University of Stavanger

Faculty of Science and Technology

MASTER'S THESIS

Study program/ Specialization: Petroleum Technology/ Drilling Technology	Spring semester, 2012 Open
Writer: Marius Aarskog	…… (Writer's signature)
Faculty supervisor: Steinar Evje External supervisor(s): -	
Titel of thesis: Extending a Drift-Flux Model for More Realistic Prediction of Transient Flow in UBO	
Credits (ECTS): 30	
Key words: UBO, UBD, unloading, drill pipe connection, two-phase flow modeling, drift-flux, slip, slug flow, bubble flow, transient, dynamic BHP	Pages: 107 + enclosure: - Stavanger, June 15th - 2012 Date/year

Abstract

The transient behavior of the bottomhole pressure during underbalanced drilling operations has been investigated. Focus has been on jointed pipe drilling with gas injection through the drill string. A description is made of a two-phase drift-flux model. The model has previously been developed in Matlab and is modeled to simulate the dynamic bottomhole pressure, during transient conditions in underbalanced operations. The original model only recognizes the slug flow regime and its corresponding slip parameters are implemented through the general slip law [29]. Extension has been made to the original model by including a model that distinguishes between bubble flow and slug flow, based on a simplified version of the suggestions made by Caetano [22]. Values for the slip parameters were chosen depending on existing flow pattern. For the transition zone, interpolation technique was used. The velocity profile coefficient, C_0, for bubble flow was suggested to be 1.0 by Caetano, however, as this made oscillations in the simulation results a value of 1.1 was adapted, as proposed by Lage and Time [34]. Simulation runs of two-phase flow in a vertical well were performed using the original model, the bubble slip parameters and the flow pattern dependent model. The results of the bubble flow model was compared to the original model, showing that after the unloading sequence, the bottomhole pressure was found to be 18.3 % lower than for the original model. The unloading sequence was also found to last 47 % longer for the bubble flow model. The results gained from the flow pattern dependent model concluded that the slug flow region is the main flow regime during the simulation. However, until break through of gas during the unloading sequence, the bubble flow regime was found to be the primary flow pattern.

Nomenclature

AUSM – Advective Upwind Splitting Method

BHA – Bottomhole Assembly

BHP – Bottomhole Pressure

BOP – Blow Out Preventer

DIV – Downhole Isolation Valve

ECD – Equivalent Circulating Density

ESDV – Emergency Shut Down Valve

FVS – Flux Vector Splitting

IADC – International Association of Drilling Contractors

MPD – Managed Pressure Drilling

MW – Mud Weight

MWD – Measurement While Drilling

NRV – Non Return Valve

OBM – Oil Based Mud

PVT – Pressure, Volume and Temperature

RAS – Rig Assisted Snubbing unit

RCD – Rotary Control Device

ROP – Rate Of Penetration

TVD – True Vertical Depth

UB – Underbalanced

UBD – Underbalanced Drilling

UBO – Underbalanced Operation

WBE – Well Barrier Element

WBM – Water Based Mud

WP – Working Pressure

Part I Introduction to Underbalanced Operations

The main purpose of part I of this thesis is to give the reader an overview of the underbalanced drilling concept, before putting focus over to two-phase flow modeling in part II. Chapter 1 will put focus on important pressure terms needed to getting an understanding of what underbalanced conditions in a wellbore is. Then, chapter 2 will give a short review of different drilling concepts with main focus on underbalanced drilling. Chapter 3 will be discussing the advantages gained by drilling underbalanced, and also the threats associated with the technique. As the underbalanced drilling concept differs quite much to conventional drilling, a short review of different well control equipment will be given in chapter 4, using the Norsok Standard [31] as basis. The purpose is just to give an overview of the system, not giving technical data and specifications. The last chapter in part I, chapter 5, is dedicated to different techniques used to achieve underbalanced conditions, main focus will be at gasified drilling fluids, as this is the technique that will be discussed in part II and also simulated in part III.

1 Definition of Important Pressure Terms

In this chapter important pressure terms and calculations will be defined. These terms will be used throughout the thesis and is based on reference [1] unless other is stated.

1.1 Formation Pressure

Formation pressure is defined as the pressure of the fluid contained in the pore space of the formation rock that is being drilled. In any formation, formation pressure may change over time as fluid is being produced from it. In old depleted reservoir, the formation pressure will have been lowered. The formation pressure will also vary with depth. There are 3 categories of the formation pressure; normal pressure, abnormal pressure and subnormal pressure. Normal formation pressure equals to a column of water reaching from the formation and up to surface. This is depending on the salinity of the water found, as the water density will vary with salinity. Subnormal formation pressure is defined as a formation pressure below normal formation pressure, and abnormal formation pressure is defined as a formation pressure greater than the pressure of a column of water to surface.

With respect to UBD, the formation pressure will typically be normal or subnormal.

1.2 Hydrostatic Pressure

The hydrostatic pressure is defined as the pressure exerted by the fluid in the wellbore when it is at rest. The hydrostatic pressure is important in drilling operations because this is the pressure the drilling personnel typically can control. The hydrostatic pressure at any point in a well is calculated by equation (1),

$$P_{Hyd} = MW \times g \times TVD \quad (1)$$

Where,

P_{Hyd} = The hydrostatic pressure

MW = The mud weight

g = The acceleration due to gravity

TVD = The true vertical depth

During circulation of fluids in the well, the hydrostatic pressure will not be the real pressure seen in the well due to friction pressure loss up the annulus. While drilling, and circulating, the equivalent circulating density (ECD) will be the important pressure parameter. The ECD can be defined as the density of the mud in addition to the contribution of the pressure losses during circulating. The mathematical expression for ECD is shown in equation (2)[10,32],

$$ECD = MW + \frac{\Delta P_A}{g \times TVD} \quad (2)$$

Where,

ECD = The equivalent circulating density

MW = The mud weight

ΔP_A = The pressure loss in the annulus

g = The acceleration due to gravity

TVD = The true vertical depth

1. 3 Formation Fracture Pressure

The formation fracture pressure is the amount of pressure it takes to permanently deform or fracture the formation. By exceeding the formation fracture pressure, the wellbore will get fractured and may lead to loss of circulation as the fluids in the well are pushed into the formation through the fractures. The fracture pressure is depending on the formation type, overburden pressure and how compacted the formation is and it is a tensile failure mode [2, 32].

1.4 Formation Collapse Pressure

The formation collapse pressure is the minimum amount of pressure that can be found in a wellbore, before the formation wall starts to collapse into the hole. It is a shear failure. Stuck pipe may be the outcome of a borehole collapse situation [2].

2 Drilling Methods

There are different approaches to drill a well. In general they can be divided into three categories; conventional-, managed pressure- and underbalanced drilling. This chapter will have a little introduction to the different drilling approaches. Figure (1) is showing a simplified pore pressure plot. The x-axis represents pressure, while the y-axis represents the depth. Most commonly the pressure is measured in specific gravity (s.g) [32]. The three lines shown in the plot represents different pressure boundaries. The brown "Borehole Stability" line corresponds to the formation collapse pressure, the blue "Pore Pressure" line corresponds to the formation pressure and the red "Frac or Lost Circulation" line corresponds to the formation fracture pressure, all addressed in chapter 1. The different coloring represents the drilling window for three different drilling techniques.

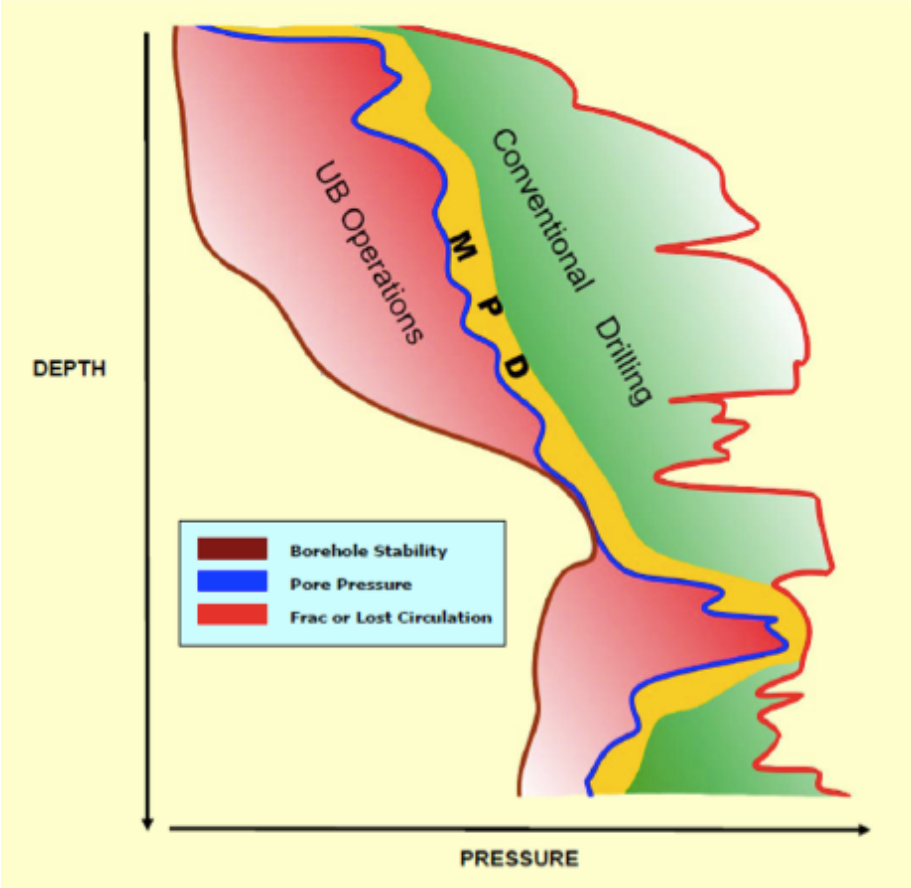

Figure (1) - Pore Plot Illustrating Different Drilling Methods [26]

2.1 Conventional Overbalanced Drilling

Conventional overbalanced drilling is the most common drilling practice used in the drilling industry [36]. In figure (1) conventional drilling window is illustrated with the green coloring, between the pore pressure line and the fracture pressure line. This is also how conventional overbalanced drilling is defined. The pressure exerted in the wellbore is greater than the formation pressure in any parts of the wellbore. By keeping a hydrostatic pressure above the formation pressure, the formation fluid will be kept in the formation by the positive differential pressure. Adjusting the mud weight and mud pump pressure during drilling operations controls the overbalanced pressure. There are, however, other concerns. As seen in figure (1), there is an upper pressure boundary, the formation fracture pressure. If the ECD exceeds the formation fracture pressure during drilling operations the formation may fracture giving a new flow path for the mud with the result of loss of circulation. As a consequence to the mud loss, the well may become unintentional underbalanced and the well may take a kick. Drilling well sections with a narrow drilling window between pore and fracture pressure are therefore a major challenge using conventional drilling methods. As mud weight is static until casing setting depth is reached, one problem is to run out of casing sizes before target depth is reached.

2.2 Managed Pressure Drilling

The MPD drilling window is illustrated in figure (1) by the yellow coloring. As for conventional overbalanced drilling, it aims to keep the wellbore pressure above the formation pressure and at the same time below the formation fracture pressure. However, the MPD approach does not require the big drilling window, as for the case with conventional drilling. Narrow drilling windows are often found in deepwater drilling and in depleted formations. To drill conventional here will have a great risk of resulting in an unintentional kick induced by either to low mud weight or due to mud losses from fracturing the formation. The MPD technique gives, as the name states, the opportunity of managing the bottomhole pressure from surface while drilling. MPD is in general divided in two categorizes [26], reactive and proactive. Reactive MPD operations are typically planned as a conventional drilling operation. However, they will have MPD equipment as a contingency to mitigate potential drilling problems as they arise.

Proactive MPD will on the other hand use the MPD method and equipment to control the pressure profile actively throughout the operation. In MPD applications the wellbore is a closed pressurized mud circulating system, as seen in figure (2). With this arrangement, the driller can better control the BHP by imposing backpressure.
There are different methods for keeping the bottomhole pressure controlled. Constant bottomhole pressure method, mud cap method, casing while drilling and dual gradient method are some of the techniques used for MPD [27].

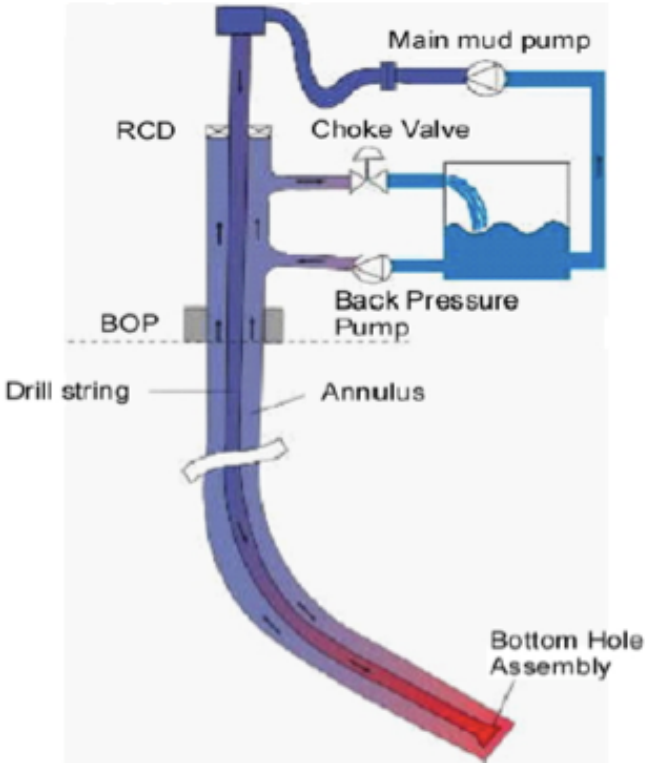

Figure (2) - MPD Flow Schematic [28]

The Underbalanced Operation and Managed Pressure Drilling Committee of the International Association of Drilling Contractors (IADC) have defined managed pressure drilling as [25];
"Managed Pressure Drilling is an adaptive drilling process used to precisely control the annular pressure profile throughout the wellbore. The objectives are to ascertain the downhole pressure environments limits and to manage the annular hydraulic pressure profile accordingly. The intention of MPD is to avoid continuous influx of formation fluids to the surface. Any influx incidental to the operation will be safely contained using an appropriate process.

MPD process employs a collection of tools and techniques which may mitigate the risks and costs associated with drilling wells that have narrow downhole environmental limits, by proactively managing the annular hydraulic pressure profile.

MPD may include control of back pressure, fluid density, fluid rheology, annular fluid level, circulating friction, and hole geometry, or combinations thereof.

MPD may allow faster corrective action to deal with observed pressure variations. The ability to dynamically control annular pressures facilitates drilling of what might otherwise be economically unattainable prospects."

2.3 Underbalanced Drilling

The underbalanced drilling window is indicated by, the red area in figure (1). This approach differs from the two described previously by the fact that the wellbore pressure is kept below the formation pressure. This means that any formation containing fluids and having high enough porosity and permeability will start producing while drilling. As seen in figure (1), the lower boundary for the wellbore pressure is the formation collapse pressure. If the pressure gets below this, the formation may collapse around the drill pipe and lead to stuck pipe. The official definition of underbalanced drilling is given by, the IADC Underbalanced Operations & Managed Pressure Drilling Committee [25],

> "A drilling activity employing appropriate equipment and controls where the pressure exerted in the wellbore is intentionally less than the pore pressure in any part of the exposed formations with the intention of bringing formation fluids to the surface."

There are several advantages with UBD, and of course, also disadvantages. Additional equipment is needed and different techniques and drilling fluids are being used to get and maintain underbalanced conditions. This will be addressed in the following chapters. First a little historical review of underbalanced operations.

2.3.1 History of Underbalanced Drilling Operations [10]

The very first drilling operations with cable tool rigs were performed underbalanced. This was not to get the advantages wanted from UBD now; it was due to the lack of knowledge and technology. A blowout simply meant discovery, while no blowout indicated a dry reservoir. As rotary drilling, with a circulating fluid to transport cuttings, was introduced in 1895, focus was set on developing better technology within the drilling industry. The mud column gave the opportunity for overbalance and the concept of primary well control. Mud systems with possibility for better viscosity properties for better hole cleaning was introduced in the 1920s. Well control with BOPs came in 1928 giving the possibility to control blowouts and being able to shut in the well. Drilling operations after this have in general been drilled overbalanced. However, it was seen that overbalanced drilling had its limitations, such as low ROP in some formations, lost circulation, differential sticking and damage to the reservoir. In the 1950s a new form for drilling was developed, air drilling. This was to be able to drill in hard rock formations. 1960s brought foam drilling to be able to drill loss zones with returns. This was, in many ways, the rebirth of underbalanced drilling technology. The first known intentional underbalanced well was drilled in the Austin chalk in the 1980s. The Canadians took it a step further when they in the late 1980s introduced the use of surface separators instead of flowing the hydrocarbons directly into surface pits, which was practiced in the Austin chalks. The use and improvements of multi-phase flow modeling and at the same time use of more advanced separation systems resulted in an increase in use of UBD. The technology is still being improved with the help of experience gained from new wells being drilled underbalanced.

3 Effects of Drilling Underbalanced

This section is based on reference [1, 3] and will give an overview of pros and cons regarding the use of UBO instead of conventional overbalanced operations. Figure (3) illustrates some of the different effects.

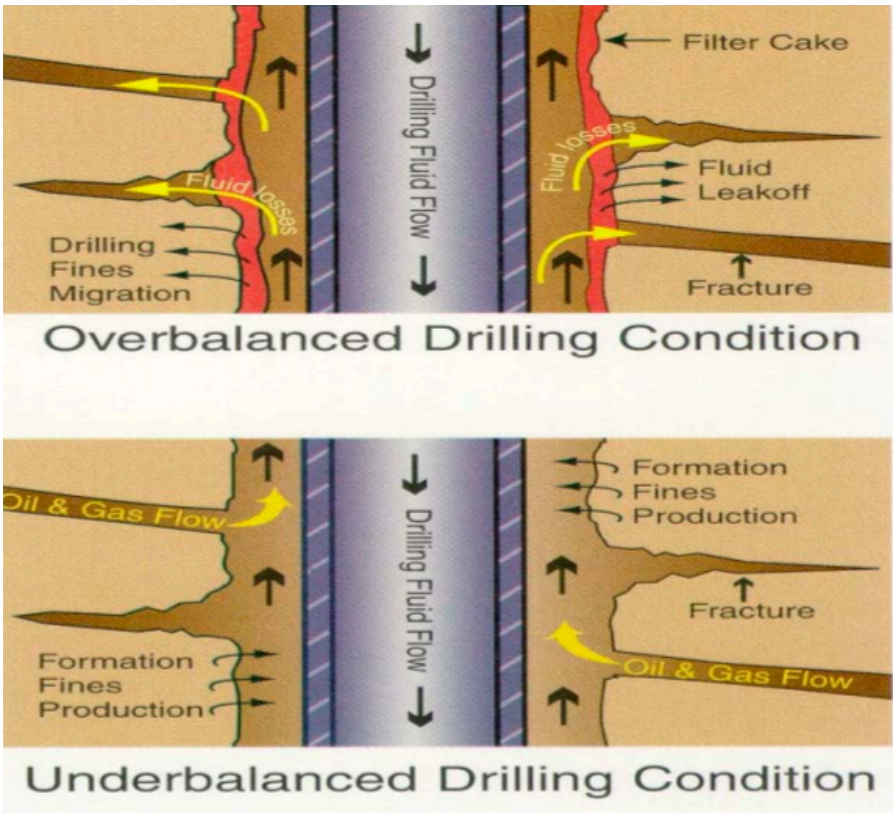

Figure (3) - Overbalanced vs Underbalanced Conditions in a Wellbore [5]

3.1 Advantages by Choosing UBD

Introduction of underbalanced drilling technology offshore has a wide area of interest. From old depleted reservoirs to new fields with special drilling problems or low reservoir pressure may all be candidates for an underbalanced drilling approach. However, drilling underbalanced requires additional equipment and more attention than the overbalanced case, which of course equals additional costs. This implies that UBO will not be considered without proven to be economical beneficial. Here are some of the most recognized benefits by drilling a well underbalanced.

3.1.1 Increased Rate of Penetration

The differential pressure down hole will affect the rate of penetration. As mud weight increase, the ROP decrease, and equally, as the mud weight is lowered the ROP will increase. The decrease in ROP in overbalanced drilling is due to the chip hold down

effect, which has a major effect on drilling rates. The chip hold down effect is a function of the differential pressure between the wellbore pressure and the formation pressure, which in conventional drilling gives a confining pressure that prevents the cuttings from releasing from the formation. This confining pressure is also strengthening the rock, making it harder to drill. Underbalanced drilling avoids this confining pressure to the rock below the bit. The differential pressure will instead give a clean up effect that helps removing the cuttings from the formation, giving a higher ROP. At least, this is true till a certain point. At some point the positive effect of decreased mud weight ends, after this point is reached the bit will begin to flounder due to inadequate cleaning of cuttings from the bit, which will cause the bit to re-drill the cuttings.

3.1.2 Minimize Lost Circulation

Lost circulation may be a huge problem in conventional drilling operations. Lost circulation occurs when drilling fluid flows into the formation due to highly porous and permeable formation or existence of natural fractures. Overbalanced drilling can also create fractures, which again cause lost circulation. This is especially a problem when the drilling window is narrow, like mentioned in chapter 2. Drilling depleted reservoirs with overbalance is very challenging due to a narrow window between pore pressure and the reduced fracture pressure. Lost circulation can be very costly in conventional drilling. The worst-case scenario in a lost circulation situation is total loss of mud column into the formation, leaving an unwanted kick situation where the well gets filled with gas. Drilling underbalanced will, when performed right, eliminate the problem with fracturing of the formation and loss of mud. The differential pressure is forcing fluids from formation into the wellbore instead of the other way around, giving no possibility for loss of drilling fluid, see figure (3) In the 90´s the main reason for drilling underbalanced was to avoid lost circulation.

3.1.3 Avoid Differential Sticking

Filter cake is formed during overbalanced drilling in permeable zones where drilling fluid is filtrated through the formation wall, leaving the clay and barite solids in the formation wall. These solids forms a rather impermeable cake called mud cake or filter cake, see figure (3). The filter cake continually builds up and also gets abraded by the rotation or the sliding of the drill pipe. The problem occurs when the drill pipe, or usually the drill collars, gets to rest against the filter cake. In this case the drill stem will

experience a low-pressure side and a high-pressure side. The drill stem gets pushed into the impermeable filter cake, due to the differential pressure. The severity of the sticking depends on the differential pressure between the wellbore and the formation, the area of drill pipe in contact with the formation and the roughness of the drill pipe, formation wall and filter cake.

In underbalanced operations one avoids these problems due to the fact that there will be no build up of filter cake. In permeable zones the flow will be from the formation into the wellbore, resulting in no filter cake at the formation wall. Horizontal wells are especially exposed to differential sticking, as the drill pipe lies resting on the bottom of the wellbore. The horizontal part of the well is also often permeable, as it usually contains the reservoir section. Some horizontal wells are therefore drilled using underbalanced operations to avoid differential sticking.

3.1.4 Improved Formation Evaluation

Drilling underbalanced gives the opportunity to evaluate the formation fluids at once, as the well is producing in reservoir zones. In permeable zones, the fluid contained in the formation will flow into the well and mix up with the drilling fluid. This makes it possible to immediately detect hydrocarbon bearing reservoirs that otherwise might have been bypassed if the well was drilled overbalanced. In addition, the fact that there is no intrusion of mud into the formation also will improve the interpretation of open-hole logs and pressure transient tests. This also gives the opportunity to start producing the reservoir as its drilled, provided the necessary surface equipment is in place.

3.1.5 Reduced Formation Damage

In conventional overbalanced drilling the reservoir is being invaded with solids and foreign fluids, which may lead to skin development and reduced productivity. As a measure to this problem, expensive and time-consuming stimulation may be required. And even now, after stimulations, full productivity may not be reached. When using an underbalanced system, fluids will flow from the reservoir to the wellbore, see figure (3). In this way, no foreign fluids and solids will enter the formation, leaving it near skin and damage free.

3.2 Disadvantages by Choosing UBD

Even though underbalanced operations have a lot of advantages compared to conventional drilling, it also has its weaknesses and appears as a poor choice under certain conditions. Potential problems and weaknesses regarding UBD must be evaluated before implementing a UBD program. Problems with different techniques regarding equipment and keeping a controlled BHP will be discussed later, while problems regarding the underbalanced conditions in the hole will be addressed below.

3.2.1 Geopressured shale

When shale is deposited in a river or lake environment it normally contains about 60 % water. As more shale and sand is deposited, the water gets squeezed out from the original clay. When the overburden pressure gets high enough it will form a shale stone, which contains approximately 5 to 20 % water. This is regular shale formation. Geopressured shale on the other hand, will have a much higher content of water. Here the deposition process is interrupted by for example a fine grain cap that prevents the water from being squeezed out. Because of this, water supports the rock structure above, and not the shale structure as in the case of regular shale formations. This is what makes these sections un-drillable with underbalanced conditions. If the well pressure is below the pressure in the shale, the shale will get squeezed into the wellbore in lumps causing hole cleaning issues and possible stuck pipe.

3.2.2 Salt formations

Drilling through salt formations will also cause problems drilling underbalanced. Salt formations tend to flow towards lower pressure, which obviously will create problems in an underbalanced wellbore. Especially the Zechstein salt domes in the North Sea flows rapidly and may cause tight holes just hours after it is drilled through. This is why overbalanced is recommended procedure when drilling through salt formations.

3.2.3 Unconsolidated sand

Sand that have not had the time to be cemented properly into sandstone are called unconsolidated sand. This is in general young sand formation. When this sand is exposed to the negative differential pressure in the well, it may collapse into the well, and cause problems with hole cleaning, stuck pipe and production of sand.

3.2.4 Hole collapse

The potential for hole collapse will be a vital part when planning an underbalanced drilling program, especially for horizontal wells. As seen in figure (1), the underbalanced drilling window is limited by the borehole stability line. Drilling with a lower well pressure than this may result in collapsing wellbore walls. Hole collapse is particularly troublesome when reentering a depleted zone, where the collapse pressure is close up to the formation pressure.

4 Well Control Equipment

In conventional overbalanced drilling, the mud system is the primary barrier against a kick or blowout. This is not possible in UBD as the drilling fluid is deliberately designed to be lighter than the expected downhole pressures. There is need of other types of equipment to be able to achieve well control. Figure (4), below, shows the well barrier schematic illustration taken from the Norsok Standard D-010 [31], regarding drilling and tripping of work string in underbalanced fluid. This is the configuration for rig-up on installations with a surface drilling BOP.

13.8.1 Drilling and tripping of work string in UB fluid

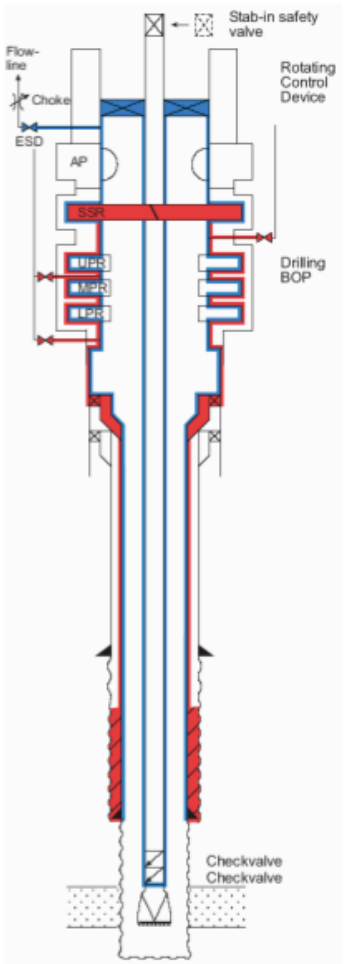

Well barrier elements	See Table	Comments
Primary well barrier		
1. Casing cement	22	
2. Casing	2	
3. Wellhead	5	
4. High pressure riser	26	
5. Drilling BOP	4	
6. Rotating control device	48	The flowline shall have two valves, one of which shall be remotely operated and failsafe close (ESDV).
7. Drilling non-return valves	50	
8. Drill string or completion string	3 25	Above NRV.
Secondary well barrier		
1. Casing cement	22	
2. Casing	2	
3. Wellhead	5	
4. High pressure riser	26	
5. Drilling BOP	4	Shear seal ram.

Notes

1. The well control configuration described is for rig-up on installations with a surface drilling BOP.
2. The work string refers to drill string (illustrated) or completion string.
3. Stab-in safety valve is readily available on the drill floor at all time with relevant connections.
4. Kill fluid to be readily available in order to perform an emergency kill.
5. For common WBEs, a risk analysis shall be performed and risk reducing/mitigation measures applied to reduce the risk as low as reasonable practicable.

Figure (4) - Well Barrier Schematic Illustrations [31]

The Norsok Standard [31] have also given following requirements and guidelines for underbalanced operations,

"a) Primary well control during underbalanced drilling is maintained by flow and pressure control. The BHP and the reservoir influx is monitored and controlled by means of a closed loop surface system including an RCD, flowline, ESDV, choke manifold and surface separation system:

1) The RCD shall be installed above the drilling BOP and shall be capable of sealing the maximum expected wellhead circulating pressure against the rotating work string and containing the maximum expected shut-in wellhead pressure against a stationary work string;
2) The return flowline shall have two valves, one of which shall be remotely operated and failsafe close (ESDV). The flowline and the valves shall have a WP equal to or greater than the anticipated shut-in wellhead pressure;
3) A dedicated UBD choke manifold shall be used to control the flow rate and wellbore pressure, and reduce the pressure at surface to acceptable levels before entering the separation equipment. The choke manifold shall have a WP equal to or greater than the anticipated shut-in wellhead pressure. The choke manifold shall have two chokes and isolation valves for each choke and flow path. Applied surface backpressure should be kept to a minimum to reduce erosion of chokes and other surface equipment;
4) A surface separation system shall be selected and dimensioned to handle the anticipated fluid/solids in the return flow. Plugging, erosion or wash-outs of surface equipment shall not impact the ability to maintain primary well control.

b) When running a work string UB, two NRVs, shall be installed in the string, as deep in the work string as practical and as close together as possible. The NRVs shall prevent wellbore fluids from entering into the work string. Installation of additional NRVs shall be considered depending on the nature of the operation (ie high-pressure gas). The NRV is a WBE and shall have a minimum WP rating equal to the maximum expected BHP.

c) Snubbing facilities shall be used or the well shall be killed with a kill weight fluid prior to tripping pipe, if the shut-in or flowing wellhead pressure can produce a pipe light condition and a DIV, a retrievable packer system or similar shut-in device, is not in use or is not functioning as designed.

d) Enough kill fluid of sufficient density shall be available on site at any time to be able to kill the well in an emergency. 1,5 times the whole volume should always be available.

e) A stab-in safety valve for the pipe in use shall be available on the rig floor. "

Equipment required that are not used in conventional drilling is described below,

4.1 Rotary Control Device (RCD) [10]

During UBO, the well will be under pressure continuously. At the same time, the drill string needs to be able to be rotated and move axially. This gives the need of an annular seal element that is in constant touch of the drill string, are able to rotate with the string and at the same time withstand the pressures expected. There are two categories of RCDs,

1) Passive seal
2) Active seal

The RCD is mounted on top of the drilling BOP, which is a conventional BOP stack. The drilling BOP is used in open position like in conventional drilling and the body of the BOP serves as a primary barrier element in figure (4), while the RCD is the primary barrier element that closes the annulus. The shear seal ram, in the drilling BOP, acts as a secondary barrier element giving the opportunity to shear the drill string and seal the wellbore.

In the passive RCD, rubber elements are in forced contact with the drill pipe. The rubber elements are often referred to as strippers and they will have a smaller inner diameter than the drill pipe outer diameter. The force fit contact between the pipe and the rubber elements are enhanced by the differential pressure across the seal. The seal elements are mounted on a bearing supported assembly. The contact force between the seal and the rotating string will give high enough friction force to rotate the bearing assembly. Due to high friction between the drill string and the rubber element, large axial loads, downwards or upwards, are developed and transferred from the seal to the bearing. The

highly loaded bearing generates heat and needs to be cooled and lubricated. This is facilitated by circulated oil in a special cooling and lubrication oil system.

In active RCD, the rubber seal element or the annular packer will be inflated or energized by hydraulic pressure. The seal elements assembly is mounted on bearings. As in rotating control heads, the bearing-supporting assembly is rotated by the grip force on the rotating pipe. As for the passive RCDs the friction force between the seal and rotating drill string is high enough to provide rotation of the bearing assembly. The bearings will also be cooled and lubricated by an oil circulation system. The hydraulic pressure, the sealing pressure, increases automatically as the wellhead pressure increases.

4.2 Flowline With Emergency Shut Down Valve [31, 36]

The Norsok Standard D-010 [31] states that the return flow line shall have two valves, where one of them is an emergency shut down valve (ESDV). The ESDV is an on/of gate valve that is controlled by hydraulic pressure. The requirement from Norsok is that it is remotely activated and also that it is fail-safe close. The ESDV is kept open by the hydraulic control pressure. That the ESDV is fail-safe close type indicates that failure of the control system will cause the valve to shut close instantly. It can also be closed by the control system from a control panel. It is all a part of the emergency shut down system that monitors the drilling conditions. This system will alert the operators if unexpected conditions are discovered. Examples of conditions that are monitored are pressures at critical points in the system, liquid levels in the separator, any release of gas and fire.

4.3 Choke Manifold [1, 31]

According to the Norsok Standard D-010 [31], the choke manifold shall be used to control the flow rate and wellbore pressure, and reduce the pressure at surface to levels that is acceptable in the separation system. To maintain redundancy and increase the reliability of the choke, it is also stated that the choke manifold shall have two chokes and isolation valve for each choke and flow path. The well control choke is an important part in UBO. It is used to hold backpressure to the annulus, in this way the drilling crew is capable of some control of the bottomhole pressure and the gas expansion in the annulus.

4.4 Four Phase Separator System [10, 36]

As UBO is expecting to produce during drilling, the returns need to be taken care of by a separator system. A four-phase separator may be used and this separates gas, light liquid (oil and condensate), heavy liquid (drilling fluid and water) and cuttings. The separator acts as a closed pressurized system separating the phases with the help of gravity. The lightest phase, gas, tends to move upwards to the top of the separator and is taken out through an outlet there. The heaviest phase, the solids, settles down at the bottom of the separator. The heavy liquids, such as mud and water is accumulated and evacuated right above the solids, while the light liquid, oil and condensate are accumulated between the heavy liquids and the gas. A schematic of a typical four-phase separator is presented in figure (5) below.

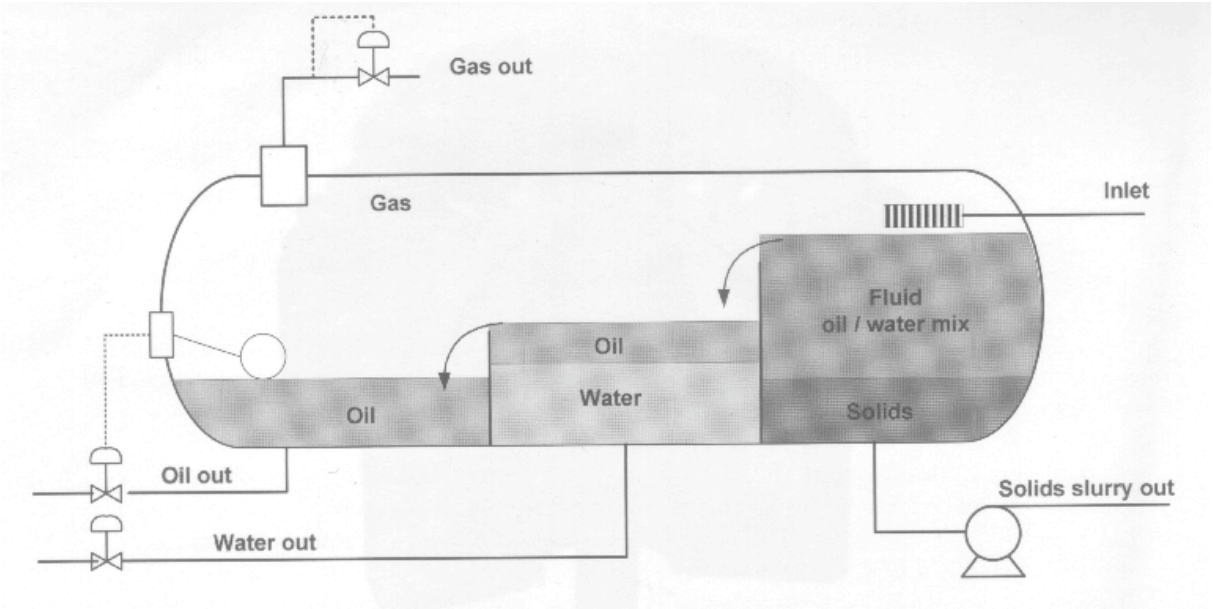

Figure (5) - Schematics of a Four Phase Separator [10]

4.5 Non Return Valve (NRV) [31]

It is a requirement from the Norsok Standard D-010 [31], that two NRVs shall be installed in a string that is run in an underbalanced well. The NRVs shall be set as deep as practical in the string and as close together as possible. A NRV allows pumping of fluids down through the string but, however, it prevents fluid from flowing back into the string. They provide the primary safety barrier inside the drill string and prevent gas and fluids in the drill string from flowing back on the drill floor when pipe connection is made. The typical valve design can be either a dart/plunger type, or a flapper type.

4.6 Snubbing Facilities [31, 36]

While tripping into a live well, situations may occur where the drill string is to light to overcome the buoyancy effect. This is also known as a pipe light situation. The Norsok Standard D-010 [31] states that prior to tripping during pipe light conditions the well shall be killed with a weighted kill fluid. This will however make the well overbalanced, ruining the advantages gained by having drilled underbalanced. An alternative provided by the Norsok Standard D-010 [31] is a snubbing unit. A rig assisted snubbing unit, RAS unit, may provide additional force to the pipe. This force will be added on the drill string to push it into a live well, until it reaches the balance point where it will be able to enter with its own weight. The RAS unit may also hold the pipe in the opposite case, where the pipe jumps out of the well. Here it will provide force to hold the pipe during tripping out, taking it out in a controlled manner.

5 Underbalanced Drilling Techniques

To drill underbalanced requires a drilling fluid that is light enough to keep the dynamic BHP below the pore pressure. The simplest way to lower the well pressure is obviously to use lightweight drilling fluids such as fresh water, diesel and lease crude. However, this may not be enough to achieve underbalanced conditions. Underbalanced operations will therefore often involve the use of compressed gas or foam as the circulating fluid. The gas may either be utilized on its own, or in conjunction with other drilling fluids depending on the drilling conditions. In theory, all kinds of gases can be used to lower the BHP. However, there are some concerns to think of when it comes to selection of a suitable gas. Cost, handling and safety, mechanical and chemical concerns all needs to be considered. Atmospheric air is known as the most common utilized compressed gas followed by natural gas and nitrogen [24]. This chapter will review different drilling fluids used to get underbalanced conditions while drilling. Main focus will be at gasified fluid drilling as this is the technique that will be used in part II and part III. Different approaches to the injection of gas into the drilling fluid are also of importance and will be discussed in chapter 5.2. If no other is stated, the literature in this chapter is based on reference [24]

5.1 Circulated Fluids in Underbalanced Drilling

The selection of drilling fluid for a particular underbalanced drilling operation depends on a wide range of considerations. The most important are,

- Reservoir pressure and depth
- The desired underbalanced conditions
- The type and physical and chemical properties of the drilled rock
- The properties of the formation fluid
- The location of the drilling site and the availability of different types of gases

These considerations indicate that one drilling fluid will not be applicable in all cases, and thus, there is need of different solutions to reach underbalanced conditions.
The fluid selection can be categorized as follows,

- Liquid drilling fluids
- Gaseous drilling fluids
- Stable foam drilling
- Mist drilling
- Gasified fluid drillings

5.1.1 Liquid Drilling Fluids

As the pore pressure often exceeds the hydrostatic pressure of oil and even water at the same depth, it may be possible to drill underbalanced using a pure liquid drilling fluid. However, even though the hydrostatic pressure alone provides underbalanced conditions, the system may become overbalanced during circulation due to ECD contribution. The liquid drilling fluid is similar to the drilling fluid used in conventional drilling operations. It may be water based or oil based and contains a variety of additives to control weight, hole cleaning and other properties. An important feature of the drilling fluid is that it is a homogeneous liquid and incompressible with constant density. When planning an underbalanced well it is important to know that the drilling fluid may become compressible if mixed with formation hydrocarbons in the annulus of the wellbore.

5.1.2 Gaseous Drilling Fluid

In gas drilling, dry gas is used as the only drilling fluid. Gas will be injected down the drill pipe, and as it has no real cuttings transport properties, like in liquid drilling fluids,

it is depending on high annular velocity of the gas. At surface, the cuttings will usually have been reduced to dust due to the high velocity contact with the wellbore.

Dry gas drilling systems have been known to provide the fastest penetration rates and also longest bit lifetime. Wells drilled with dry gas have also typically less deviated holes, better cement jobs, better completions and better production than wells drilled with conventional drilling fluids. On the downsides, dry gas drilling systems is restricted by water producing formations, unstable wellbores and also high formation pressure. When water producing zones are being drilled, the wet cuttings will be glued together and stick to the formation wall. After a while the hole will be packed, circulation stopped and the drill pipe will get stuck.

As mentioned before, atmospheric air is the most utilized gas when it comes to gaseous drilling fluids, followed by natural gas and nitrogen. A problem with dry air drilling is the possibility of downhole explosions and fire in the presence of natural gas, due to the fact that air and natural gas is a highly flammable mixture. Using natural gas instead of air as the circulating fluid will prevent the formation of a flammable gas mixture when producing hydrocarbons. However, when natural gas is released to surface, a highly flammable mixture is formed. Using nitrogen as the circulating fluid will also prevent the formation of a flammable gas mixture when producing hydrocarbons. Another advantage is that the nitrogen supply is unlimited as it is taken out of air.

5.1.3 Stable Foam Drilling

Drilling operations with stable foam has been performed for more than 30 years. Stable foam are typically produced by injecting water containing 1-2 volume percent foaming agent at injection pressure into a stream of gas. The result is stable foam with consistency quite similar to an average shaving cream. The foam has an excellent carrying capacity for cuttings, about 8 times as high as for water, due to the viscosity.

The injection water with foaming agent provides a mechanism for also introducing other chemical additives like polymers, clay and shale stabilizers and corrosion inhibitors. In this way there are possibilities for designing the foam individually for each individual well. Since stable foam contains water and foam, the potential for a down hole explosion or fire are pretty much eliminated. This, combined with the fact that it has such good

hole cleaning properties and water transportation abilities makes stable foam drilling one of the most complete reduced pressure drilling systems. It is however also one of the most costly, due to the needed quantities of foaming agent and other additives.

5.1.4 Mist drilling

Mist drilling is basically a modification to the dry gas drilling that is used when water producing zones are drilled. Like mentioned previously, dry gas drilling in water producing zones may lead to stuck pipe. In mist drilling small quantities of water containing foaming agent, typically 0.10-0.25% foaming agent by volume percent water, is injected into the gas stream at surface. This will produce system where gas is the continuous phase with water mist that is being carried by the gas.
Typically mist system has less than 2.5 % liquid content. The liquid mist is introduced to assist in cleaning the face of the drill bit and to assist to lift the very small and powered like cuttings surrounding the bit. The foaming agent reduces the interfacial tension between the water and the drill cuttings allowing small water and drill cutting droplets to be dispersed as fine mist in the return flow instead of packing of the hole like in the case of dry gas. The ROPs generated through mist drilling are quite similar as for dry gas drilling, it is however more expensive due to additives like foam agents and corrosion inhibitors.

5.1.5 Gasified Fluid Drilling

This is a method that will provide underbalanced conditions, and at the same time keep the advantages of the mud. This is also the technique that will be investigated more in part II and part III of this thesis. To create a gasified drilling fluid, gas is injected into the drilling fluid. As the gas is mixed into the drilling fluid results in an expansion of the fluid, it will result in a reduced density per unit of volume. In gasified fluid drilling, the cuttings transport properties are given by the lifting and carrying properties of the drilling fluid. The drilling fluid can be water, crude oil, diesel, WBM or OBM. Drilling with gasified drilling fluid is considered as the most corrosive of all underbalanced drilling techniques. However, by using corrosion inhibitors, adjusting pH and careful select the fluid, gasified fluid drilling is successfully in use worldwide.
The two-phase flow behavior of gasified mud is rather complicated to accurately model, which makes the prediction of the pressure profile in the well hard. It is of importance to find the right ratio between gas and liquid to ensure a stable circulation system. Two-

phase flow models are important in this work; this will be focused on in part II of this thesis. In general, too low gas injection will cause overbalance while too high amounts of gas may lead to slugging.

5.2 Gasified Fluid Injection Techniques

From now on, the focus in the thesis will be on gasified fluid drilling.
To gasify the drilling fluid there are several different techniques. The most common way is to inject the gas and liquid through the drill string. Injection through a parasite string is another option, as well as annular injection through a concentric string. The two latter may also be combined. The purpose of this chapter is to identify the different methods, how they affect the BHP will be discussed in part II, chapter 7.2.

5.2.1 Drill String Injection

As stated above, injecting the gasified drilling fluid through the drill string is the most common technique used to inject gasified drilling fluid. The gas is injected at the standpipe manifold and here it mixes with the drilling fluid, see figure (6). One of the advantages with drill string injection is that it does not require any special equipment downhole. Other benefits of using this technique is that it requires a smaller upper hole and smaller casing sizes, it can be used in horizontal wells where gas expansion helps aiding in cuttings transport, and it also requires a lower gas volume than if the gas was injected partially up the annulus. The biggest disadvantage using this method is that the gas injection is shut down during each connection; this will be further discussed in chapter 7.2. Another problem is that MWD equipment normally utilizes mud pulse-telemetry to communicate. This system requires an incompressible drilling fluid to be able to operate. As gas is a compressible fluid, a maximum of 20 % gas may be mixed in the drilling fluid before the pulse-telemetry cease to function [10]. If higher gas volume fractions are needed, the use of electromagnetic MWD tools will be an opportunity.

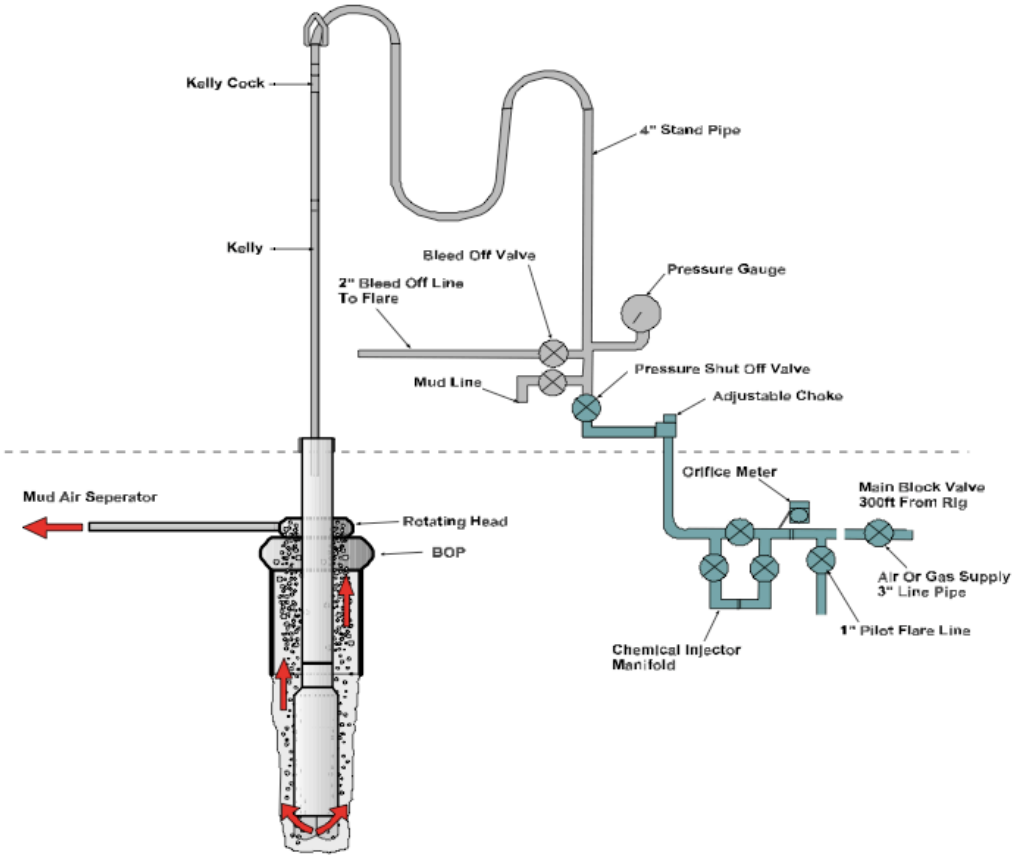

Figure (6) - Injection through drill string [24]

5.2.2 *Parasite String Injection*

As stated above, the main problem with drill string injection is that gas injection is stopped during connections, and also during tripping in and out of hole. One of the problems with this is that the gas boils out of the gaseous fluid leaving fluid slugs at the bottom. The result is an unwanted pressure fluctuation, which may ruin the whole operation; this will be discussed in chapter 7.2. However, this may be avoided by injecting the gas through a parasite string. The use of this parasite string gives the possibility to inject gas also during connections and while tripping in or out of hole. A parasitic string is basically a coiled tubing string, or similar, connected and strapped to the casing. Drilling fluid is pumped down the drill string while the gas is injected down the parasite string and mixed into the drilling annulus at some point where the parasite string is connected to the casing. The single phase and incompressible drilling fluid in the drill string gives the opportunity of efficient operation of mud pulse telemetry during MWD and also running of downhole motors. Parasitic string gas injection is almost only used in vertical wells [10]. Compared to the case with gas injection through the drill string, injection through a parasite string requires higher gas rates to achieve

wanted underbalanced conditions. Gas costs are not the only disadvantage, the parasite string also requires a larger surface hole to fit at the outside of the casing [1]. Figure (7) shows a typical parasitic gas injection system.

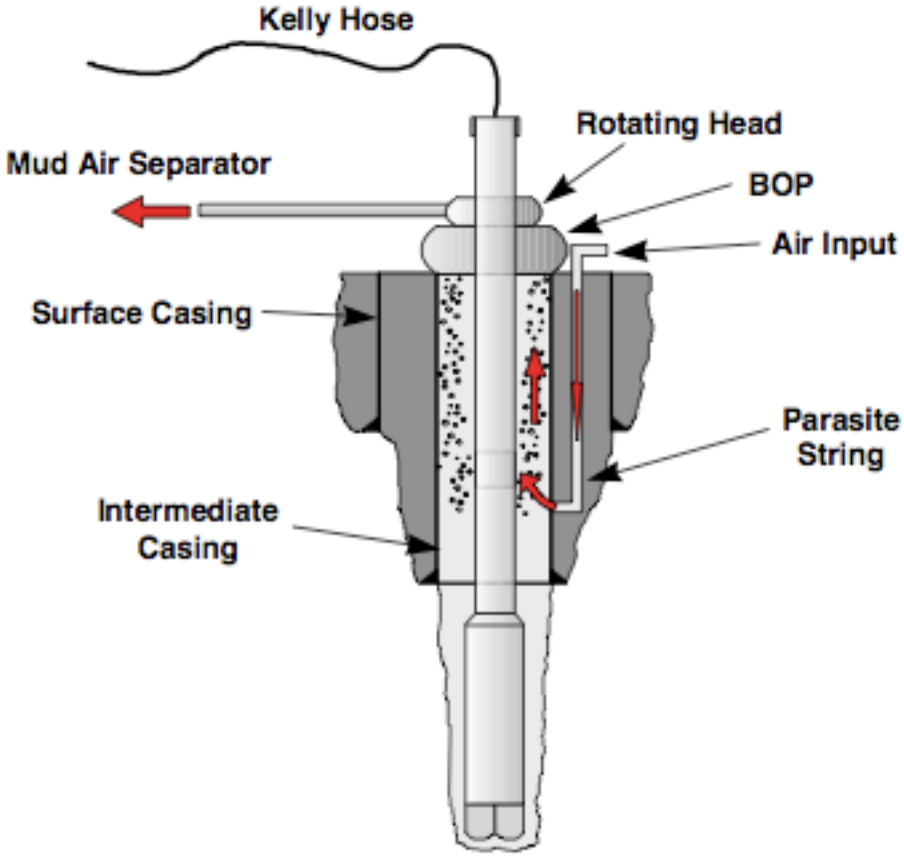

Figure (7) Gas injection through a parasite string [24]

5.2.3 Annular Injection

The idea behind the annular injection is to use two casing strings, dual casing, and inject gas in the annulus between them. As for the parasite string, annular injection will provide a possibility to inject gas also during connections and tripping, and provide an environment where conventional MWD equipment can be used. Due to a larger annular volume, higher gas rates are needed than for the parasitic string. A dual casing string may also be set in inclined and horizontal wells. After the casing is cemented in place, the temporary casing string is set. It can either be centralized at bottom or set with a packer. The greatest problem using this injection method is that it reduces the hole size and will leave a step in the hole size after it is pulled. It is of importance to know that this method is going to be used at the preplanning phase of the well, to be sure that final hole size is feasible. Special slim hole couplings are required and the technique will also increase the casing expense. However, if multiple wells at the field are going to be drilled

in the same manner the inner string can be reused and will therefore be more cost effective [1]. As it is time consuming to trip in and out with the temporary casing string, rig costs will also increase using this method. Figure (8) shows an annular gas injection system.

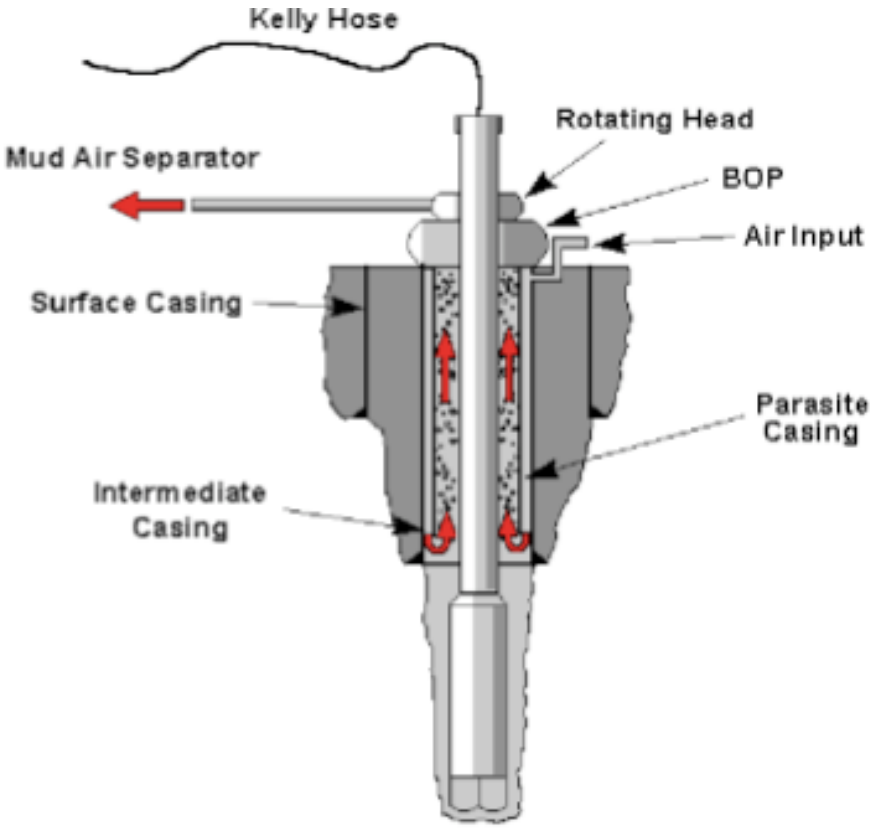

Figure (8) Annular injection [24]

Part II Two-Phase Flow Modeling

At this point the reader should have gotten an idea of the concept of underbalanced operations and also some knowledge of the different techniques available. The purpose of part II is to give an overview of two-phase flow modeling, which is of huge importance for getting a successful operation when drilling underbalanced with gasified drilling fluids. Chapter 6 will be describing different approaches to two-phase flow modeling and how it has evolved. Chapter 7 will try to give an overview of dynamic modeling of two-phase flow and its use in underbalanced operations. Chapter 7.1 is dedicated to a short introduction to two-phase modeling with respect to UBO. Chapter 7.2 will give a presentation of the transient behavior of the bottomhole pressure when experiencing changes in the system. This is important to keep in mind for part III, where some of these deviations from steady state will be simulated. The focus will be on gasified fluid drilling with injection through the drill pipe. At last in chapter 7, a proposed modeling sequence will be presented, to show how a multi-phase flow simulator is vital for planning of an UBO. Chapter 8 will give an overview over multiphase flow parameters, which again are needed in chapter 9, where the drift-flux model is described. The drift-flux model will be used in part III of the thesis.

6 Approaches to Flow-Modeling

Multiphase flow modeling has been and still is a difficult task. Up through the years there have been different approaches to describe the flow. Starting with simple unrealistic assumptions, and adding more realistic and better descriptions as these areas were better researched. The first approach was a flow model that neglected slippage between the phases, and treated the gasified fluid as a homogeneous fluid. Thereof the homogeneous approach. As this is found to be a too simple way of describing the flow [30], empirical correlations were implemented into the model to correct for slip between phases and also recognition of different flow patterns [16]. Then the mechanistic, or phenomenological, approach was developed. This approaches tries to describe the different mechanisms, instead of using empirical correlations, in the multiphase flow. It recognizes that different flow patterns exists and that they requires separate models to predict main parameters [22, 33, 34].

6.1 Homogeneous Models

The homogeneous approach provides the simplest technique for analyzing two-phase flow. The idea behind the homogeneous model is that both liquid and gas phase moves at the same velocity. With this assumption, slip ratio will be set equal to one and this is why the model also is known as zero slip model (see chapter 8.6 to find the definition of slip flow). This approach considers the two-phase flow as a single-phase flow with average fluid properties depending on the mixture quality. The frictional pressure drop in the model is calculated by assuming a constant friction coefficient between the inlet and the outlet section of the pipe [14]. Guo et al [13] was the first to use the homogeneous flow model approach in 1996. They developed a computer program that predicted the optimum gas injection rate that would ensure maximum ROP and also provide adequate hole cleaning. The model was simplified by only considering the dispersed bubble region of flow. The dispersed bubble regime is the only flow pattern where the assumption of no slip is valid [11]. The model was validated with field data from three specific wells at different depths [13].

6.2 Empirical Correlations

The empirical correlations are formulated by establishing a mathematical relation based on experimental data. Models that use empirical correlation are limited to the data range used when generating the correlation [30]. The empirical approach typical involves flowing different fluids through a pipe. The flow rates, phase fractions and pressure drops are carefully measured, while flow patterns are observed. This can all be done at different pipe diameters and pipe inclinations. All tests are however done at steady state conditions with constant gas and liquid rates. These measured data are then use to develop empirical correlations that can predict flow patterns, liquid hold up and friction factor for the different cases. Then a pressure gradient equation is developed that uses these empirical correlations [15]. The Beggs and Brill [16] correlation is one of the most used empirical correlations in different UBD simulators [17]. This correlation was made from experimental data gained in a small-scale test facility, which consisted of 90 ft long transparent acrylic pipes. Fluids used were air and water. The parameters used for the study are shown in table (1).

Table 1 - Parameters Studied by Beggs and Brill [16]

Parameter	Range
Gas flow rate	0-300 Mscf/D
Liquid flow rate	0-30 gal/min
Average system pressure	35-95 psia
Pipe diameter	1 and 1.5 in.
Liquid holdup	0-0.87
Pressure gradient	0-0.800 psi/ft
Inclination angle	-90°-+90°
Flow patterns	All horizontal flow patterns

6.3 Mechanistic Models

The mechanistic approach postulates the existence of different flow regimes and gives separate models for each of these flow patterns to predict the main parameters, such as gas fraction and wellbore pressure. This is the reason that mechanistic models are being used with increasing frequency for the design of multiphase production systems, rather than the empirical correlations, which are found too inaccurate [18].

One of the first steady state UBD program designed based on the mechanistic approach was developed by Bijleveld et al [19].

Hasan and Kabir [20] developed a mechanistic model to estimate gas fraction during upward concurrent two-phase flow in annuli. Hasan [21] also developed a mechanistic model to estimate gas fraction during downward concurrent two-phase flow in pipes for the bubbly- and slug flow region.

7 Dynamic Modeling of Two-Phase Flow in UBO

In this chapter a short introduction to multi-phase flow modeling in UBO is presented. The purpose of the introduction is to get an understanding of why flow modeling is critical in the planning of an UBO. After the introduction, section 7.2 will go through the dynamic behavior of the BHP during UBD. Then in section 7.3, a proposed use of a modeling sequence prior to an underbalanced drilling operation will then be presented, to get an understanding of how it is done.

7.1 Introduction

A successful UBO are expected to keep the BHP below the formation pressure during the entire operation. Exceeding this pressure just for a little while could ruin the whole operation. Proper well planning is vital prior to any drilling operation, regardless if it is conventional drilling, MPD or UBD. However, an UBO will in most cases involve multi-phased flow, which is associated with a dynamic BHP as will be discussed in in chapter 7.2. Multiphase flow calculations is said to be amongst the most complex fluid-engineering calculations known to the industry [10]. UBD is combining drilling, with two phase drilling fluid, and production of reservoir giving a system with many variables that is very difficult to describe. As well control also essentially becomes flow control, the circulation system is becoming the most critical element in the operation. As a result, flow modeling and simulations has become more and more important in the planning phase of an underbalanced operation [4]. The main motivation for multiphase flow modeling in underbalanced operations is to establish a pressure profile along the entire circulating path. Flow models are in general divided into two groups, transient models and steady state models. The transient models, known as dynamic models, will be used for situations where the flow situation changes with time. Such situations will be discussed in chapter 7.2. The steady-state models are time independent and is generally used to work out the operations drilling window and give advise on how the system

should be operated during full production. A complete underbalanced flow modeling software program should in general at minimum include following features [8],

- A flow regime model, which predicts what kind of flow that exist at any given location in the well.
- A liquid hold up model, that calculates the liquid fraction at any given location in the well, which also is taking the slip between the phases into account.
- A model for prediction of frictional pressure losses along the two-phase flow system.
- A model that account for the effect of temperature and pressure on the phase behavior and transport properties based on thermal, PVT and property data.
- A hole cleaning model which shows the hole cleaning performance.

7.2 Dynamic Bottomhole Pressure

Being able to keep the BHP underbalanced and stable is a major challenge in underbalanced operations performed with jointed pipe and gasified fluid drilling [7]. As stated above, getting overbalanced conditions may ruin the operation, even if it is just temporarily. Interruptions in the circulation system will cause fluctuations in the pressure. The flowing bottomhole pressure can be expressed as [9],

$$P_{wf} = P_{hyd} + P_{fric} + P_{acc} + P_{choke} \quad (3)$$

Where,

P_{wf} = The flowing BHP

P_{hyd} = The hydrostatic Pressure

P_{fric} = The pressure loss due to friction in the wellbore

P_{acc} = The pressure loss/gain due to fluid acceleration

P_{choke} = The back pressure from the adjustable choke

The BHP may be controlled during steady state conditions. However, all of the four parameters in equation (3) are dynamic and depending on time, and the state of the system. By changing rates of gas or liquid, which happens during, e.g., drill pipe connections or change in influx from a reservoir, all the four parameters will be affected causing a fluctuation of the BHP. In part III of the thesis, a drift-flux model will be used to perform simulations of an underbalanced drilling operation. In these simulations there will be two different scenarios that will cause fluctuations in the BHP, and these will be

discussed below and then simulated and explained through plots gained from the simulations in part III.

7.2.1 Unloading the Well

The unloading of the well is the process of making the well underbalanced. Prior to the unloading, the well is filled with liquid. The unloading process starts when the gas injection is initiated and ends at the time the gas reaches the choke at the top of annulus and the well has reached wanted steady state conditions. As the gas enters the wellbore, the BHP will increase until the well starts flowing. Now the gas will expand upwards the well displacing the liquid and creating a lower pressure profile upwards the wellbore. The gas expands upwards according to Boyles general gas law [37] due to the pressure experienced will decrease up the wellbore. At constant temperature this is shown as (4),

$$P_1 V_1 = P_2 V_2 \quad (4)$$

Where,

P_1 - Is the pressure at a reference point 1

V_1 - Volume occupied by the gas at reference point 1

P_2 - Is the pressure at a reference point 2

V_2 - Volume occupied by the gas at reference point 2

As the gas breaks through at the surface, the decrease in BHP will happen more rapidly until steady state conditions is reached. Throughout this process, both the frictional part and the hydrostatic part of equation (3) will be changing, giving a dynamic bottomhole pressure. This will be illustrated through simulations in part III, chapter 10.2.1.

7.2.2 Drill Pipe Connections

Drill pipe connections, in jointed pipe drilling, are considered to be the most critical factor regarding fluctuations in BHP. As stated in chapter 5.2.1, a disadvantage by using injection through the drill string is that the circulation of gasified fluid is shut down during each connection. This is making a change in the steady state conditions. As the circulation is stopped, the friction part, P_{fric}, of equation (3) will be removed or reduced. There will still be some friction force if the well continuous to produce during the connection. This drop in pressure may lead to increased production from the reservoir, as the differential pressure between the reservoir and wellbore is increased. This might be a problem, especially in horizontal wells, with a long production zone. Here the production rates of hydrocarbons may become so high that overbalanced conditions will

be seen when regaining circulation in the well after the connection has been made. This may potentially ruin the reservoir properties, as discussed in chapter 3.1.5. Figure (9) shows a plot of the BHP as a function of time, where two drill string connections are made. As seen in the figure, the BHP decreases at approximately 20 min and 90 min corresponding to the annular friction. Here the circulation is shut down and connection is being made. This pressure decrease might also damage the formation. The BHP might get lower than the formation collapse pressure, and the formation will be destabilized or start to collapse into the wellbore. This must be properly modeled before starting to drill the section.

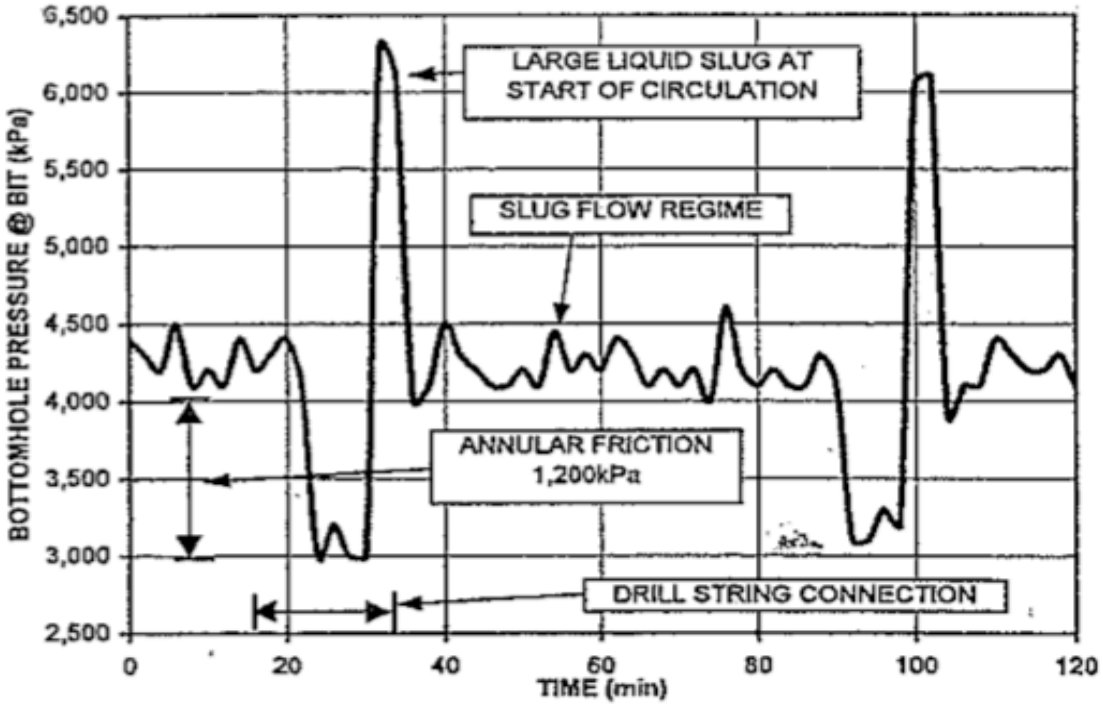

Figure (9) - BHP During Drill Pipe Connections [7]

Figure (9) describes another important incident, after the connection is made and circulation is started. At time equal to approximately 32 min and 100 min a sudden pressure spike occurs. What would be expected is that the BHP simply would increase equaling the annular friction from circulation. However, as the injection is shut down, the fluids start to separate both in the drill pipe and in the well due to gravity displacement. Liquid slugs are formed both in annulus and in the drill pipe that change the profiles of hydrostatic pressures in the well and drill pipe. There will be accumulation of liquid slugs in the lower parts of the well and drill pipe, while the gas tends to move upwards. As the circulation is re-established, the drill string will pump a

liquid slug into the well increasing the hydrostatic term in addition to the friction force. As a result, overbalanced conditions may appear at the bottom of the well. The liquid slug separation process is directly related to the time without injection and circulation [7]. This indicates that it is important to optimize connection operations and also make all shut downs as time efficient as possible.

During the connections, a decision whether annulus should be kept open or closed has to be made. This depends on the well and its capability to flow on its own. If the reservoir has enough energy to produce freely on its own, the annulus should be kept open to avoid high shut in pressures and thereby avoid big increases in BHP. However, if the reservoir has not got enough energy to produce on its own during a connection, or produce negligible volumes of liquid, the annulus should be kept closed during the connection. By doing this, the fluid separation process will be reduced as well as the annular gas phase energy is stored [7, 24].

7.3 Proposed Modeling Sequence

Part II of this thesis has up till now focused on the difficulties and importance of two-phase modeling in UBO. As stated in the introduction part of this chapter, multiphase flow simulation is a vital element in the initial engineering regarding design of circulation system, well controllability analysis, and equipment selection process for any underbalanced drilling operation. There is thus a need of software to be able to plan and execute these operations in a proper way. The SPT group [23] states on their website that they are the leader in flow modeling for the oil and gas industry. "*We have the leading dynamic and steady state flow simulators covering drilling, wells, pipelines and complex gas fields".* The SPT group offers two solutions for dynamic modeling of UBD, Drillbench and Wellflo. The simulators consists of both steady state and transient modules and is used for both planning, evaluation of executed drilling operations and for training of personell. For more information regarding Drillbench and Wellflo, the reader is encouraged to visit the SPT groups website [23]. Below is a proposed methodology for feasibility study with the use of an UBD multiphase flow simulator. The proposition is found in [8]

Step 1 – Model Annular Pressures and Velocities with no Influx

The first step is to model the annular pressures and velocities with the assumption of no influx from the formation. This is done to find the combination of liquid and gas that will

give the desired pressure drawdown across the reservoir section. By specifying the surface choke pressure and the rates of gas and liquid that will be injected, the annular pressures and velocity is modeled.

Step 2 – Determining the UBD Operating Window

The next step is to find the UBD operating boundaries. These boundaries are typically,

- Upper pressure boundary: Designed to be low enough to keep the well underbalanced also during situations that may cause pressure spikes, as discussed in chapter 7.2.
- Lower pressure boundary: The maximum pressure drawdown that is possible without risking hole collapse, too high return rates and water- gas coning.
- Lower fluid injection boundary: Typically found as minimum liquid velocity that gives adequate hole cleaning.
- Upper fluid injection boundary: Typically bound by maximum tolerance by motor.

Figure (10) below shows a suggested operational window, found in [8].

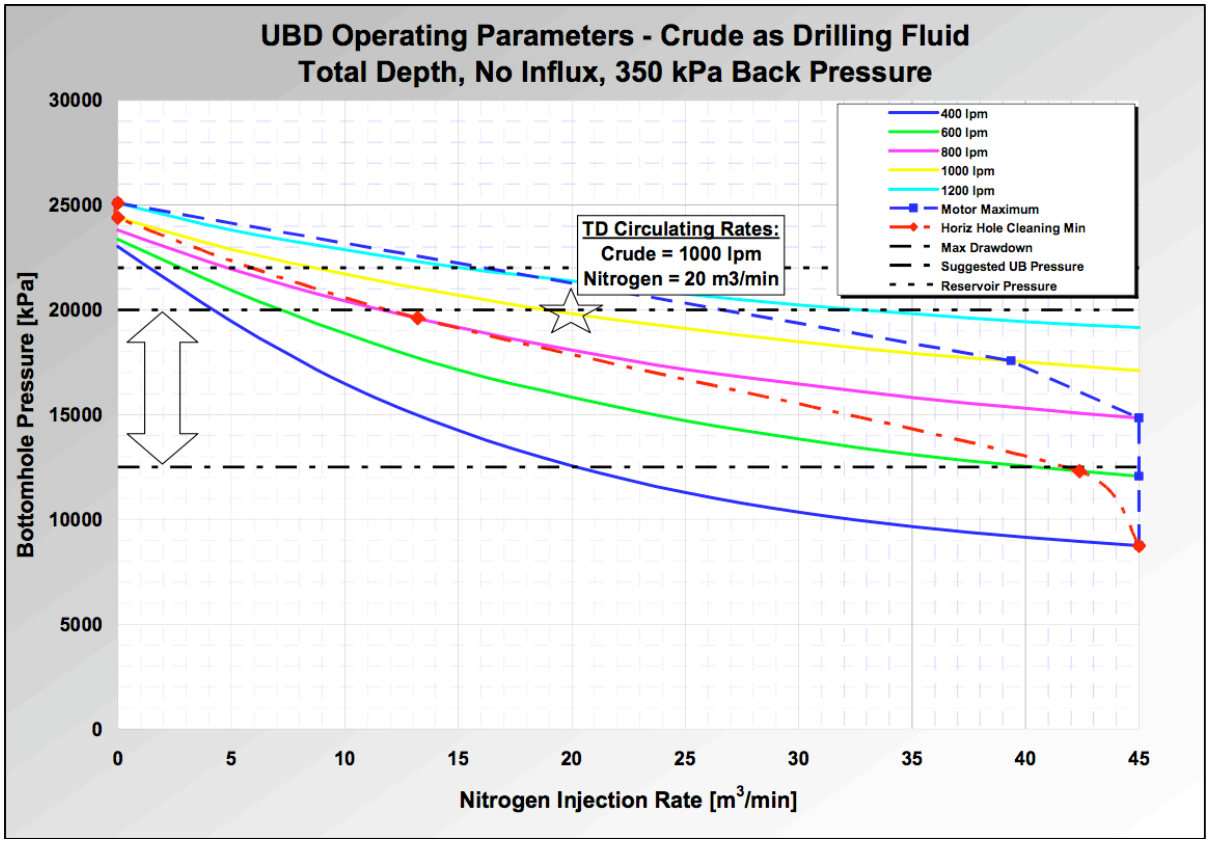

Figure (10) - Operational Window Presented in [8]

Step 3 – Modeling injection pressure and MWD operability

Step 3 in the modeling sequence is to calculate the injection pressures and the liquid volume through the motor that fits to step 1 and step 2. From this the gas volume fraction profile in the drill pipe is determined. This is of importance when it comes to check MWD operability, like stated in chapter 5.2.1. Figure (11) gives the MWD operability window; the boundary is set at 22% gas fraction, before MWD is not functional.

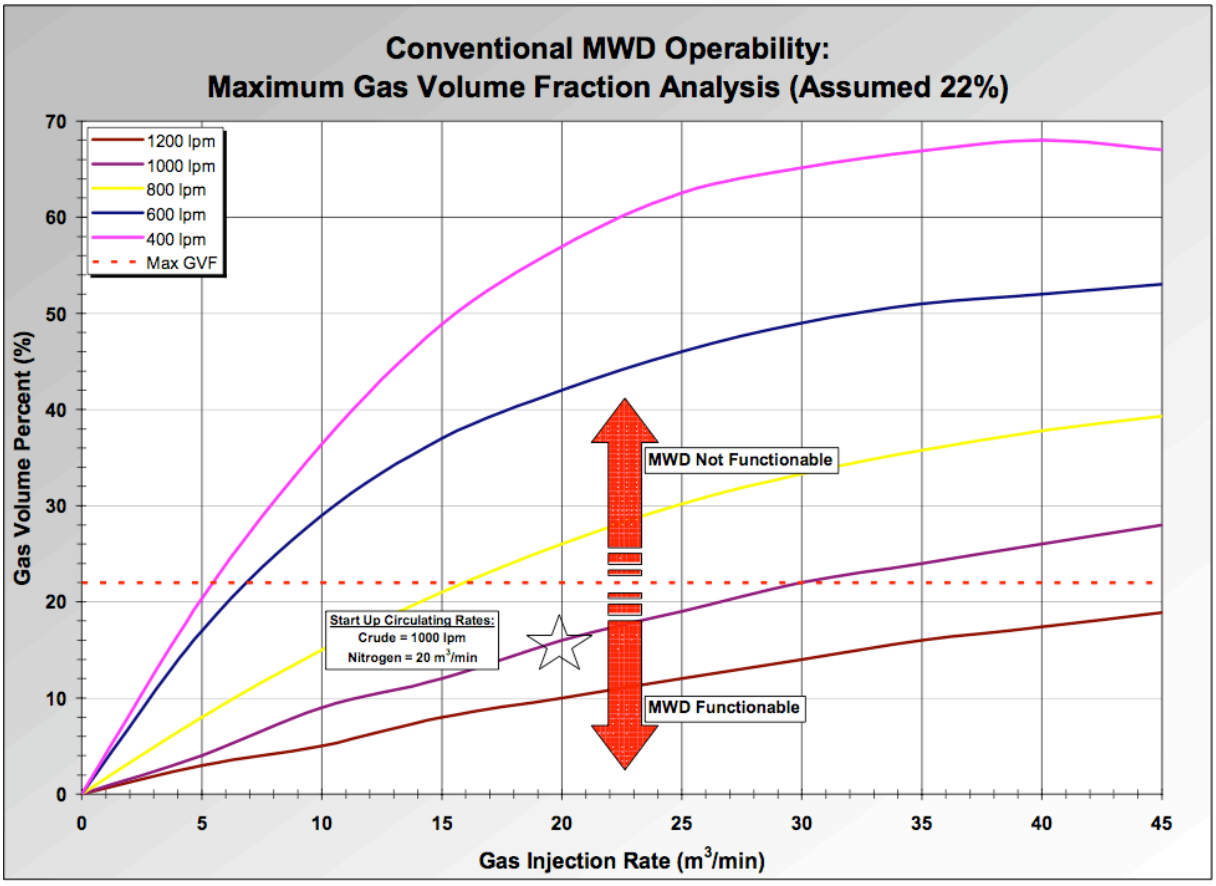

Figure (11) - MWD Operability Window [8]

Step 4 – Modeling with reservoir inflow

The next step is to do the modeling over again, also taking influx from reservoir into account and see how this impacts the operating window. The modeling must assure that underbalanced conditions are kept throughout the operation as well as the motor limits are not exceeded and that adequate hole cleaning is possible.

Step 5 – Well Controllability

Now the well controllability is analyzed. This is an analysis of how controllable the BHP is by varying the surface choke setting. It is important to know the relationship between them, and how to adjust the choke in certain parts of the operation.

Step 6 – Equipment specifications

The final step is to check that all equipment can handle the environment that is expected during the operation. If equipment is rated below the parameters found in step 1-5, the equipment needs to be changed, to ensure a safe and successful operation.

8 Multiphase Flow Parameters

To be able to predict what is happening in the wellbore during drilling operations it is important to be able to describe the multiphase flow and its parameters as precise as possible. This chapter will present some multiphase terms and parameters needed to better understand multiphase flow. See figure (12) for illustration.

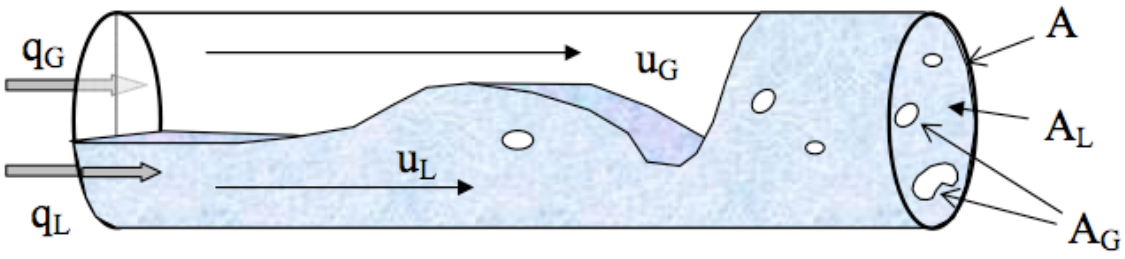

Figure (12) - Some parameters in two-phase flow in a pipe [11]

8.1 Superficial Velocity

The superficial velocity is the velocity of a phase if it was to flow through the entire cross sectional area of the pipe alone. The equations are as follows,

$$u_{SL} = \frac{q_L}{A} \quad (5)$$

and,

$$u_{SG} = \frac{q_G}{A} \quad (6)$$

Where, subscript L is liquid phase, subscript G is gas phase and,

u_S = Superficial velocity

q = Volumetric flow rate

A = Cross sectional area of pipe

8.2 Phase Velocities

The phase velocities are defined as the real velocity of the flowing phase and are given by following equations,

$$u_L = \frac{q_L}{A_L} \quad (7)$$

and,

$$u_G = \frac{q_G}{A_G} \quad (8)$$

Where, subscript L is liquid phase, subscript G is gas phase and,

u = Phase velocity

q = Volumetric flow rate

A_L = Cross section occupied by liquid phase

A_G = Cross section occupied by gas phase

8.3 Phase Fraction

The phase fraction is defined as the fraction of the pipe that is occupied by either liquid or gas. It may be averaged over flow area by following equations,

$$\alpha_L = \frac{A_L}{A} \quad (9)$$

and,

$$\alpha_G = \frac{A_G}{A} \quad (10)$$

Where, subscript L is liquid phase, subscript G is gas phase and,

α = Phase fraction

A_L = Cross section occupied by liquid phase

A_G = Cross section occupied by gas phase

A = Area

For two-phase liquid and gas flow it is therefore found that the two phase fractions sums up to one. This may be expressed as,

$\alpha_L + \alpha_G = 1 \quad (11)$

8.4 Densities as a Function of Pressure

The pressure profile of the well is affecting the densities of gas and liquid. This can be expressed as,

$$\rho_G = \frac{p}{a_G^2} \quad (12)$$

and,

$$\rho_L = \rho_{L,0} + \frac{p - p_{L,0}}{a_L^2} \quad (13)$$

Where, subscript G is liquid phase, subscript L is gas phase and,

ρ = Density as a function of pressure

p = Common pressure

a = Velocity of sound in medium

ρ_0 = Reference density at a given reference pressure

p_0 = Reference pressure

8.5 Mixture Properties

8.5.1 Mixture Velocity

The mixture velocity is given by following equation,

$$u_{mix} = \alpha_L u_L + \alpha_G u_G \quad (14)$$

Where,

u_{mix} = The mixture velocity

8.5.2 Mixture Viscosity

The mixture viscosity is given by following equation,

$$\mu_{mix} = \alpha_L \mu_L + \alpha_G \mu_G \quad (15)$$

Where,

μ_{mix} = Viscosity of mixture

μ_L = Viscosity of liquid

μ_G = Viscosity of gas

8.5.3 Mixture Density

The mixture density is given by following equation,

$$\rho_{mix} = \alpha_L \rho_L + \alpha_G \rho_G \quad (16)$$

Where,

ρ_{mix} = Density of mixture

ρ_L = Density of liquid

ρ_G = Density of gas

8.5.4 The Mixture Reynolds Number

The Reynolds number is a dimensionless number that gives a measure of the ratio of inertial forces to viscous forces. The Reynolds number is often used to discriminate between laminar and turbulent flow in pipelines, and are also part of some friction factors. The equation for determining the mixture Reynolds number,

$$Re_{mix} = \frac{\rho_{mix} u_{mix} d}{\mu_{mix}} \quad (17)$$

Where,

Re_{mix} = Reynolds number for mixture

d = Diameter of flow path

8.6 Slip Flow

Slip flow occurs when the liquid and gas phases travels at different velocities. The general slip law [29] that will be used in this thesis can be expressed as equation (18),

$$u_G = C_0 u_{mix} + C_1 \quad (18)$$

Where,

u_G = Is the gas flow velocity

C_0 = Is the profile parameter (distribution coefficient)

u_{mix} = Is the mixture velocity

C_1 = Drift velocity of the gas

The general slip relation [29] describes the slip between liquid and gas as a combination of two mechanisms, which results in the parameters C_0 and C_1. This is shown in figure (13), on the next page.

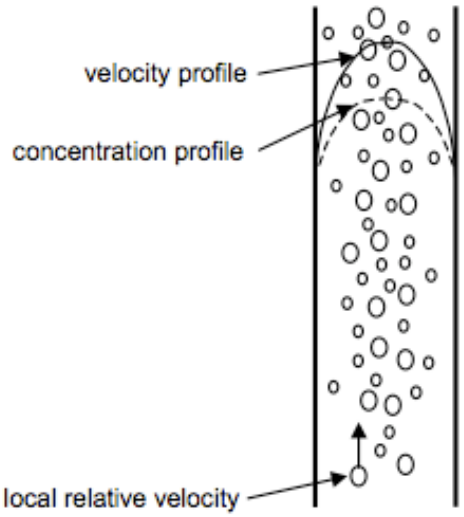

Figure (13) - Velocity profile for mixture and Concentration profile for gas [30].

As seen in figure (13), both the concentration of gas and the velocity of the mixture in a vertical pipe are highest in the center of the pipe. This indicates that the velocity of the gas, on average, is higher than the liquid and this is what parameter C_0 is describing in the equation. When it comes to the second mechanism, the C_1 parameter, this is indicating the buoyancy effect that gas will experience in the wellbore. The gas will get a higher velocity due to being a lighter fluid. The two constants C_0 and C_1 will vary in value, depending on which flow pattern that exists in the two-phase flow. This will be further discussed in part III of the thesis.

8.7 Two Phase Flow Patterns in Vertical Flow

One of the reasons for two phase flow is much more complicated to describe and understand compared to single-phase flow due to the many different flow patterns that may exists in two phase flow. Single-phase flow usually just gets discriminated between laminar and turbulent flow regimes[11]. Whereas for the two-phase flow case, the flow gets discriminated between flow regimes that are characteristic for the time and space distribution of gas and liquid flow [11, 13]. Fluid distribution will change greatly in different flow regimes, which again will affect the pressure gradient, both inside the and outside the drill pipe. Two-phase flow regimes are depending on flow rates and amount of the different phases, wellbore geometry, and the fluid properties of the phases, this will be addressed for the bubble- to slug flow transition in chapter 11, part III. Variation in wellbore pressure and temperature may also change the flow pattern. Flow patterns

expected in two-phase flow in a vertical well are bubble flow, dispersed bubble flow, slug flow, churn flow and annular flow [12] and they are shown in figure (14).

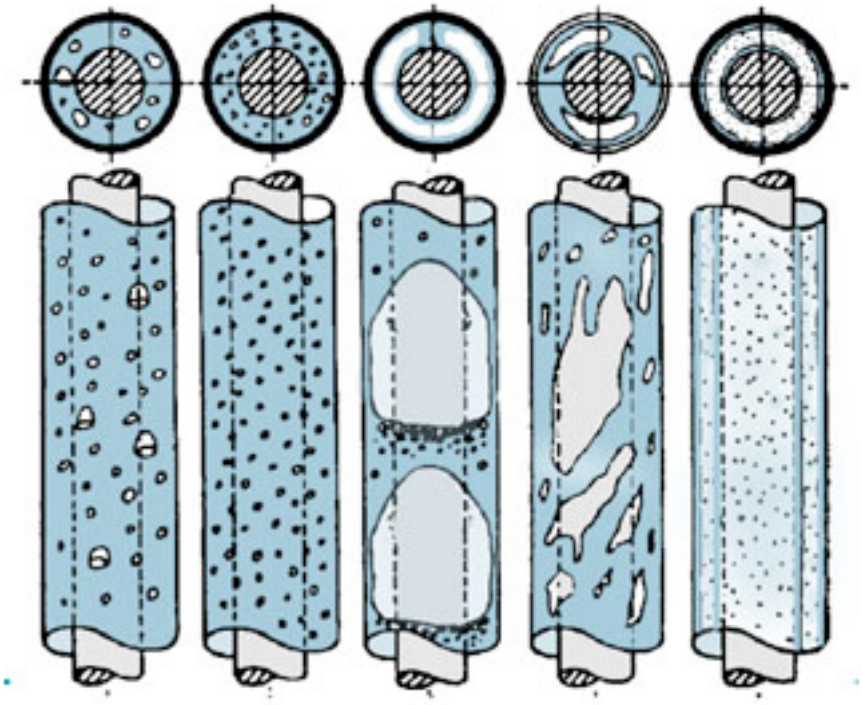

Figure (14) - Flow Patterns in a Vertical Well [38]

8.7.1 Bubble Flow

The bubble flow is characterized by discrete gas bubbles distributed in a continuous liquid phase. The shape and size of the bubbles will differ within the flow. There will be slippage between the two phases due to buoyancy forces [12]; the effect of this will be discussed further in chapter 11.2.1. Bubble flow will typically occur at low to medium superficial velocities and low fractions of gas, at higher velocities the bubbles will break up into smaller bubbles creating the dispersed bubble flow. At higher gas fractions the bubbles will typically collide and form bigger bubble slugs. A simple boundary between bubble flow and slug flow is presented in chapter 11.1.

8.7.2 Dispersed Bubble Flow

The dispersed bubble flow is characterized by small discrete gas bubbles being homogeneous distributed in the continuous liquid phase [18]. This is the only flow pattern where no slippage between the phases can be assumed [11], as the flow essentially is homogeneous. This flow pattern is common when having a two-phase flow with low fractions of gas. The reason for that is that in low velocity flows, with high

fractions of gas, the gas bubbles collide and form bigger bubble slugs, as with the case of bubble flow. However, as flow velocity increases, turbulent flow conditions tend to break up these big bubble slugs into smaller bubbles again.

8.7.3 Slug Flow

In slug flow, the gas bubbles grows together into larger bubbles that eventually will fill the entire pipe cross section [13]. In vertical flow these gas pockets are known as Taylor bubbles, and surrounding these Taylor bubbles are a film of liquid that is forced downwards relative to the gas bubble [18]. The Taylor bubbles moves upwards with a lower velocity than the dispersed bubbles. Between the large bullet-shaped gas bubbles are liquid slugs that contains smaller gas bubbles. These smaller bubbles will catch up with the Taylor bubble, collide and melt into it. Slug flow is typical for two-phase flow with high gas fractions and/or low velocities.

8.7.4 Churn Flow

As the flow velocity increases, the bubble slugs tend to collapse creating a chaotic turbulent flow with both phases dispersed [13]. Churn flow is characterized by an alternating direction of the flow of the liquid phase [18].

8.7.5 Annular Flow

As gas velocity and amount of gas increases further, the liquid will be pushed into the pipe wall. Now, the gas is the continuous phase in the core of the pipe or annulus cross-section area. The liquid is flowing upwards as a thin film along the wellbore, and as dispersed droplets in the gas phase in the core of the pipe. Annular flow will in general exist at flows experiencing high gas superficial velocities and relatively low liquid fractions [12].

9 Description of The Drift-Flux Model

The main goal for this thesis is to extend a drift-flux model to be able to better predict transient flow scenarios found in UBO. Dr. Steinar Evje developed the drift-flux model that is used in this thesis in MATLAB. For information regarding the build up of this drift-flux model, reference [39] is given. However, some modifications have been done. This drift-flux model will from now on be referred to as the original model, or the slug flow model. It consists of two conservation equations for mass, one for each phase, and one combined conservation equation for momentum using mixed fluid properties. This puts the drift-flux model into the category of homogeneous models. The model does include slip between the phases by utilizing the general slip law [29], it does however only recognize the slug region. Drift-flux models are known to be well suited to be used for simulations, as they are quite simple, continuous and differentiable [30]. The model uses a set of three conservation laws combined with a set of closure laws to describe the flow. The soluble equation system is then solved numerical; this will be further discussed in this chapter. It is important to understand that the model will not describe the real nature of the two-phase flow system, as the system is considered to be isothermal and also there is an assumption of no mass exchange between the phases.

9.1 A set of conservation laws

Three conservation laws are what in general make up the drift-flux model. With the assumption of an isothermal system without any mass transfer between the phases the drift-flux model will be made up by two mass conservation equation, one for each phase, and one combined momentum conservation equation.

9.1.1 Conservation of Mass

The conservation of mass criteria states that mass is to be preserved. The net change in mass within a given control volume, for a single-phase fluid system, equals to the mass added or subtracted from the control volume. The conservation of mass equations for the two phases are given by,

$$\partial_t(\alpha_G \rho_G) + \partial_x(\alpha_G \rho_G u_G) = q_G \quad (19)$$

and,

$$\partial_t(\alpha_L \rho_L) + \partial_x(\alpha_L \rho_L u_L) = q_L \quad (20)$$

Where subscript G is gas phase, subscript L is liquid phase and,

α = Phase fraction

ρ = Fluid density

u = Phase velocity

q = Source or sink term

For this model,

$$q_G = q_L = 0 \quad (21)$$

There will be assumed no mass transfer between the phases, or production of oil or gas, giving the mass balance equations the form,

$$\partial_t(\alpha_G \rho_G) + \partial_x(\alpha_G \rho_G u_G) = 0 \quad (22)$$

and,

$$\partial_t(\alpha_L \rho_L) + \partial_x(\alpha_L \rho_L u_L) = 0 \quad (23)$$

9.1.2 Conservation of Momentum

The conservation of momentum criteria states that net change in momentum within a control volume equals to the sum of volume and surface forces acted on the control volume. The conservation of momentum equation is based on Newton´s second law of motion on a fluid element and is combined for the two phases,

$$\partial_t(\alpha_G \rho_G u_G + \alpha_L \rho_L u_L) + \partial_x(\alpha_G \rho_G u_G^2 + \alpha_L \rho_L u_L^2) + \partial_x p = -q \quad (24)$$

Where subscript G is gas phase, subscript L is liquid phase and,

α = Phase fraction

ρ = Fluid density

u = Phase velocity

p = Common pressure

q = Source term related to gravity and friction

The source term in equation (21) is the sum of viscous and frictional forces, and the gravitational forces,

$$q = q_{friction} + q_{gravity} \quad (25)$$

$q_{friction}$ and $q_{gravity}$ will be presented in 9.2.2 and 9.2.3.

9.2 Closure Laws

There are now seven unknown variables in the three conservation equations.

α_G	α_L	ρ_G	ρ_L	p	u_G	u_L

To get a soluble system, a set of closure laws is needed;

9.2.1 The Relation of Fractions

Equation (11) gives the relation of volume fractions.

9.2.2 The Frictional Model

The viscous forces and the friction forces between the wall and the fluids are taken into account through the frictional force term, $q_{friction}$. The friction force is found through [33],

$$q_{friction} = \frac{2f}{(d_o - d_i)} \rho_{mix} u_{mix} |u_{mix}| \quad (26)$$

Where,

$q_{friction}$	= Represents the viscous forces and the frictional forces
d_o	= The inside diameter of the annulus
d_i	= The outside diameter of the drill pipe
f	= Friction factor
ρ_{mix}	= Mixed density, as defined in equation (16)
u_{mix}	= Mixed velocity, as defined in equation (14)

The friction factor is depending on the state of the flow, if it is turbulent or laminar flow. This is done by calculating the mixture Reynolds number and comparing this to specific transition boundaries. The mixture Reynolds number is found through equation (17).

For $Re_{mix} \geq 3000$, turbulent flow is recognized and following equation will be used,

$$f_{turb.} = 0.052 \times Re_{mix}^{-0.19} \quad (27)$$

For $Re_{mix} < 2000$, laminar flow is recognized and following equation will be used,

$$f_{lam.} = \frac{24}{Re_{mix}} \quad (28)$$

For $2000 < Re_{mix} < 3000$, a transition zone between laminar and turbulent flow is found, giving a interpolated friction factor by following formula,

$$f_{trans.} = \left(1 - \frac{Re_{mix} - 2000}{1000}\right) \times f_{lam.} + \frac{Re_{mix} - 2000}{1000} \times f_{turb.} \quad (29)$$

9.2.3 The Gravitational Model

The gravitational part of the source term, $q_{gravity}$, has the form,

$$q_{gravity} = \rho_{mix} g \cos\theta \quad (30)$$

Where,

$q_{gravity}$ = Represents the gravitational forces acting on the fluid.

ρ_{mix} = Mixture density, as defined by equation (16)

g = Gravitational constant

θ = Inclination relative to vertical direction

9.2.4 Density Models

Equation (12) and (13) gives the density of gas and liquid as a function of pressure.

9.2.5 The Slip Law Model

As mentioned, the original drift-flux model utilized in this thesis only recognizes the slug flow regime. The slip term used for this model is found in [33], and can be expressed as,

$$u_G = 1.2 \times u_{mix} + 0.35\sqrt{g \times (d_o + d_i)} \quad (31)$$

Where,

u_G = The gas flow velocity

u_{mix} = The mixture velocity

g = The gravitational constant

d_o = The inside diameter of the casing

d_i = The outside diameter of the drill pipe

To simplify the equation,

$$C_{0,S} = 1.2 \quad (32)$$

$$C_{1,S} = 0.35\sqrt{g \times (d_o + d_i)} \quad (33)$$

Where subscript S represents that the parameter is for slug flow.

Giving the equation the form in equation (18),

$$u_G = C_{0,S} u_{mix} + C_{1,S} \quad (34)$$

However, the model has implemented a special case for high gas fractions. In this way no slip will be included as the fluid enters one-phase gas flow. For $0.75 < \alpha_G \leq 1$, slip parameters become as follows,

$$C_0 = \frac{\alpha_G - 0.75}{0.25} C_{0,NS} + \left(1 - \frac{\alpha_G - 0.75}{0.25}\right) C_{0,S} \quad (35)$$

and

$$C_1 = \frac{\alpha_G - 0.75}{0.25} C_{1,NS} + \left(1 - \frac{\alpha_G - 0.75}{0.25}\right) C_{1,S} \quad (36)$$

Where,

$$C_{0,NS} = 1.0 \; and \; C_{1,NS} = 0$$

Subscript NS represents the no slip case. As seen here, when gas fractions reach 1, the system will be experiencing no slip, as the gas is the only flowing phase.

Now there are seven unknown variables and seven different equations, making it a soluble system.

9.3 Discretization of Conservation Equations

To be able to calculate the variables at different positions in the well with time, a space- and time grid must be applied. The conservation equations then have to be related to the grid, by discretization, to be able to solve them. The discrete equations can then be solved implicit or explicit. Implicit solutions are based on "new" values, while explicit solutions are based on the "old" values. For this MATLAB drift-flux model, the explicit method is used. A simple explicit discretization of the conservation equation will be presented below. First, the set of conservation law equations that are making up the drift-flux model, (19), (20) and (21) can also be written as,

$$\partial_t U + \partial_x f(U) = q \quad (37)$$

Where,

$$U = \begin{pmatrix} \alpha_G \rho_G \\ \alpha_L \rho_L \\ \alpha_G \rho_G u_G + \alpha_L \rho_L u_L \end{pmatrix} = \begin{pmatrix} U_1 \\ U_2 \\ U_3 \end{pmatrix}$$

$$f(U) = \begin{pmatrix} \alpha_G \rho_G u_G \\ \alpha_L \rho_L u_L \\ \alpha_G \rho_G u_G^2 + \alpha_L \rho_L u_L^2 + p \end{pmatrix}$$

$$q = \begin{pmatrix} 0 \\ 0 \\ -q_{friction} - q_{gravity} \end{pmatrix}$$

A space- and time grid must be applied to give the opportunity to and a discretization of (37) is made to relate them together. An illustration of the grid is given in figure (15) on the next page.

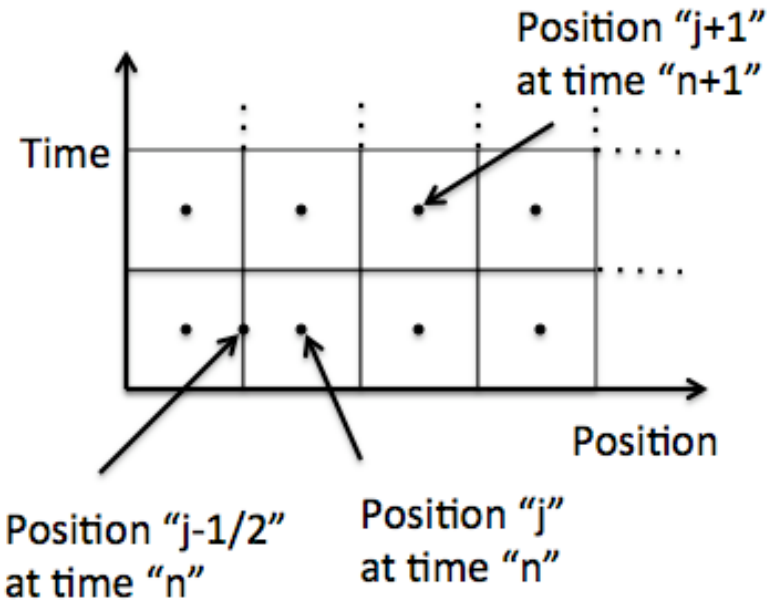

Figure (15) - Illustration of the Time- and Space Grid Used in Matlab. Drawn in Power Point.

As seen in figure (15), the position moves along the x-axis, each box center is a whole step, while the box edges indicates half steps. For the drift-flux model, the calculations are performed in the box center. The time steps are indicated along the y-axis.

An explicit discretization of equation (37) is performed below; here it is visual that the equation becomes related to the time and space grid. First, the time dependent part of the equation is related to the time grid in equation (38),

$$\partial_t U = \frac{U_j^{n+1} - U_j^n}{\Delta t} \quad (38)$$

Where,

$\partial_t U$ = The time derivate of U

Δt = $t^{n+1} - t^n, n+1 = new\ time, n = old\ time$

U_j^{n+1} =Value of U at position j, and time step $n+1$

U_j^n = Value of U at position j, and time step n

The flux vector, $f(U)$, is position dependent, as it is related to the position grid it becomes,

$$\partial_x f(U) = \frac{1}{\Delta x}\left(f^n_{j+1/2} - f^n_{j-1/2}\right) \quad (39)$$

Where,

$\partial_x f(U)$ = The position derivate of $f(U)$

Δx = $x_{j+1/2} - x_{j-1/2}$, position at both box edges

$f^n_{j+1/2}$ = The flux term at position $j + 1/2$, and time step n

$f^n_{j-1/2}$ = The flux term at position $j - 1/2$, and time step n

The source/sink term, q, is integrated to the time- and space grid by,

$$q = q_j^n \quad (40)$$

Now, by inserting these new expressions into equation (37),

$$\frac{U_j^{n+1} - U_j^n}{\Delta t} + \frac{1}{\Delta x}\left(f^n_{j+1/2} - f^n_{j-1/2}\right) = q_j^n \quad (41)$$

And, by solving with respect to the value for the new time step, $n + 1$,

$$U_j^{n+1} = U_j^n + \frac{\Delta t}{\Delta x}\left(f^n_{j-1/2} - f^n_{j+1/2}\right) + q_j^n \Delta t \quad (42)$$

An explicit discretization of equation (37) has been performed.

9.4 Calculation of Variables

To be able to get an updated U_j for the new time step, $n + 1$, both U_j^n and the flux term f^n needs to be determined. U_j^n is known through initial conditions, while f^n is not. To calculate f^n, the variables presented in chapter 9.2 needs to be determined for time step n. Recall that $U_1 = \alpha_G \rho_G$, $U_2 = \alpha_L \rho_L$ and the relation of fraction $\propto_L + \propto_G = 1$, giving following equation,

$$\frac{U_1}{\rho_G} + \frac{U_2}{\rho_l} = 1 \quad (43)$$

Combining this with the density models presented in 8.4, equation (12) and (13), are giving,

$$\frac{U_1 a_G^2}{p} + \frac{U_2}{\rho_{L,0} + \dfrac{p - p_{L,0}}{a_L^2}} = 1 \quad (44)$$

By rearranging this equation with respect to pressure, p, a second order polynomial as follows,

$$p^2 + Bp + C = 0 \quad (45)$$

Where A and B is defined as,

$$B = a_L^2 \left(p_{L,0} - \frac{p_{L,0}}{a_L^2} - U_2 - \left(\frac{a_G}{a_L}\right)^2 U_1 \right) \quad (46)$$

$$C = U_1 (a_G a_L)^2 \left(\frac{p_{L,0}}{a_L^2} - p_{L,0} \right) \quad (47)$$

The equation can be solved by,

$$p(U_1, U_2) = \frac{-B \pm \sqrt{B^2 - 4C}}{2} \quad (48)$$

Only the positive solution is a real solution, as there cannot be a negative pressure. After the pressure is determined the densities are calculated from equation (12) and (13).

The volume fractions are calculated by,

$$\alpha_G = \frac{U_1}{\rho_G} \quad (49)$$

and,

$$\alpha_L = \frac{U_2}{\rho_L} \quad (50)$$

At last the phase velocities are determined. From definition of U_3 from equation (37)

$$\alpha_G \rho_G u_G + \alpha_L \rho_L u_L = U_3$$

Substituting in U_1 and U_2,

$$U_1 u_G + U_2 u_L = U_3 \quad (51)$$

By using the definition of the slip formulation in equation (18) and the definition of the mixed velocity (14),

$$C_1 = -C_0 \alpha_L u_L + (1 - C_0 \alpha_G) u_G \quad (52)$$

Combining equation (51) and (52) gives a soluble system of two equations and two unknowns,

$$u_L = \frac{U_3 (1 - C_0 \alpha_G) - U_1 C_1}{U_2 (1 - C_0 \alpha_G) + U_1 C_0 \alpha_L} \quad (53)$$

and

$$u_G = \frac{U_2 C_1 + U_3 C_0 \alpha_L}{U_2 (1 - C_0 \alpha_G) + U_1 C_0 \alpha_L} \quad (54)$$

9.5 Flux Splitting and the AUSMV Scheme

The flux term, $f(U)$, given in equation (37) is divided into a convective and a pressure term, giving,

$$f(U) = f(U)_C + f(U)_p = \begin{pmatrix} \alpha_G \rho_G u_G \\ \alpha_L \rho_L u_L \\ \alpha_G \rho_G u_G^2 + \alpha_L \rho_L u_L^2 \end{pmatrix} + \begin{pmatrix} 0 \\ 0 \\ p \end{pmatrix} \quad (55)$$

Here, subscript C is for the convective term and p for the pressure term.
The convective part of equation (55) is then split into one part for gas phase and one part for the liquid phase in equation (56), subscript G is for gas phase while L represents liquid phase.

$$f(U)_C = f(U)_{C,G} + f(U)_{C,L} = \alpha_G \rho_G u_G \begin{pmatrix} 1 \\ 0 \\ u_G \end{pmatrix} + \alpha_L \rho_L u_L \begin{pmatrix} 0 \\ 1 \\ u_L \end{pmatrix} \quad (56)$$

There are different ways for handling the flux splitting at the interface between boxes, giving different numerical schemes for analyzing the two-phased flow. For this drift-flux model generated in matlab, the AUSMV (Advection Upstream Splitting Method) scheme is used. This is a modified version of the AUSM scheme that was introduced by Liou and Steffen, which is based on the FVS (Flux Vector Splitting) scheme. For a more thoroughly review of the theory behind the numerical splitting schemes and why the AUSMV scheme is to be preferred in this drift-flux model, the reader is encouraged to read the work done by Dr. Steinar Evje and Dr. Kjell Kåre Fjelde [40] and Molvik [39].

Part III Simulations and Extensions to the Drift-Flux Model

The final part of the thesis will be used to perform simulations with the drift-flux model presented in chapter 9. The simulations will all be of a base case, which will be presented in chapter 10. These simulations are performed using the original matlab code, as described in chapter 9. In chapter 11 some extensions will be made to the model. The modifications will take the homogeneous approach used in the original model a step towards a mechanistic approach. First, there is a need of a way to predict the existing flow pattern, as the original model only recognize the slug flow region. The model will then be able to recognize two different flow patterns, bubble flow and slug flow. Different values for the slip flow variables C_0 and C_1, remember the slip law presented in chapter 9.2.5, will be used, depending on the flow pattern recognized. Then, chapter 12 will be presenting simulations with the new model. The simulations will be compared to the original model.

10 The Base Case

In this chapter the base case will be presented. The scenario, which is going to be simulated, will be reviewed and the most important results will be investigated. The simulation will be performed by the original drift-flux model, which was presented in chapter 9. The results from the base case will be used for comparison with the extensions made to the model in chapter 11. The plots gained from the simulations will also be used to describe the transient behavior of the BHP, as discussed in chapter 7.2.

10.1 Simulation Scenario

The scenario that will be simulated with the drift-flux model is the unloading of a well prior to drilling of the reservoir section. As steady state flow conditions are achieved, after the unloading process, a simulation of a drill pipe connection will be made. Results gained from the simulation consist of several plots, which will be used to give an understanding of the different scenarios.

10.1.1 Description of the Well

The simulation well is a vertical well reaching 2000 m TVD, drilled using jointed pipe drilling with a surface drilling BOP, see typical well rig up schematics in figure (4) in chapter 4. From now on the reservoir section follows, and it is chosen to drill underbalanced. The annulus in the well consists of a $9\,^5/_8\,''$ casing and a $5''$ drill pipe. Inner diameter of the casing string is set to be $8.535''$. For simplicity reasons, the annulus diameter is considered to be constant throughout the well, neglecting the BHA section. To achieve underbalanced conditions, gasified fluid drilling is chosen; see chapter 5.1.5, where a mixture of water and air is chosen as fluids. The injection is through the $5''$ drill pipe, see chapter 5.2.1, and the annulus is kept fully open throughout the simulation, there will be no manipulation of the choke. To keep it as simple as possible there will be no production of reservoir fluids or formation cuttings during the simulation. The gas and liquid will also be mixed at the bottom of the well, the downward flow through the drill pipe will not be considered.

10.1.2 Parameters Used

The well is divided into 25 boxes, each one with a length of 80 m TVD. The calculations shown in 9.3 will be performed in these boxes. The simulation runs through 3000 seconds. Mass rates used are shown in table (2), where the label “During circulation” are

when full circulation is reached, and "During shutdown" is when the circulation stops. The startup and shut down of circulation will be performed with linearly increase and decrease over a timeline of 10 seconds. The reason for using a linear increase/decrease in start ups and shut downs of circulations is because sudden changes may induce excessive pressure pulses.

Table (2) - Mass Rates Used in th Base Case

Event	Gas (kg/s)	Liquid (kg/s)
During circulation	2.0	22.0
During shutdown	0.0	0.0

Other input to the model are shown in table (3) below,

Table (3) - Parameter values used by the drift-flux model

Parameter	Value
$p_{L,0}$	$10^5 Pa$
$\rho_{L,0}$	$1000\ {}^{kg}/_{m^3}$
a_L	$1000\ {}^{m}/_{s}$
a_G	$316\ {}^{m}/_{s}$
μ_G	$0.000005\ Pa \cdot s$
μ_L	$0.05\ Pa \cdot s$
g	$9.81\ {}^{m}/_{s^2}$
d_o	$0.2168\ m$
d_i	$0.127\ m$
C_0	1.2
C_1	0.64

The definitions and equations for the different parameters presented in table (3) are shown in chapter 8. Also remember the flow pattern recognized by the model is limited to slug flow, for description of flow patterns see chapter 8.7.

10.1.3 Timeline

As stated above, the total time of the simulation run is 3000 seconds. During this time, different scenarios are modeled. Table (4) gives an overview over the timeline of the simulation.

Table (4) - Timeline of the Simulation

Time (in seconds)	Event	Method
0-100	Making the well vertical.	Linearly increasing the gravitational constant.
150-160	Start circulation of well. (Unloading)	Linearly increasing the flow rates of gas and liquids at inlet.
160-1700	Constant flow rates of gas and liquid.	Keeping flow rates of gas and liquid constant.
1700-1710	Start making a drill pipe connection.	Linearly decrease the flow rates of gas and liquid at inlet.
1710-2000	Drill pipe connection, no circulation.	Keeping the flow rates of gas and liquid at zero.
2000-2010	Drill pipe connection performed.	Start circulation by linearly increase the flow rates and liquid at inlet.
2010-3000	Well is circulating again at constant flow rates of gas and liquid, achieving steady state conditions again.	Keeping the flow rates of gas and liquid at inlet constant.

At time equal to zero the pressures and densities are initialized at standard conditions with the gravity constant set to be zero. Due to the no existing gravity constant, the well is basically horizontal at this stage. To make it vertical, the gravity constant is linearly increased from 0 to 9.81 m/s^2 during a time step of 100 seconds. This corresponds to hoisting the well from a horizontal position to a wanted vertical position. The BHP should now be equal to the hydrostatic pressure, given by equation (1) in chapter 1.2. The pressure profile is given in figure (16). A general comment to the figures with depth as y-axis is that the depth starts at 40 and ends at 1960, this is due to the fact that the calculations are performed in the center of the box, see chapter 9.3.

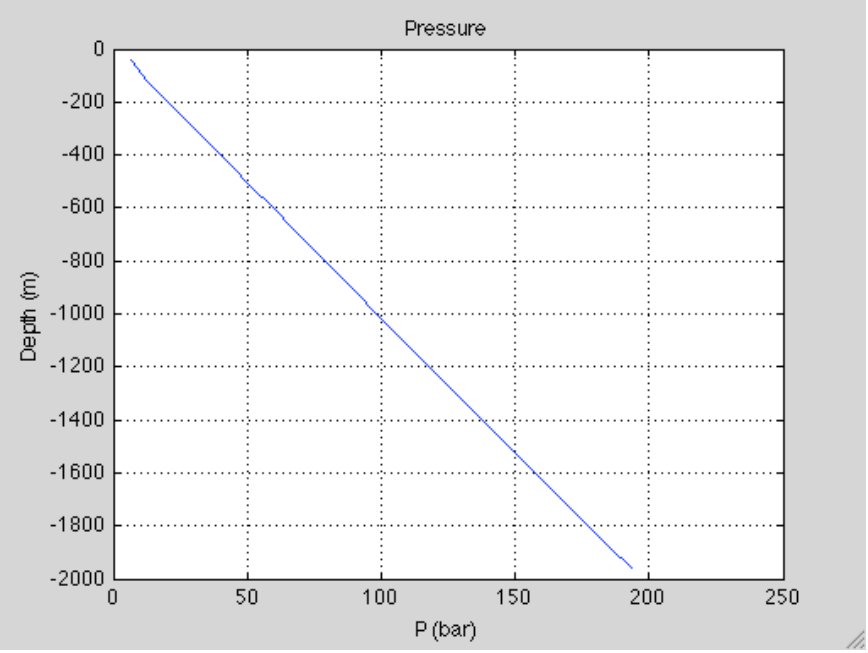

Figure (16) Pressure Profile of the Well at Initial Conditions

The next 50 seconds, nothing happens. The circulation of the well starts at 150 seconds and the initiating process is over after 10 seconds. From 160 seconds to 1700 seconds the well is circulating at constant mass rates. After 1700 seconds the drilling crew have to perform a drill pipe connection. The well stops the circulation over a time period of 10 seconds. The drill pipe connection is performed from 1710 seconds to 2000 seconds, and at this point the circulation is gradually increased over a time period of 10 seconds. From 2010 seconds until the end of the simulation at 3000 seconds the well is circulating at constant mass rates again. Table (2) above shows the mass rates used.

10.2 Simulation

The important processes, which will be further investigated, are the unloading sequence starting at time equal to 150 seconds and the drill pipe connection that will be made at time equal to 1700 seconds. These two scenarios are described in chapter 7.2.1 and 7.2.2, where the dynamic pressure is addressed, and the results of the simulation will be described below. Three plots from the simulation will first be presented, and these will help describe the different scenarios. Figure (17) shows the pressure as a function of time during the whole simulation run. The red line represents the pressure found at the choke, while the blue line represents the BHP.

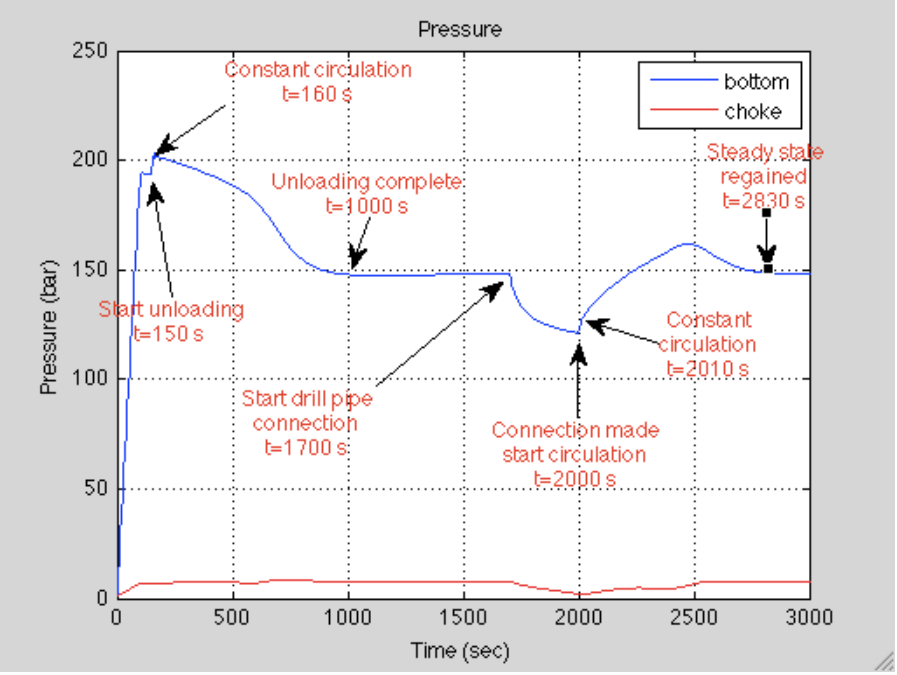

Figure (17) -Pressure as a Function of Time

Table (5) below gives an overview over important scenarios and corresponding values of the BHP during the simulation. The difference values, in the parentheses in the "Pressure Peak" event, gives the pressure difference with respect to the BHP at time equals 1700 seconds. All other differences are from the previous event.

Table (5) - Overview Slug Flow Model

Event	Time [s]	BHP [bar]	Difference [bar]	Difference [%]
Start Unloading	150	194	-	-
Constant Circulation	160	203.5	+9.5	+4.9
Unloading Complete	1000	147.8	-55.7	-27.4
Start DP Connection	1700	148	+0.2	+0.14
Regain Circulation	2000	121	-27	-14.2
Pressure Peak	2480	161.8	+40.8 (+13.8)	+33.7 (+9.32)

Figure (18) and (19) below illustrates the liquid mass rates and the gas mas rates as a function of time. Like in figure (17), the red line represents the choke, while the blue line represents the bottomhole.

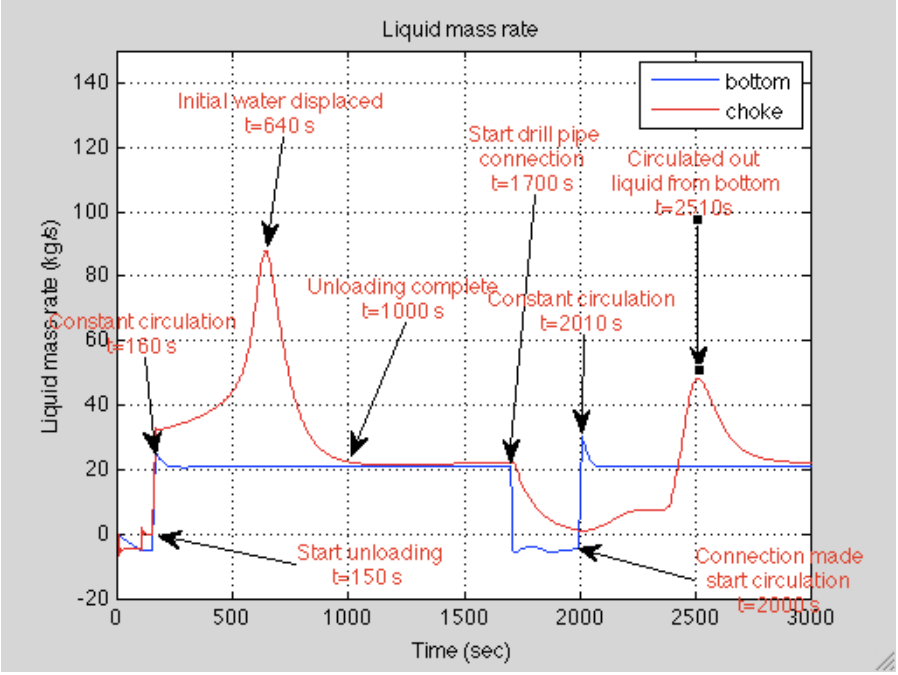

Figure (18) Liquid Mass Rate as Function of Time

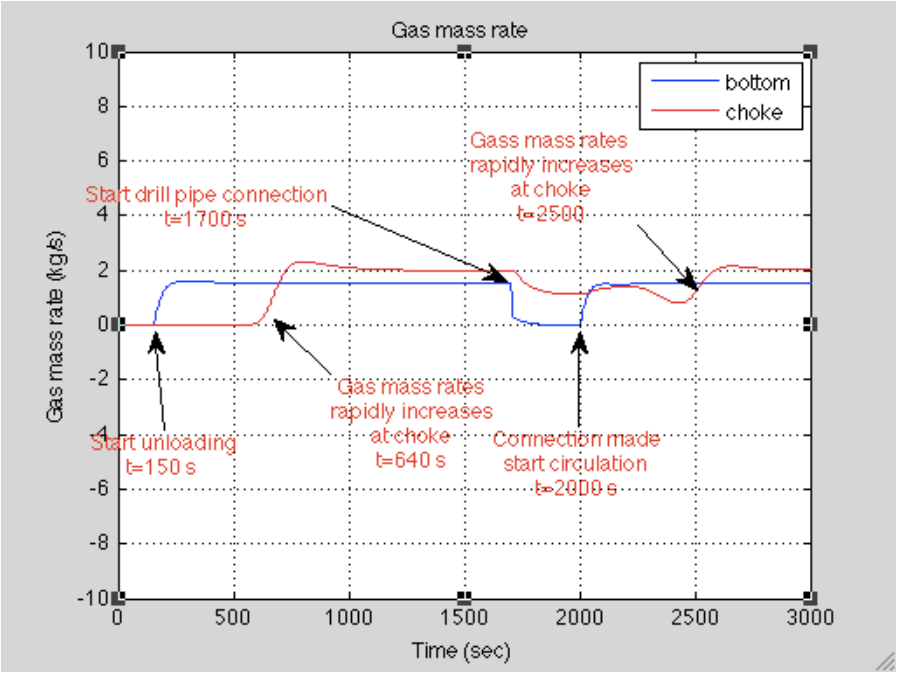

Figure (19) Gass Mass Rate as Function of Time

10.2.1 Unloading of the well

As figures (17), (18) and (19) illustrates, the unloading scenario starts at time equals 150 seconds. The gas and liquid rates are linearly increased up to values showed in table (2) over a time of 10 seconds. From here of there will be constant circulation until the drill pipe connection at time equal 1700 seconds. Prior to the unloading process, the well is filled with water. This is circulated out with a mixture of air and water, creating a

lower pressure profile. The unloading process is over when the BHP is experiencing steady state conditions, after about 1000 seconds. From figure (17), it is seen that the BHP decrease experienced during the unloading process can be divided in two. The first part is from time equals 160 seconds to about time equals 640 seconds. This part of the unloading represents the time it takes to displace the initial water in place in the annulus. The BHP decreases as the gas is circulated up the annulus, due to the heavier water is displaced with a mixture of air and water, generating a lower hydrostatic pressure profile in the well. The pressure profile at time equals 640 is shown in figure (20); here it is visual that the pressure profile has shifted to the left compared to the pressure profile at initial conditions in figure (16), giving a lower BHP.

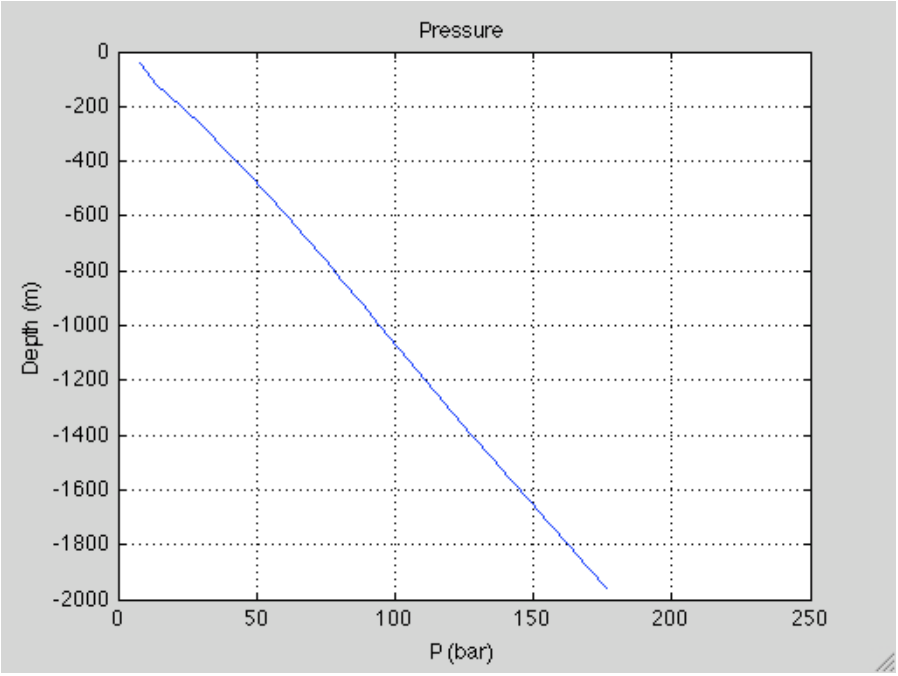

Figure (20) Pressure Profile at Time Equals 640 seconds

Figure (21) shows the gas volume fraction as a function of depth at 640 seconds. The gasified drilling fluid is has been circulated up all the annulus, and is expanding in volume as it reaches the choke.

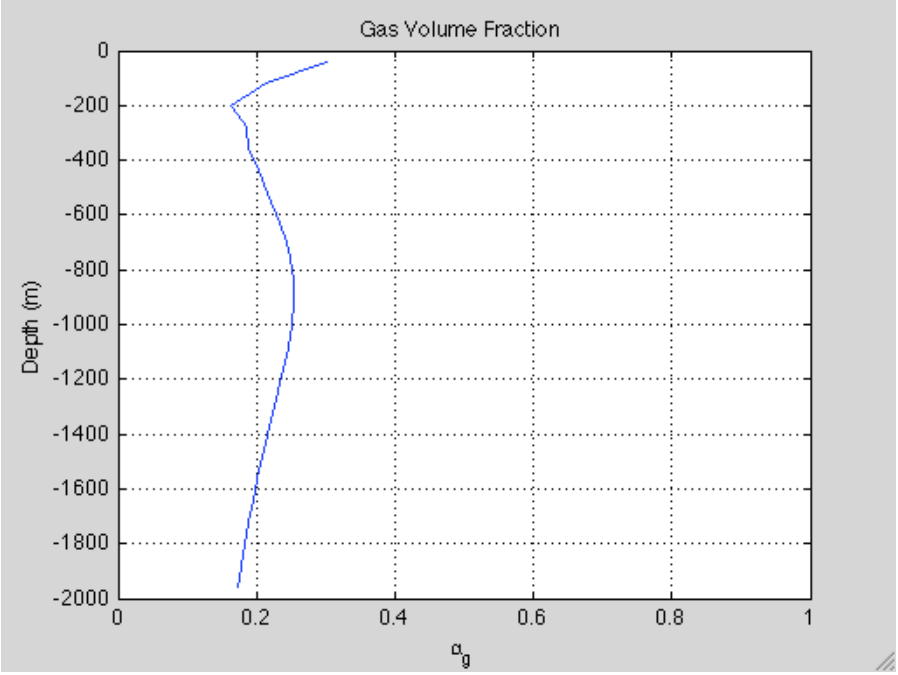

Figure (21) Gas Volume Fraction as a Function of Depth at Time Equals 640 Seconds

From time equals 640 to 1000 second; a more rapid decrease in BHP is seen in figure (17). This is due to the liquid mass rate at the choke is rapidly decreasing, see figure (18), and the gas mass rate at the choke is increasing in figure (19). The BHP is decreasing down to wanted value at time equals 1000 seconds, the pressure profile in the well is then given by figure (22), shifted even more to the left compared to the pressure profile at initial conditions in figure (16) and also compared to the pressure profile at time equals 640 seconds in figure (20).

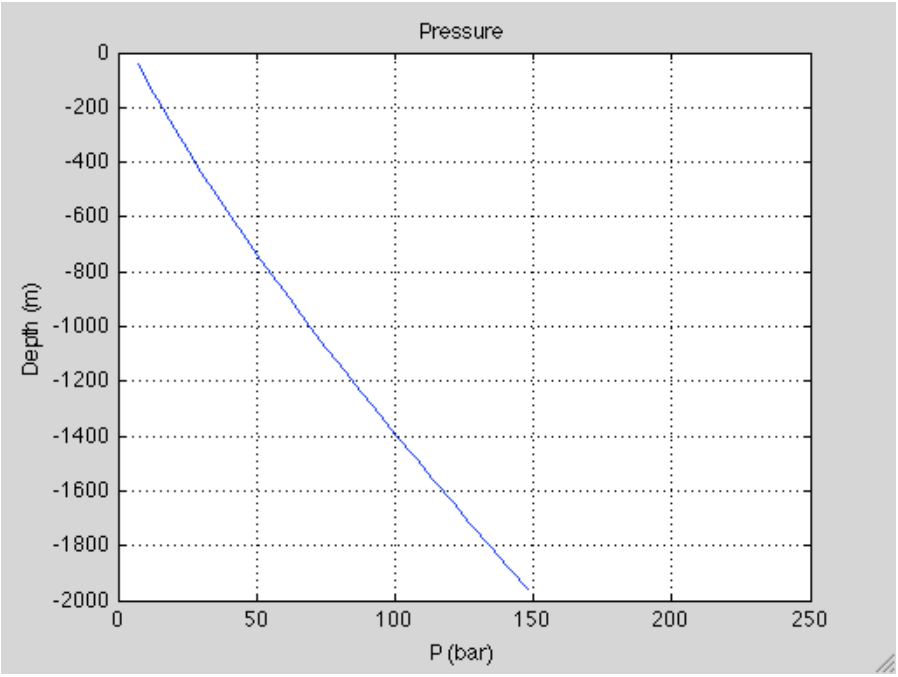

Figure (22) Pressure Profile at Time Equals 1000 seconds

The gas volume fraction verses depth, at time equals 1000 seconds, is given by figure (23). The gas is expanding upwards in the wellbore, as described in chapter 7.2.1 by Boyles general gas law [37], equation (4).

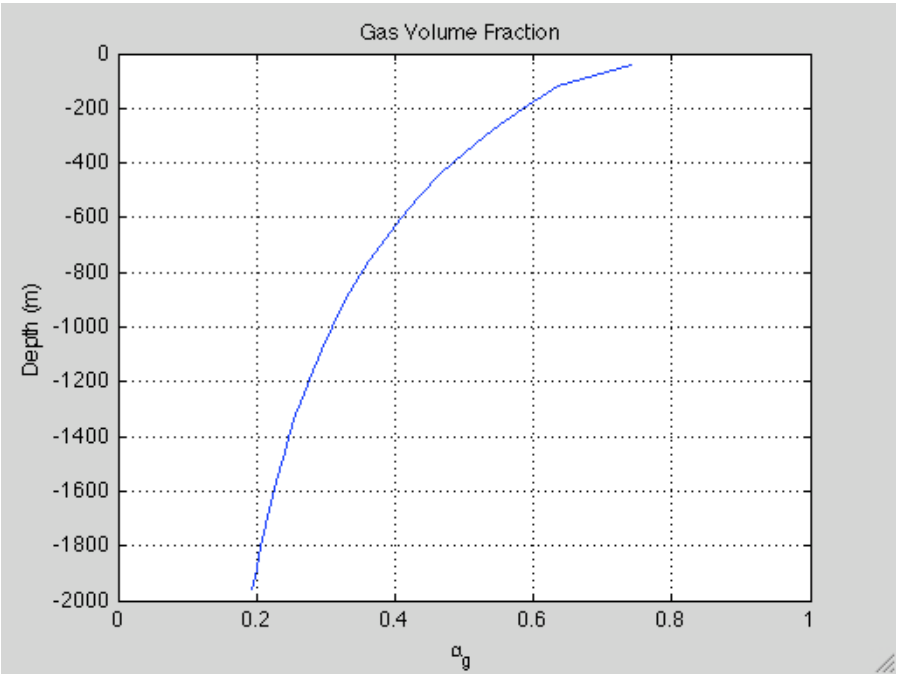

Figure (23) Gas Volume Fraction as a Function of Depth at Time Equals 1000 Seconds

10.2.2 Drill pipe connection

As stated in table (4), the drill pipe connection starts at time equals 1700 seconds. The circulation is gradually shut down in a timeline of 10 seconds. The problems regarding the drill pipe connections is discussed in chapter 7.2.2 and also illustrated in figure (9). It is expected that the BHP will drop, equaling the frictional part of equation (25), if there is no circulation of the well. As the choke is kept open throughout the connection operation there will still be some flow of the well. From figure (17) and (18) it is shown that the bottomhole line experience a sudden drop as the circulation is shut down, however, the choke line illustrates a much slower decrease in mass rates. The liquid mass rates, figure (18), at the choke is approaching zero at time equals 2000 seconds, where circulation is regained. The gas mass rate, figure (19), never approach zero, it keeps flowing through the whole connection procedure. Due to this, the BHP line in figure (17) will not experience the sudden drop equaling the frictional pressure drop, but have a more smooth decrease. This is also shown in figure (24) and (25) below which gives the different phase velocity as a function of depth at time equals 2000 seconds.

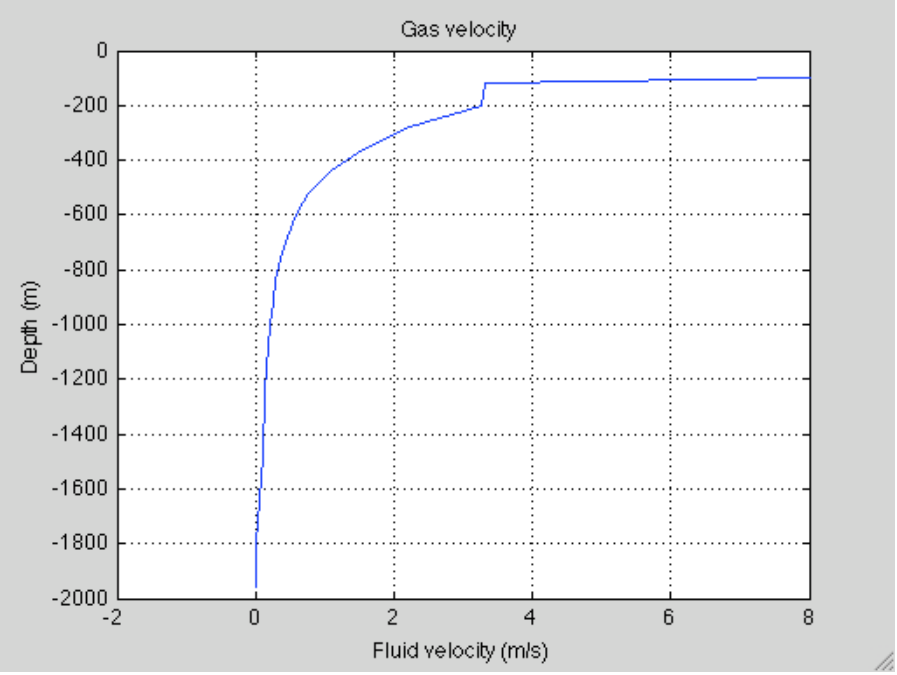

Figure (24) Gas Velocity as a Function of Depth at 2000 Seconds

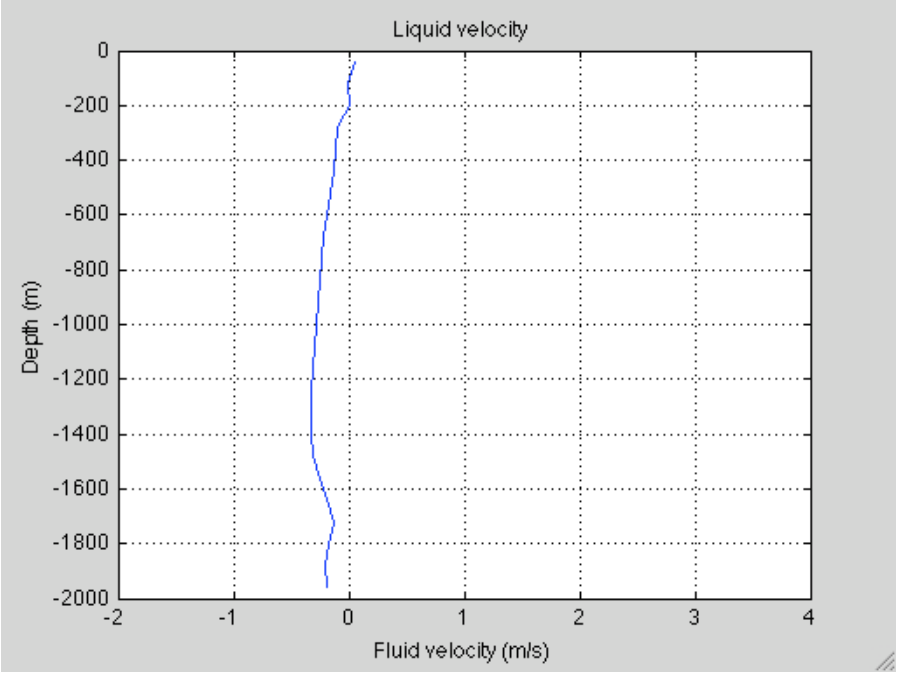

Figure (25) Liquid Velocity as a Function of Depth at 2000 Seconds

The pressure profile at the start of the connection, time equals 1700 seconds, will be the same as in figure (22). Figure (26) shows the pressure profile at time equals 2000 seconds, where the connection has been made. The pressure profile has shifted even more to the left, due to stop in circulation. This might lead to problems discussed in chapter 3.2.4 and 7.2.2.

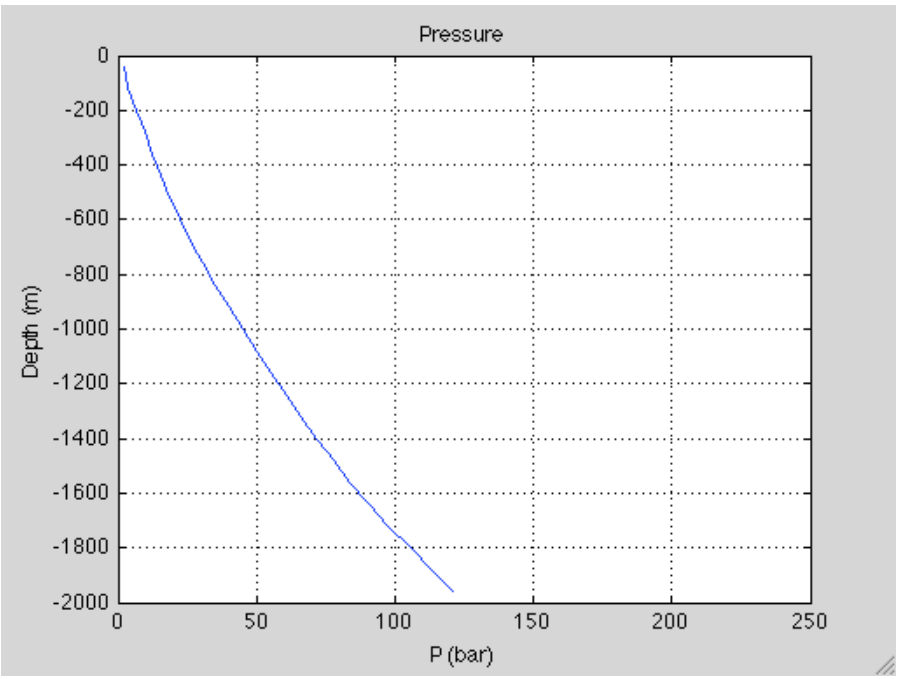

Figure (26) Pressure Profile at Time Equals 2000 Seconds

Now the connection has been made, and circulation is regained from time equals 2000 – 2010 seconds. From chapter 7.2.2, the expected outcome would be a pressure spike,

creating sudden overbalanced conditions due to the frictional pressure loss and the gravitational separation of the two fluids. Figure (27) shows the gas volume fraction at time equals 2000, this shows that the air is occupying the upper parts of the annulus, and the water the lower parts.

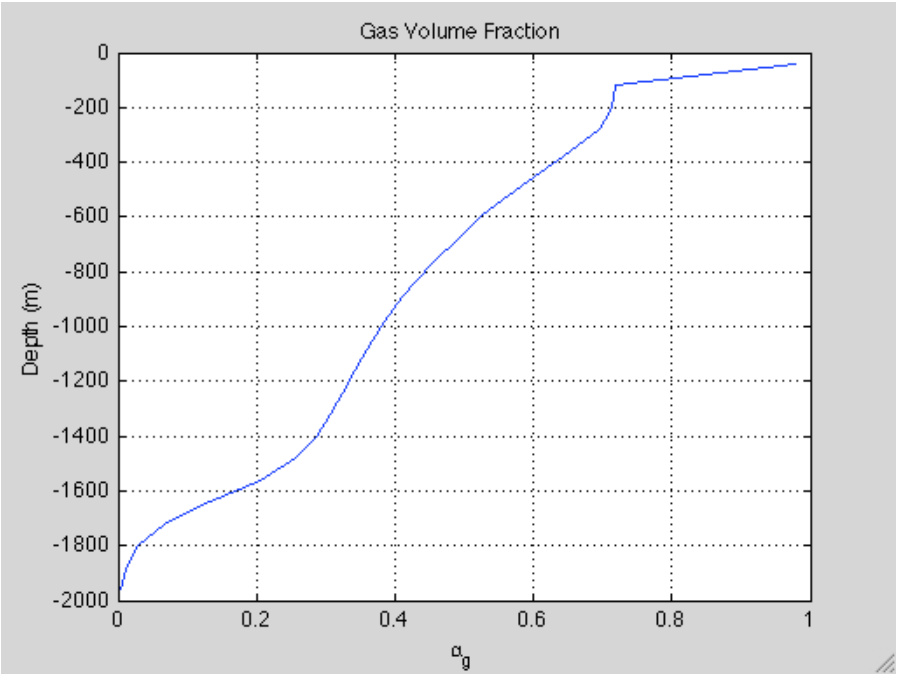

Figure (27) Gas Volume Fraction as a Function of Depth at Time Equals 2000 Seconds

From figure (17) it is seen that the BHP is increasing as the circulation is regained, and is experiencing a top at time equals 2480 seconds. Figure (18) and (19) shows that the mass rates at bottom is rapidly running at constant rates, whereas the choke rates are behaving different. As seen in figure (27) the lower parts of the annulus is dominated by water, and as this is circulated out the BHP increases. The gas mass rate decreases at the choke as the water dominant part is circulated out, while the liquid mass rate naturally increases. After 2510 seconds the liquid part is circulated out and the liquid mass rate decreases while the gas mass rate increases towards steady state. This makes the BHP in figure (17) approach steady state underbalanced conditions again at time equals 2830 seconds giving the pressure profile as in figure (28) below.

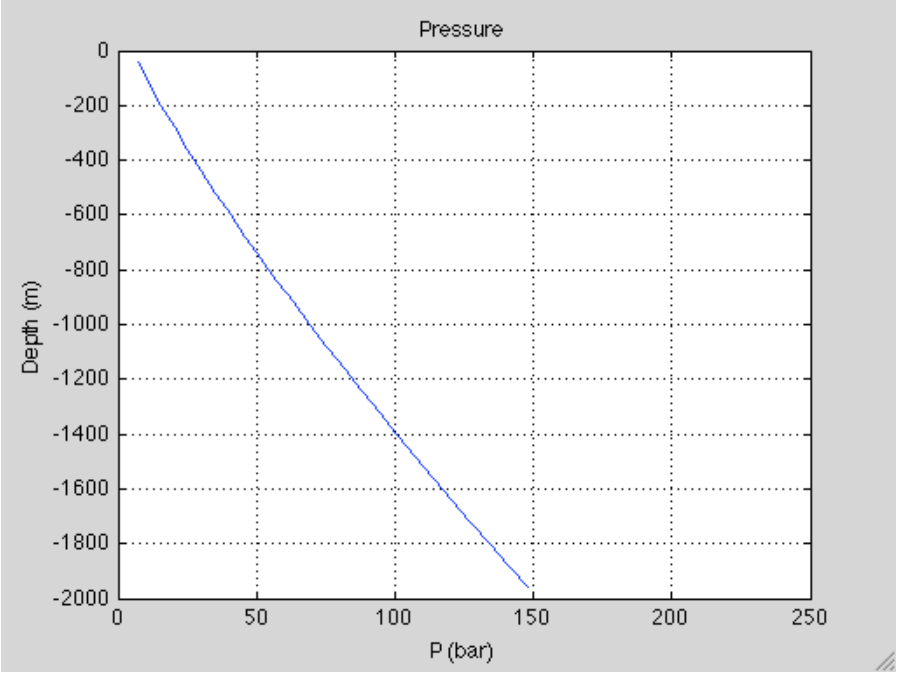

Figure (28) Pressure Profile at Time Equals 2830 Seconds

11 Extension of Model

The drift-flux model described in chapter 9 has its limitations. It only recognizes one flow pattern, the slug flow region. As mentioned in chapter 8.6, the slip flow will have different values depending on what flow pattern that exist. In this chapter the drift-flux model will be taken a step towards a mechanistic approach, by including a model that distinguish between bubble flow and slug flow. As stated in the description of the different flow patterns in chapter 8.7, the bubble flow region will have slippage between the two phases. The idea is to have two sets of values for C_0 and C_1, from equation (18), one set for bubble flow and one set for slug flow. In the transition zone between bubble flow and slug flow, interpolating technique will be used between the two sets of parameters. The extensions will be used for simulations in chapter 12, first by using only the bubble flow model, before the flow pattern depending model will be used.

11.1 Flow Pattern Detection

The first step will be to develop a method to differentiate between bubble and slug flow. The transition conditions are taken from Lage et al. [33]. They have refined the work done by Taitel et al. [35] in 1980, which considered five different flow patterns in upwards two-phase flow in pipe and formulated boundaries between them. The patterns recognized were, like described in chapter 8.7, bubble flow, dispersed bubble flow, slug flow, churn flow and annular flow. Lage et al. developed the boundaries between the flow patterns to consider a concentric annulus instead of pipe flow. A flow map showing the transition boundaries is shown in figure (29) below. The x-axis consists of the superficial gas velocity shown in equation (6), while the y-axis consists of the superficial liquid velocity as shown in equation (5).

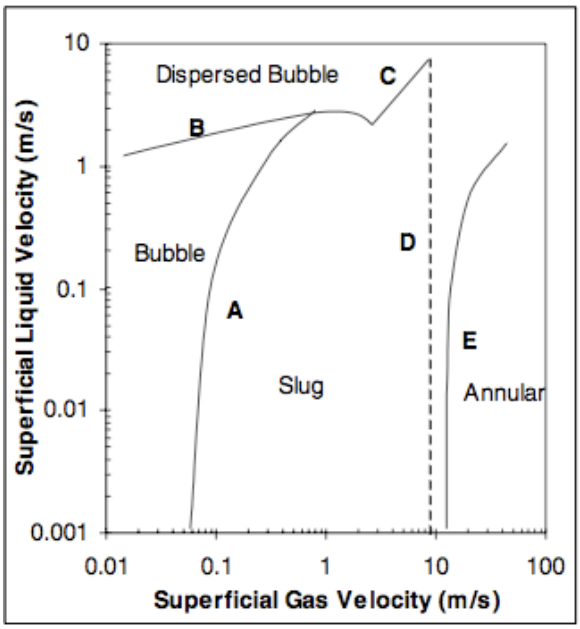

Figure (29) Flow Pattern Map [33]

This thesis puts the focus on the transition line between the bubble flow and slug flow, shown as transition "A" in figure (29). Taitel et al. [35] found that if the rise velocity of small discrete bubbles is larger than the rise velocity for the Taylor bubble, bubble flow cannot occur. When the discrete bubbles approaches the Taylor bubbles from behind, they collide and merge into the Taylor bubble. On the other hand, when the rise velocity of the Taylor bubble is larger than the rise velocity for the discrete bubbles, coalescence does not take place. This is giving a condition where bubble flow is possible. The rise velocity for a single bubble rising in an infinite medium is given by equation (57),

$$u_{0\infty} = 1.53\left[\frac{(\rho_L - \rho_G)g\sigma}{\rho_L^2}\right]^{1/4} \quad (57)$$

Where, subscripts L is for liquid phase, subscript G is for gas phase and,

$u_{0\infty}$ = Rise velocity of a single bubble rising in an infinite medium

ρ = Density as a function of pressure

g = The gravitational constant

σ = Interfacial tension

The rise velocity for a Taylor bubble on the other hand is given by equation (58),

$$u_{TB} = 0.35\sqrt{g(d_o - d_i)} \quad (58)$$

Where,

u_{TB} = The rise velocity of a Taylor bubble

g = The gravitational constant

d_o = The inside diameter of the casing

d_i = The outside diameter of the drill pipe

Combining equation (57), (58) and the statement that u_{TB} must be larger than $u_{0\infty}$ gives a geometrical limitation for the existence of bubble flow in the annulus [22],

$$(d_o - d_i) \geq 19.7 \left[\frac{(\rho_L - \rho_G)\sigma}{g\rho_L^2}\right]^{1/2} \quad (59)$$

Where, subscripts L is for liquid phase, subscript G is for gas phase and,

d_o = The inside diameter of the casing, see figure (30) below

d_i = The outside diameter of the drill pipe, see figure (30) below

ρ = Density as a function of pressure

σ = Interfacial tension, a constant value of 0.0722 N/m is used in this thesis

g = The gravitational constant

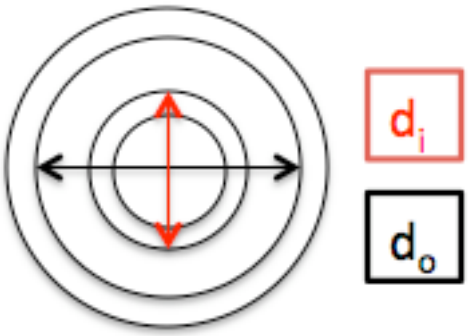

Figure (30) - Illustration of the Concentric Annulus. Drawn in Power Point.

The value for the interfacial tension that will be used is found in [11], and is valid for the fluid system water and air for temperatures at 15 degree Celsius and a pressure of 1 atm. It is stated in [11] that the interfacial tension is more sensitive to changes in temperature than for pressures, as this is an isothermal model, σ will for simplicity reasons be chosen to be constant at 0.0722 N/m. The criteria given in equation (59) must be fulfilled to have conditions that allows for bubble flow. If the annulus presents a geometry that enables bubble flow the coalescence of small gas bubbles into large Taylor bubbles is the basic mechanism for transition from bubble flow to slug flow.

There are different opinions of what gas fractions that is needed to provide this mechanism, in this thesis the experiments performed by Caetano [22] is used. Here an average transition value for α_G is found to be 0.20. At values below this, bubble flow is chosen. Based on this the transition line "A" in figure (29) is given by equation (60) [33],

$$u_{SL} = 4.0u_{SG} - 0.8u_0 \quad (60)$$

and equation (61) gives a correction proposed to correct $u_{0\infty}$ to apply for a bubble rising in a swarm of bubbles,

$$u_0 = u_{0\infty}(1 - \alpha_G)^n \quad (61)$$

Where, subscript L is liquid phase, subscript G is gas phase and,

u_S = Superficial velocity

u_0 = Rise velocity for a bubble rising in a swarm of bubbles

$u_{0\infty}$ = Rise velocity of a single bubble rising in an infinite medium

α = Phase fraction

n = Exponent, found to be 0.5 in this case

The transition boundaries used in this thesis will be given as shown in table (6), the geometrical limitation is for simplicity reasons not considered. The case for gas fractions over 75 %, as given in chapter 9.2.5 for the original model will still be valid.

Table (6) Transition Boundaries

$0.20 > \alpha_G$	Bubble Flow
$0.20 \leq \alpha_G \leq 0.25$	Transition Between Bubble and Slug Flow
$0.75 > \alpha_G > 0.25$	Slug Flow
$0.75 \leq \alpha_G \leq 1$	Approaching One-Phase Flow

11.2 Flow Behavior Models

The next step will be to calculate the slippage between gas and liquid for the flow pattern found. The pressure drop calculations for the different flow patterns will, for simplicity reasons, be the same for bubble flow, slug flow and the transition flow zone. As the different models will have different values for the slip parameters, subscripts are used to differentiate between the different sets.

11.2.1 Bubble Flow Model

As stated above, for gas fractions below 20 %, bubble flow is the chosen flow pattern. The slippage between gas and liquid for bubble flow will then be determined by equation (62) [33],

$$u_G = C_{0,B}u_{mix} + u_0 \quad (62)$$

By inserting equation (27) and (31) in for u_0 gives the relation,

$$u_G = C_{0,B}u_{mix} + 1.53\left[\frac{(\rho_L - \rho_G)g\sigma}{\rho_L^2}\right]^{1/4}\sqrt{(1-\alpha_G)} \quad (63)$$

To simplify the equation,

$$C_{1,B} = 1.53\left[\frac{(\rho_L - \rho_G)g\sigma}{\rho_L^2}\right]^{1/4}\sqrt{(1-\alpha_G)} \quad (64)$$

Giving equation (65) the same form as the general slip law in equation (18),

$$u_G = C_{0,B}u_{mix} + C_{1,B} \quad (65)$$

The equation is based on the same as for the slip model for the base case, where $C_{0,B}$ is the velocity profile coefficient for bubble flow and $C_{1,}$ is the drift velocity of the gas in bubble flow. The velocity profile coefficient will be a constant. Caetano [22], found that a value of 1.0 was the best fitting, while Lage and Time [34] found that a value of 1.1 gave the best fitting between their model and an experimental database. Both values will be tried in simulations for this thesis.

11.2.2 Transition Flow Model

For gas fractions between 0.2 and 0.25, a transition zone is chosen if the geometrical limitation is fulfilled. In this zone, an interpolation between the two sets of C_0 and C_1 will be performed,

$$C_{0,T} = \left(1 - \frac{\alpha_G - 0.2}{0.05}\right)\times C_{0,B} + \frac{\alpha_G - 0.2}{0.05}\times C_{0,S} \quad (66)$$

and,

$$C_{1,T} = \left(1 - \frac{\alpha_G - 0.2}{0.05}\right)\times C_{1,B} + \frac{\alpha_G - 0.2}{0.05}\times C_{1,S} \quad (67)$$

Where,

$C_{0,T}$= The profile parameter (distribution coefficient) for the transition zone

$C_{0,B}$= The profile parameter (distribution coefficient) for the bubble zone

$C_{0,S}$= The profile parameter (distribution coefficient) for the slug zone

$C_{1,T}$= Drift velocity of the gas for the transition zone

$C_{1,B}$= Drift velocity of the gas for the bubble zone

$C_{1,S}$= Drift velocity of the gas for the slug zone

11.2.3 Slug Flow Model

For situations where the gas fraction is higher than 25 % and below 75 %, slug flow is chosen. The slip parameters are already determined and shown in chapter 9.2.5,

$$C_{0,S} = 1.2$$

and,

$$C_{1,S} = 0.64$$

And equation (18) is applied.

11.2.4 Approaching One-Phase Flow

The slip parameters for the gas fractions above 75 % will be determined as shown in chapter 9.2.5, equation (35) and (36).

11.3 Implementing the Extensions in Matlab

Now, there are defined different flow models for bubble flow, slug flow and the transition zone in between. The next step is to implement them into the matlab code. First the bubble flow model will be used for the entire simulation, this is done to see that the model will give reasonable results, and also to see how the two different values for C_0 will influence the results. Figure (31), below, shows how the bubble flow model is implemented into the matlab code. Note that $C_{0,B}$ here is set to be 1.1. The densities, in the expression for $C_{1,B}$, are found by using the density models, as shown in chapter 9.2.4.

```
 %Bubble Flow  (variable parameters)
C0_B = 1.1;
C1_B = 1.53*(((dlo(j)-dgo(j))*grav*0.0722)/dlo(j)^2)^(0.25)*(1-eg(j))^0.5;
```

Figure (31) - Bubble Flow Model Implemented into Matlab

After simulations are performed with the bubble flow model, the flow pattern depending model will be implemented into the code. Figure (32) shows how this is done, for this

figure the C_0 parameter is set to be 1.1. The gas fraction criteria shown in table (6) is used in three different "if" statements. The first states that if the gas fraction is below 0.20, then bubble flow model should be used, 11.2.1. Then a new "if" statement occurs, if the gas fraction is between 0.2 and 0.25 the transition flow model is used, like in 11.2.2. The last "if" statement is for the slug flow regime, here the slug flow model is used, like in 11.2.3.

```
%Bubble Flow  (variable parameters)
C0_B = 1;
C1_B = 1.53*(((dlo(j)-dgo(j))*grav*0.0722)/dlo(j)^2)^(0.25)*(1-eg(j))^0.5;

%Slug Flow
C0_S = 1.2;
C1_S = 0.64;

%Flow Pattern Depending
%Bubble Flow Model
if ((eg(j)<0.20))
    C0=C0_B;
    C1=C1_B;
end

%Transition Flow Model
if ((eg(j)>=0.20) & (eg(j)<=0.25))
    C0=((1-((eg(j)-0.2)/0.05))*C0_B+((eg(j)-0.2)/0.05)*C0_S);
    C1=((1-((eg(j)-0.2)/0.05))*C1_B+((eg(j)-0.2)/0.05)*C1_S);
end

%Slug Flow Model
if ((eg(j)>=0.25) & (eg(j)>0.75))
    C0=C0_S;
    C1=C1_S;
end
```

Figure (32) – Flow Pattern Dependent Flow Model Implemented into Matlab

12 Simulations and Observations

The simulations performed after implementing the new flow models will simulate the same case as presented in chapter 10 and follow the timeline presented in table (4). In chapter 12.1, the bubble model for slip flow will be used as described in chapter 11.2.1. As there where two different values proposed for $C_{0,B}$ these two will first be tested to see what value that fits the best. Simulations will then be done, using the $C_{0,B}$ found in 12.1, results and observations are shown in chapter 12.2. The focus of the observations in 12.2 will be at the events given in table (5) in chapter 10.2. The results gained in the new simulations will be compared to the results gained from simulations with the original model, see chapter 10.2. In chapter 12.3, the simple flow pattern detecting model will be used for simulations, see figure (32) in chapter 11.3. Also here the value for $C_{0,B}$ determined in 12.1 will be used for the bubble flow part. The results and observations for this model will be investigating the unloading sequence and the pressure peak. The gas volume fraction as a function of depth plot will be used to investigate which model that is being used during these events. Then, in chapter 12.4, an

overview of the results will be presented. As the reasons for the dynamic BHP in both the unloading- and the drill pipe connection sequence already are described in chapter 7.2 and 10.2, this will not be further discussed in this chapter. Although the values of the pressures, rates and velocities will differ in the simulations presented below, the mechanisms behind will be as for the base case.

12.1 Selecting Value of the Velocity Profile Coefficient, $C_{0,B}$

As stated in chapter 11.2.1, the velocity profile coefficient for bubble flow, $C_{0,B}$, has two different options in value. The two different values are 1.0 and 1.1. The two will be used for simulations below, and based on the results; one of them will be preferred for the rest of the thesis.

12.1.1 $C_{0,B} = 1.0$

The results from using $C_0 = 1.0$ are presented below in figure (33), (34) and (35), showing the pressure, the liquid mass rates and the gas mass as a function of time respectively. As stated in chapter 10, the blue line represents bottomhole conditions and the red line represents choke conditions, this is valid for all simulation results given in this thesis.

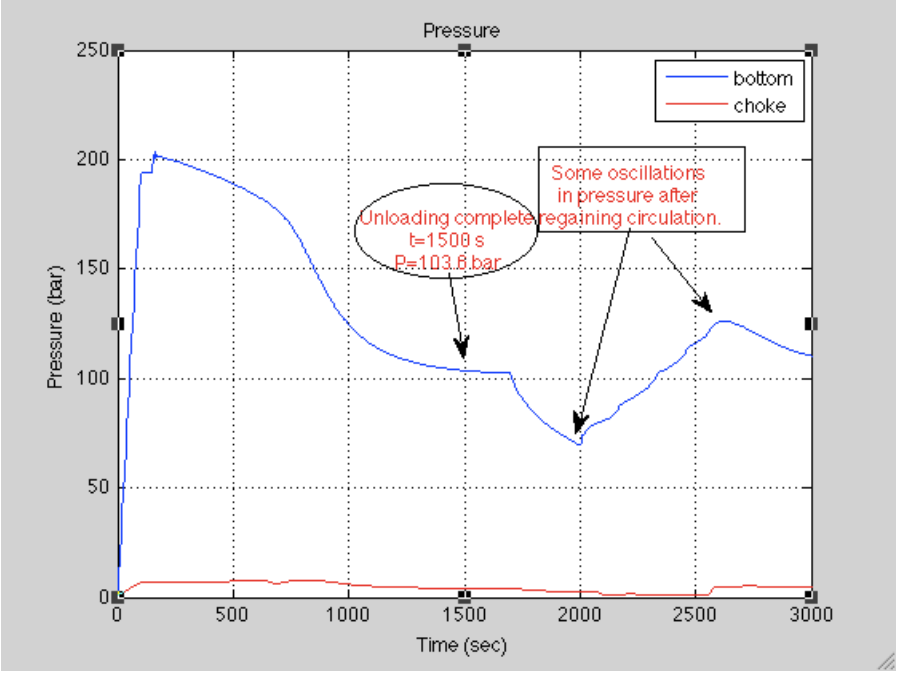

Figure (33) - The Pressure as a Function of Time

- The first observation that can be made in figure (33) is that the unloading sequence, that is lasting about 1500 seconds, gives a BHP equaling 103.8 bars. As seen in table (5), in chapter 10.2, the BHP after the unloading sequence, which in that case lasts in 1000 seconds, equal 147.8 bars for the original model.
- The second observation is that there are some oscillations in the BHP after the drill pipe connection has been made and the circulation is regained. The pressure at the choke is also lowered and quite stable at approximately 1 bar, indicating that gas fraction is very high.

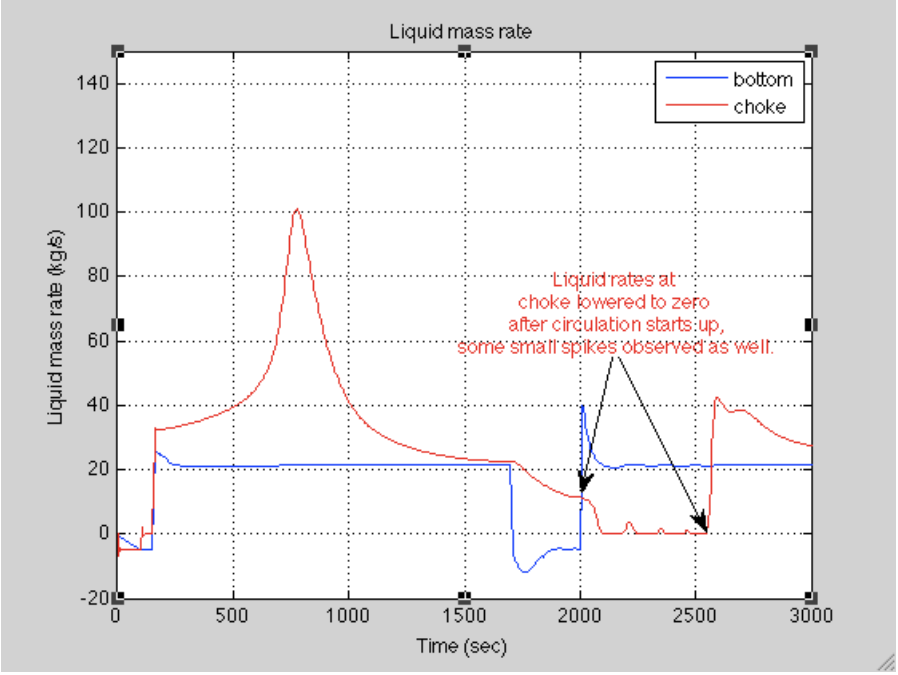

Figure (34) - Liquid Mass Rate as a Function of Time

- Figure (34), showing liquid mass rates, shows that the liquid mass rates at the choke decreases to zero after circulation in the well is regained. This indicates, as suggested from figure (33), that the well is only flowing gas at the choke, at the time, and that the top part of the well is filled with gas.

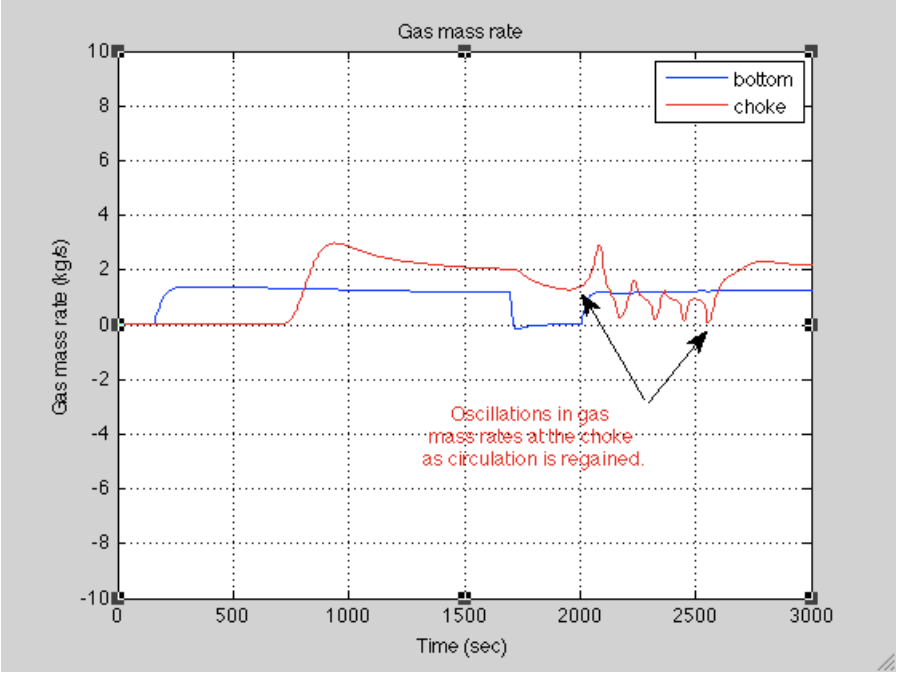

Figure (35) - Gas Mass Rate as a Function of Time

- In figure (35), showing the gas mass rates as a function of time, quite large oscillations can be observed at mass rates at the choke after circulation is regained. Figure (36), below, shows the gas fraction as a function of depth at time equaling 2140 seconds. At this time the circulation is regained.

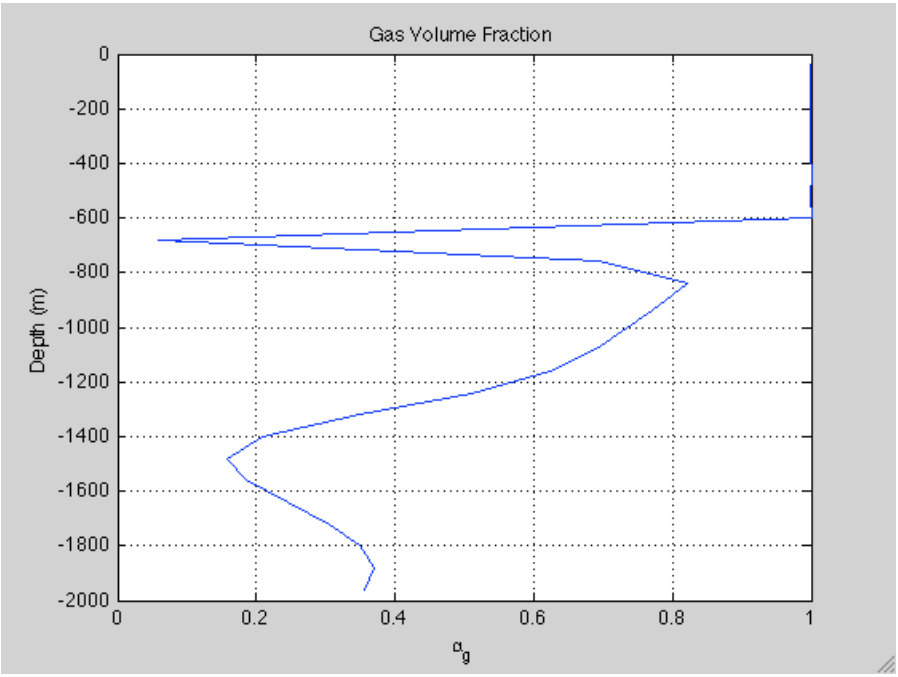

Figure (36) - Gas Fraction Profile at Time Equaling 2140 s

- As seen here, from a depth of 600 meters and up to surface, gas fraction equals 1. This agrees with the choke pressure in figure (33) and the liquid mass rates at

the choke in figure (34). The gas fraction profile, in figure (36), is rather strange looking, suggesting that there are huge fractions of liquid at a depth of about 700 meters.

12.1.2 $C_{0,B} = 1.1$

Results from using a value of 1.1 for C_0 gives the results as shown in figure (37), (38) and (39), showing the pressure, the liquid mass rates and the gas mass as a function of time respectively.

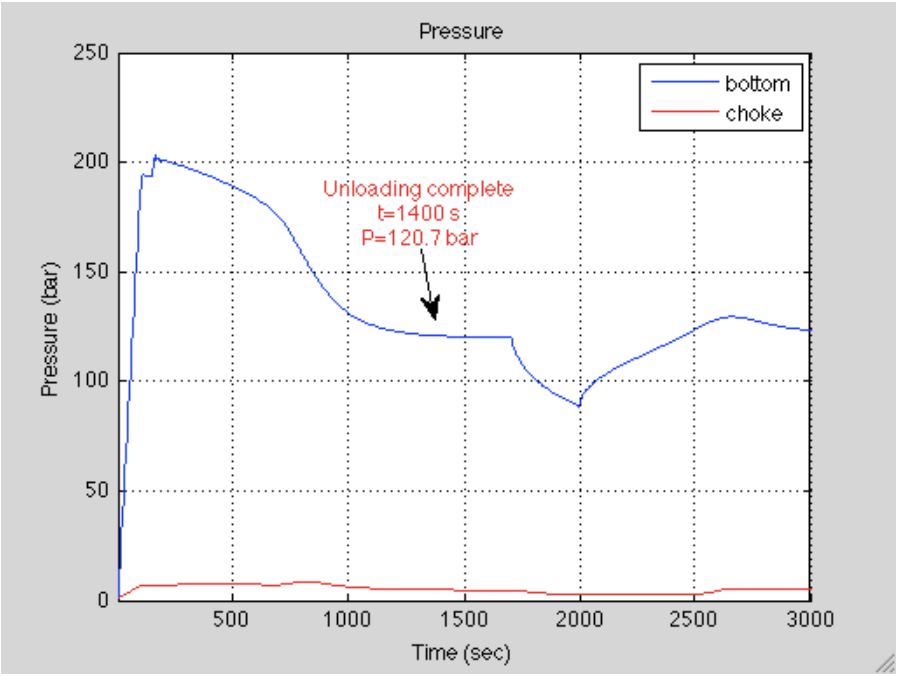

Figure (37) - The Pressure as a Function of Time

- Here, in figure (37), the unloading sequence is done after 1400 seconds, 100 seconds before the results from the case with $C_{0,B} = 1.0$. The BHP ends up at a value of 120.7 bars, 16.9 bars higher than for $C_{0,B} = 1.0$.

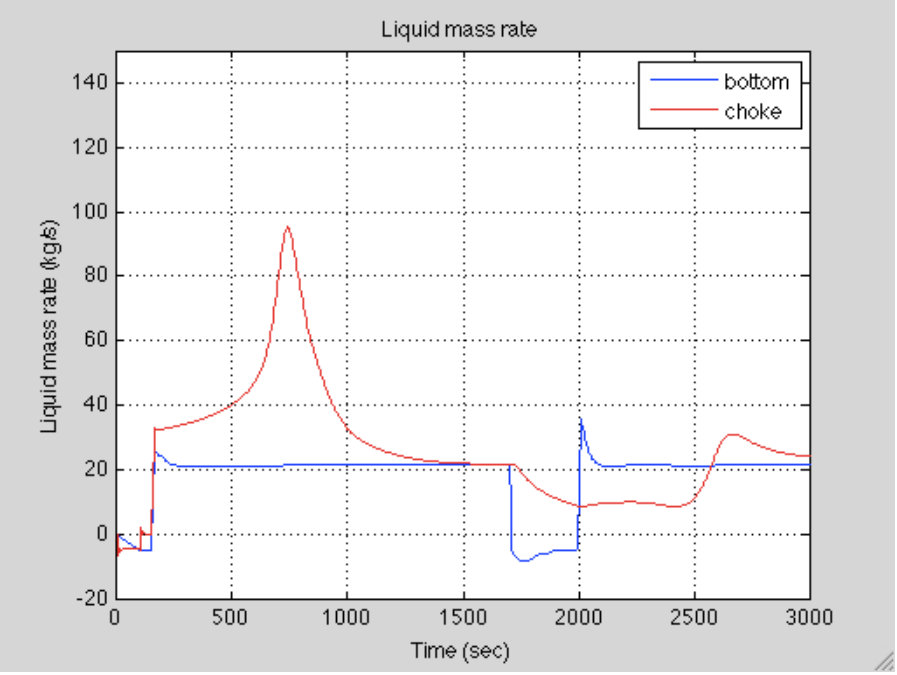

Figure (38) - Liquid Mass Rate as a Function of Time

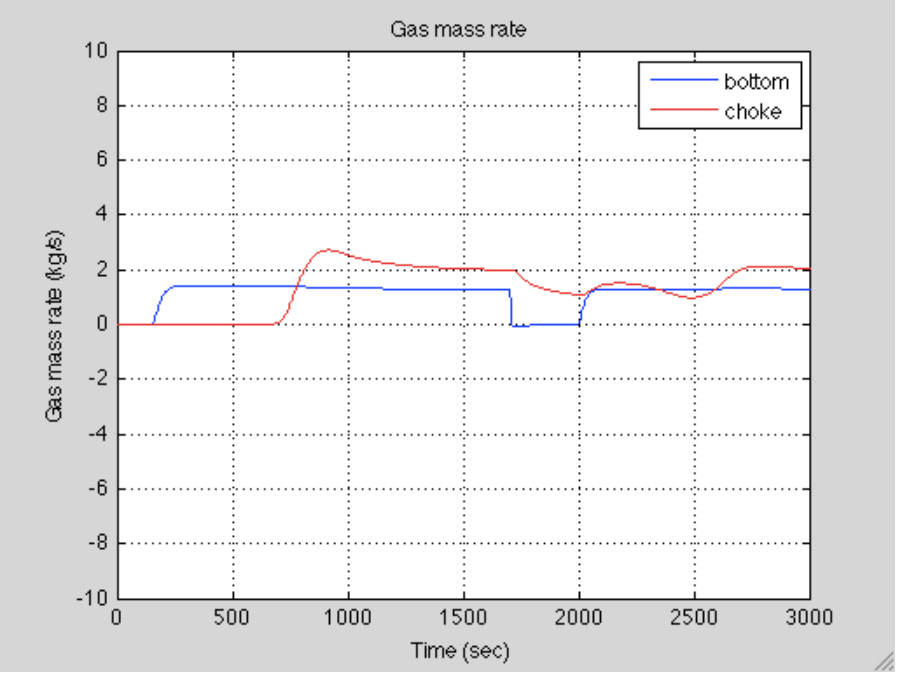

Figure (39) - Gas Mass Rate as a Function of Time

- The curves presented in figure (38) and (39) are smooth and show no sign of unphysical oscillations.
- The gas fraction as a function of depth plot at time 2140, shown in figure (40), shows a more reasonable profile than the profile presented in figure (36). As the circulation has started up again, the liquid that was at the bottom during

connection is now being circulated up the wellbore. The profile above the liquid part shows that the gas is expanding upwards the well, as the pressure decreases.

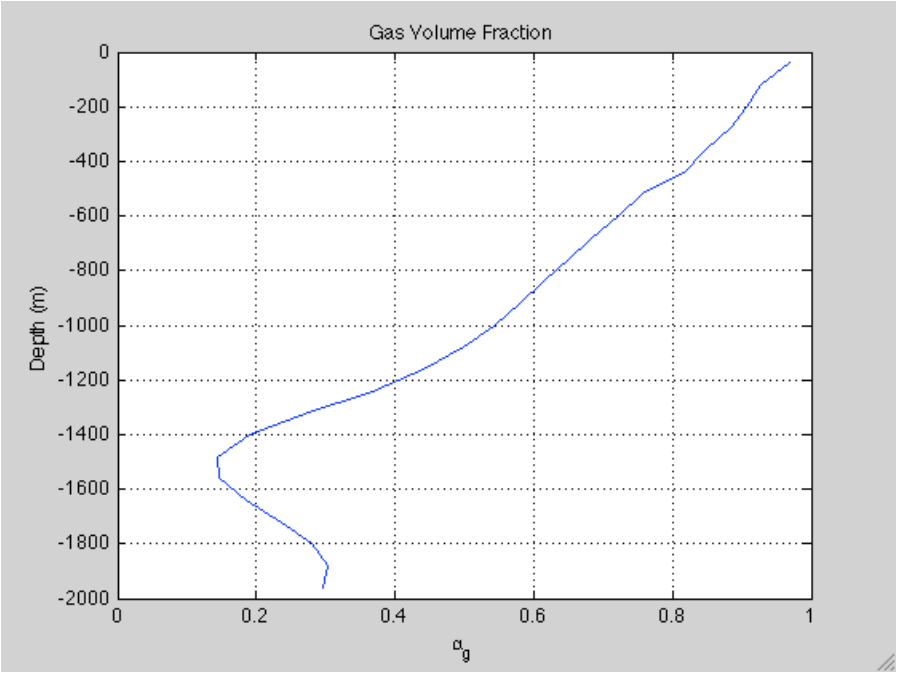

Figure (40) - Gas Fraction Profile at Time Equaling 2140 s

12.1.3 Conclusion of the Observations

As the results gained from the $C_{0,B} = 1.0$ case gave such big oscillating curves, where the $C_{0,B} = 1.1$ case gave smooth curves. And due to the look of the gas fraction profile in figure (40), for $C_{0,B} = 1.1$, was found to be more reasonable than the one presented in figure (36), for $C_{0,B} = 1.0$, the $C_{0,B} = 1.1$ case will be used for further simulations in this thesis, as proposed by [34].

12.2 Results and Observations Using Bubble Flow Model

In this chapter, the results gained from using the bubble flow model for slip parameters will be compared to the results from the simulations using the original model, which is using the slug flow model. The observations will be based on comparisons with the results gained from the original simulations, shown in table (5). Figure (41) is basically the same as presented in figure (36), only difference being comments regarding the events that will be observed. The figure corresponds to figure (17), for the original model. Remember that the timeline in the two simulations is the same.

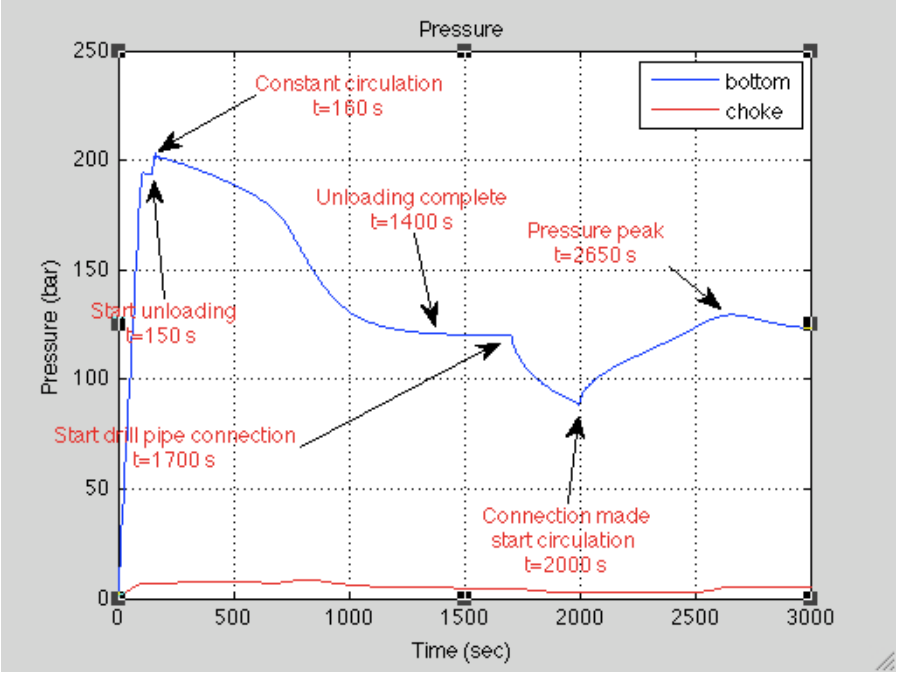

Figure (41) – Pressure as a Function of Time

The same applies for figure (42) and (43) presented below. These correspond to figure (18) and (19) for the original simulations presented in chapter 10.2, giving the mass rates for liquid and gas respectively. These plots will also be referred to when doing observations.

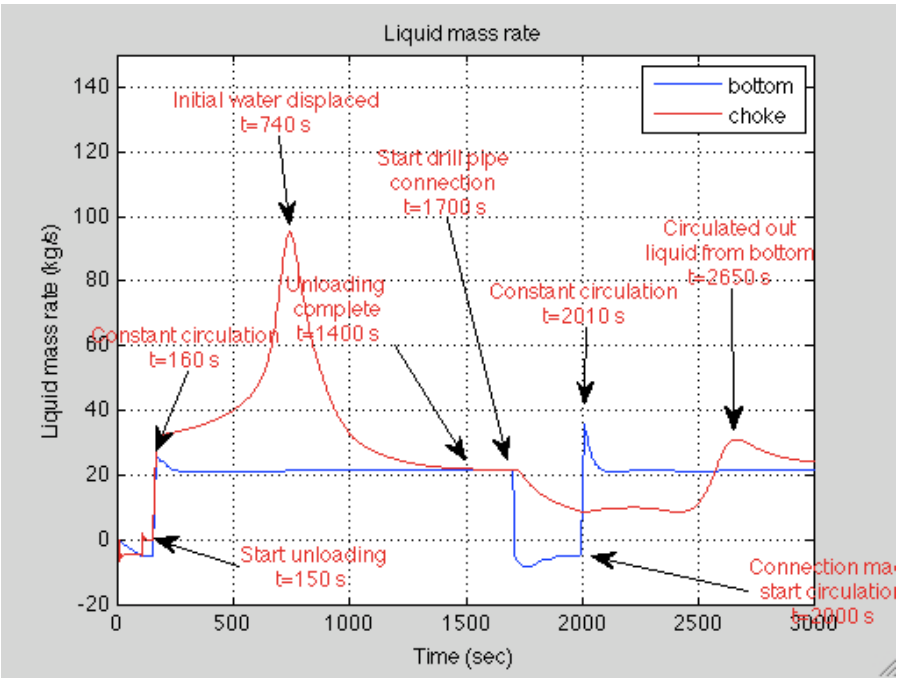

Figure (42) - Liquid Mass Rates as a Function of Time

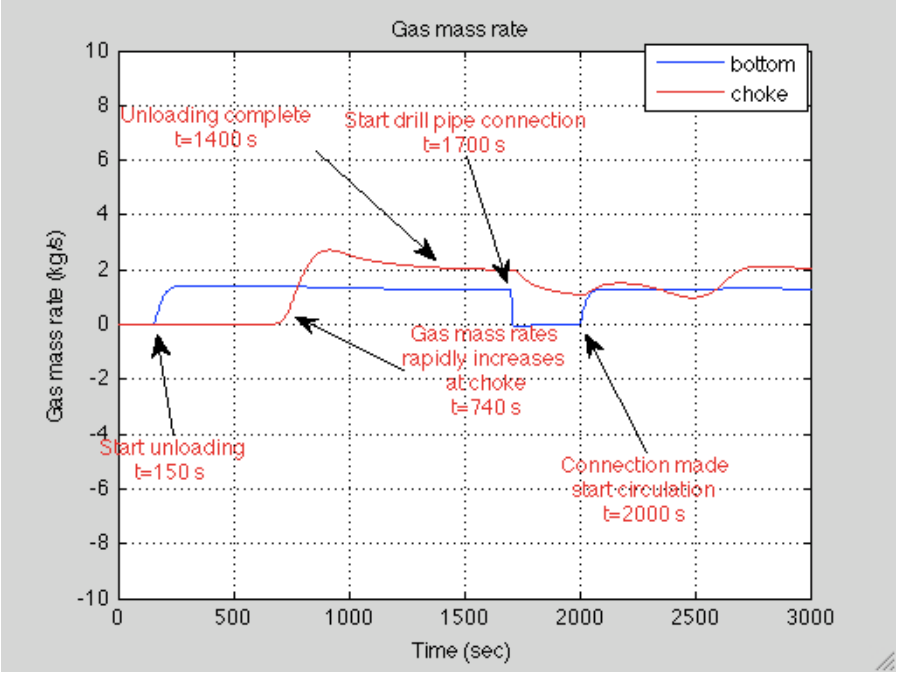

Figure (43) - Gas Mass Rate as Function of Time

The first 160 seconds will be the same for the two cases. However, comparing figure (41) to figure (17), the pressure as a function of time plots, gives differences in the BHP after this time. The BHP during the events presented in table (5) will be investigated in the following subchapters. A corresponding table has been made using the results gained from figure (41), (42) and (43). The result is table (7) below. The difference values, in the parentheses in the "Pressure Peak" event, gives the pressure difference with respect to the BHP at time equals 1700 seconds. All other differences are from the previous event.

Table (7) - Overview Bubble Flow Model

Event	Time [s]	BHP [bar]	Difference [bar]	Difference [%]
Start Unloading	150	194	-	-
Constant Circulation	160	203.5	+9.5	+4.9
Unloading Complete	1400	120.7	-82.8	-40.7
Start DP Connection	1700	120.4	-0.3	-0.25
Regain Circulation	2000	88.6	-31.8	-26.4
Pressure Peak	2650	129.4	+40.8 (+9)	+46 (+7.5)

12.2.1 Unloading Sequence

- Observation 1:

  The unloading sequence lasts 1250 seconds in this simulations, see comment in figure (41), (42) and (43). In the original model the unloading sequence was done after 850 seconds. See values in table (5). This is a time difference of about 400 seconds, or 47 %.

- Observation 2:

  At time equals 1400 seconds; the pressure experienced in the bottom of the well will only be 120.7 bar. In the original model on the other hand, the pressure will be stable at 147.9 bars at steady state conditions. This is a pressure difference of 27.2 bars, which corresponds to 18.4 % lower BHP for the bubble flow case.

Comments to the unloading sequence:

The gas break through at surface will be at time equals 740 seconds, while the time of break through for the original model was 640 seconds. The time of gas break through is seen as the spike in figure (42), liquid mass rate. This indicates that the gas is flowing slower in this case, than for the original model. The gas fraction profile at gas break through in the original model is shown in figure (20). The gas fraction profile for the bubble flow model at time equals 640 seconds is shown in figure (44) below, and shows that the gas has not reached surface yet giving support to the indication that the gas is traveling at a slower velocity than for the slug flow model presented in chapter 10.

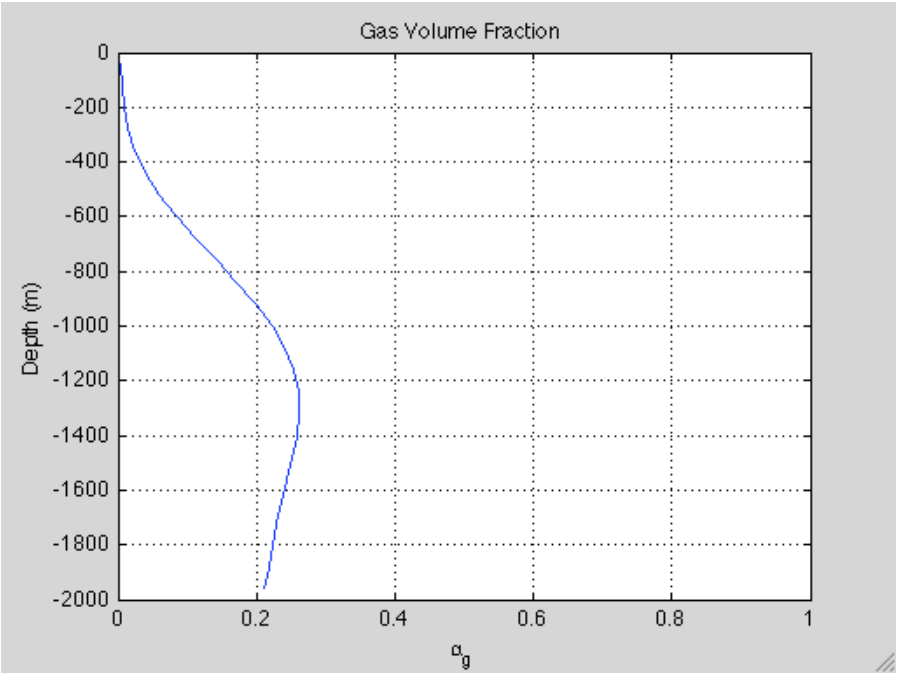

Figure (44) - Gas Volume Fraction as a Function of Depth at Time Equals 640 s

This is also indicating a higher fraction of gas in the well than for the original model after the unloading sequence, which will result in the lower BHP addressed in observation 2. Figure (45) shows the gas fraction profile after the unloading sequence. Comparing this to the gas fraction profile after unloading sequence for the original model, in figure (23), shows that there are higher fractions of gas in the well for the bubble flow model. This will give a lower BHP, as stated in observation 2.

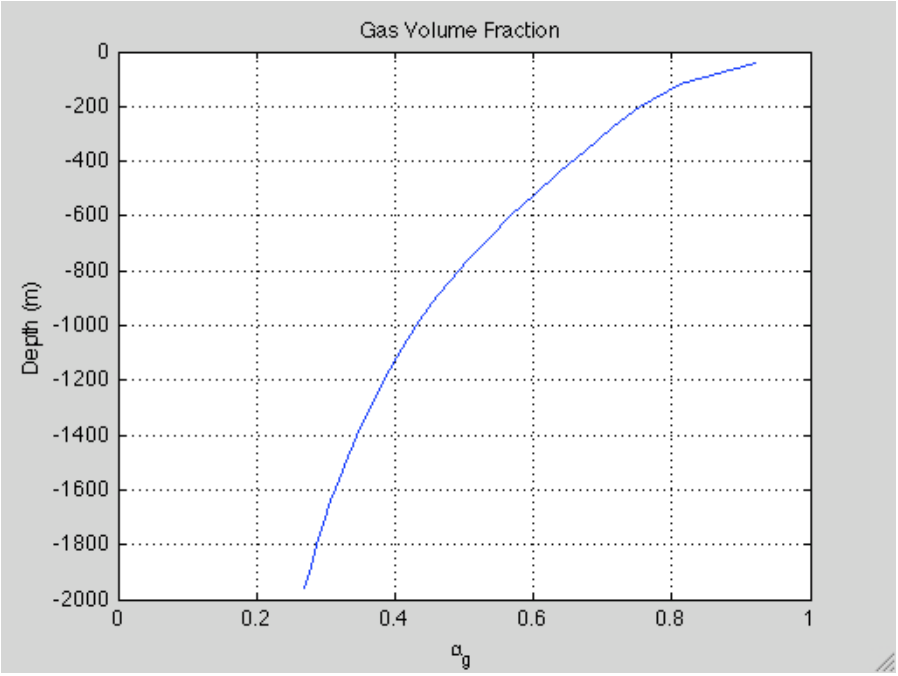

Figure (45) - Gas Volume Fraction as a Function of Depth at Time Equals 1400 s

12.2.2 BHP During Drill Pipe Connection

- Observation 3:

  Reaching 1700 seconds, the circulation of liquid and gas is linearly shut down over a timespan of 10 seconds, illustrating a drill pipe connection. The BHP at 1700 seconds is 120.4 bars for the bubble flow model, and 148 bars for the original slug flow model. The circulation starts up again at time equal 2000 seconds. The BHP calculated by the bubble flow model is then 88.6 bars, giving a pressure difference of 31.8 bars from the steady state pressure at 1700 seconds, equaling a pressure drop of 26.4 %. For the original model, the pressure ends up at 121 bars at 2000 seconds, giving a pressure difference of 27 bars, or 18.2 %.

Comments to the drill pipe connections influence on the BHP:

The differences here are not as big as for the unloading sequence. Here the circulation is shut down and a pressure drop is expected. The gas fraction profile for the well at 2000 seconds is given in figure (46). Comparing this to figure (27), which is the corresponding figure for the original model shows that there in general are higher gas fractions in the bubble flow model. Giving the lower pressure profile as indicated in observation 3.

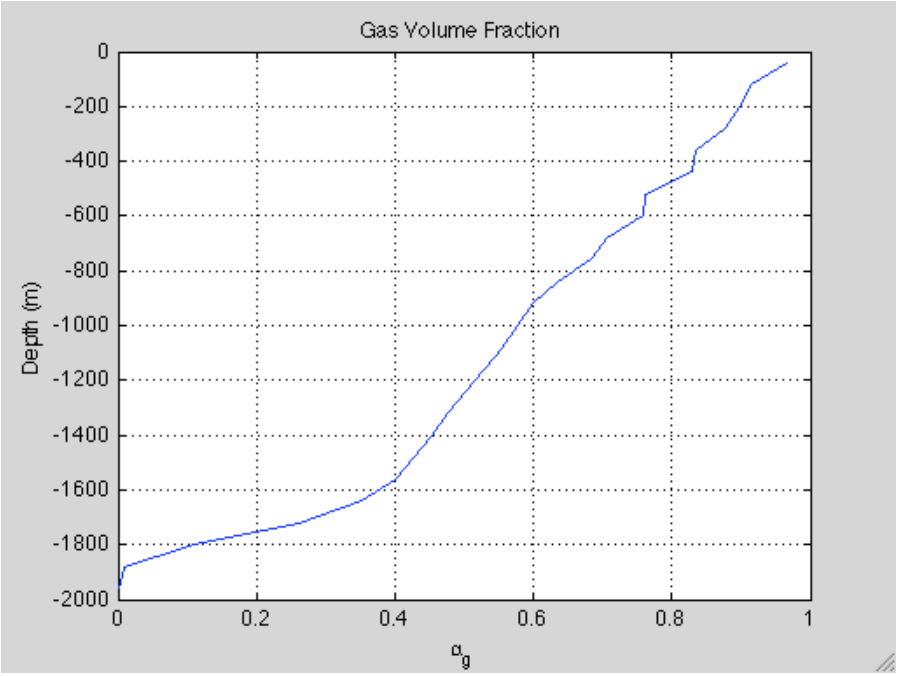

Figure (46) - Gas Volume Fraction as a Function of Depth at Time Equals 2000 s

12.2.3 Pressure Peak After Drill Pipe Connection

- Observation 4:

  As the circulation starts again, the pressure build up modeled by the bubble flow model gives a pressure peak of 129.4 bar at time equals 2650 seconds, before the pressure decrease down towards steady state again. This is a pressure increase of 9 bars, compared to the BHP at 1700 seconds. The slug flow model will give a pressure peak of 161.8 bars at time equals 2480 seconds. This is a pressure increase of 13.8 bars from steady state conditions at 1700 seconds.

Comments to the pressure peak:

The pressure peak gained, relative to the steady-state conditions, from the bubble flow model is lower than for the original model. As the pressure peak is induced by the circulation of liquid gathered at the bottomhole after shut down in circulation, this is as expected. From observation 3 it was found that there were higher gas fractions in the well when using bubble flow model. This gives that there is less liquid to be circulated

out, and thus lower pressure peak. This is also found in when comparing the liquid mass rate plots, figure (42) for the bubble flow model and figure (18) for the original model. Figure (47) and (48) shows the gas fraction profile at the time of the pressure peak for bubble flow model and slug flow model, respectively.

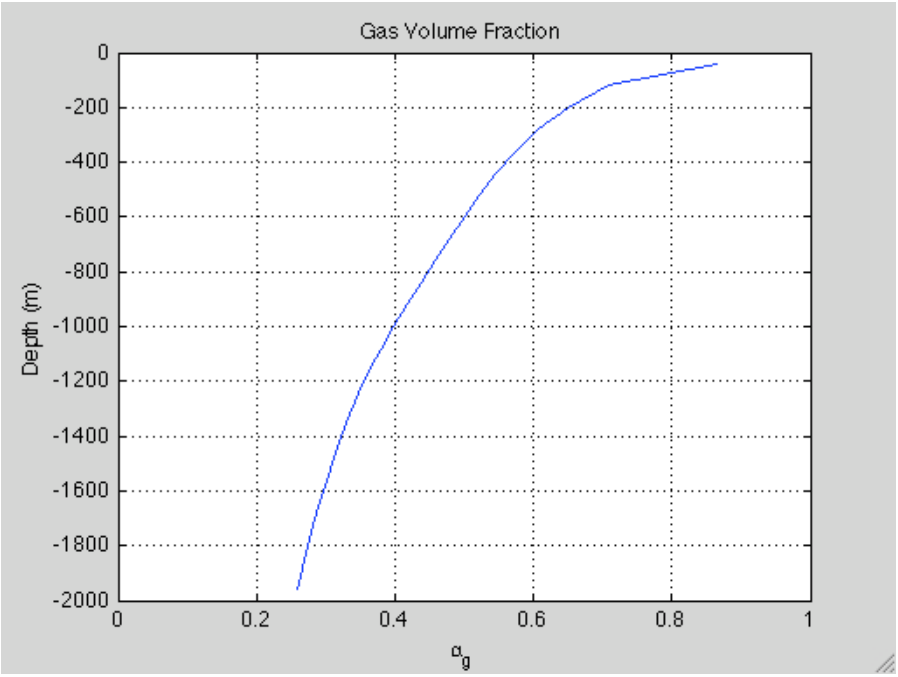

Figure (47) - Gas Volume Fraction as Function of Depth at Time Equals 2650. Bubble Flow Model.

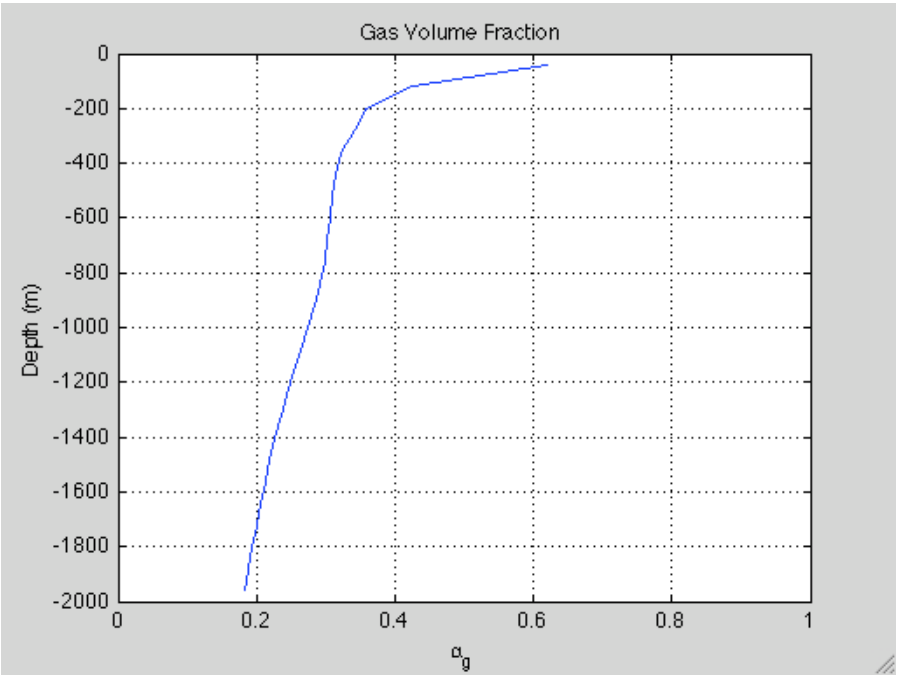

Figure (48) - Gas Volume Fraction as Function of Depth at Time Equals 2480 s. Original Model.

Comparing these two shows that by using bubble flow parameters instead of slug flow parameters gives higher fractions of gas, thus lower fractions of liquid, resulting in a lower pressure profile.

12.3 Results and Observations Using Flow Pattern Depending Slip Parameters

In this chapter, the results gained from using the flow pattern dependent model for slip parameters will be compared to the results from the simulations using the original model and the bubble flow model. From figures of the gas volume fractions in both the slug flow model and bubble flow model the fractions is typically above 0.25 along most of the wellbore. Exceptions are during the unloading sequence, and when the circulation is regained and the liquid that had gathered at the bottom is circulated out. Because of this, these are the two scenarios that will be investigated in this chapter.

Figure (49), below, shows the pressure as a function of time corresponding to figure (17), for the original model.

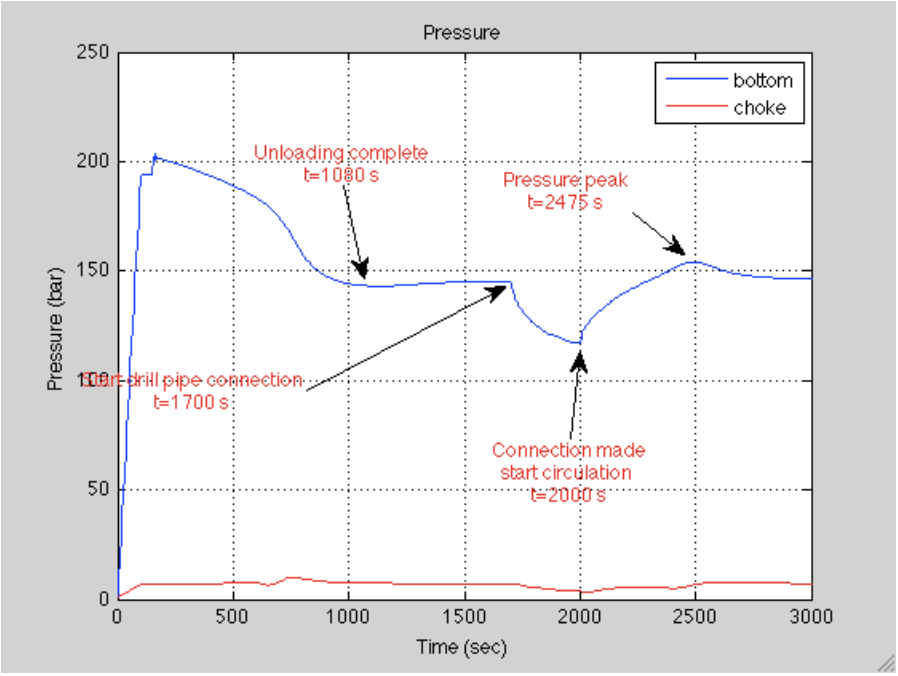

Figure (49) – Pressure as a Function of Time

Figure (50) and (51), presented below, shows the liquid- and gas mass rates as a function of time, and corresponds to figure (18) and (19) for the original model.

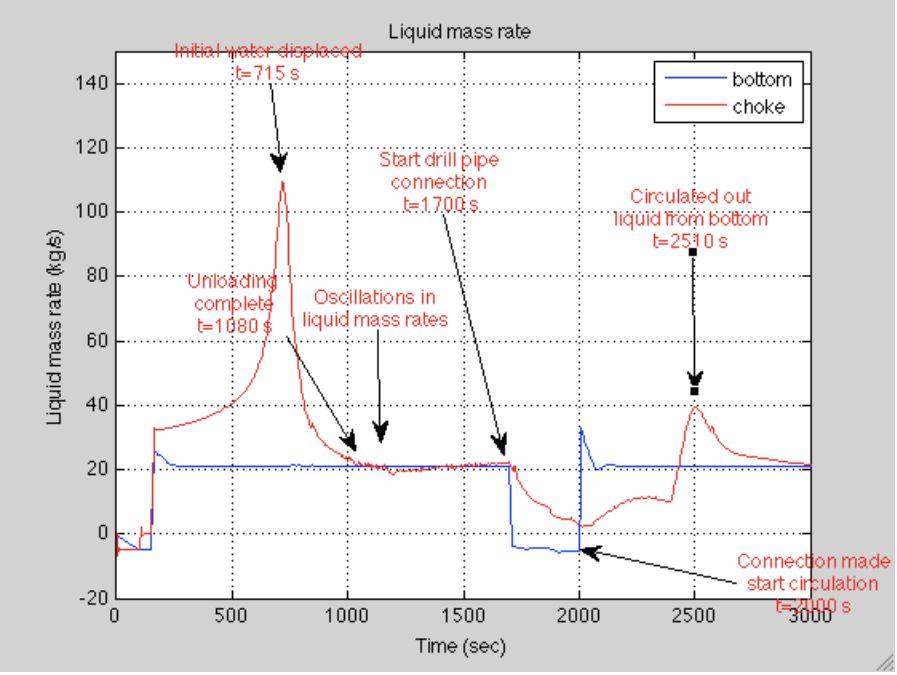

Figure (50) - Liquid Mass Rate as Function of Time

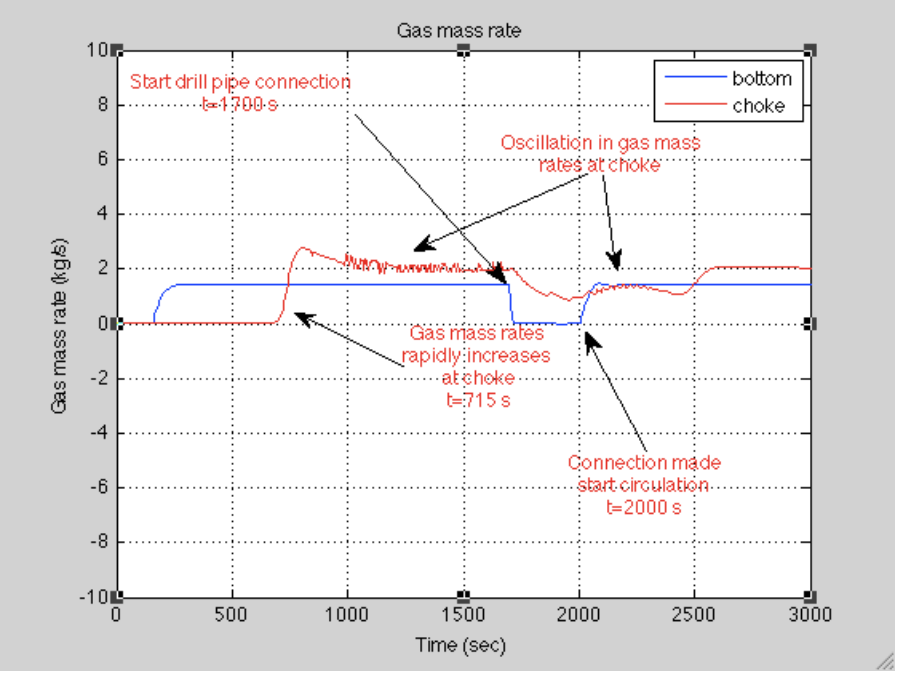

Figure (51) - Gas Mass Rate as Function of Time

Figure (50) and (51) shows some oscillations in rates at the choke, this is found to be due to the slip values chosen as the gas fraction reaches 75 % as shown in chapter 11.2.4. By lowering this boundary to a value of 60 % instead of 75 % the mass rates are smooth with no oscillations, as shown in figure (52) and (53).

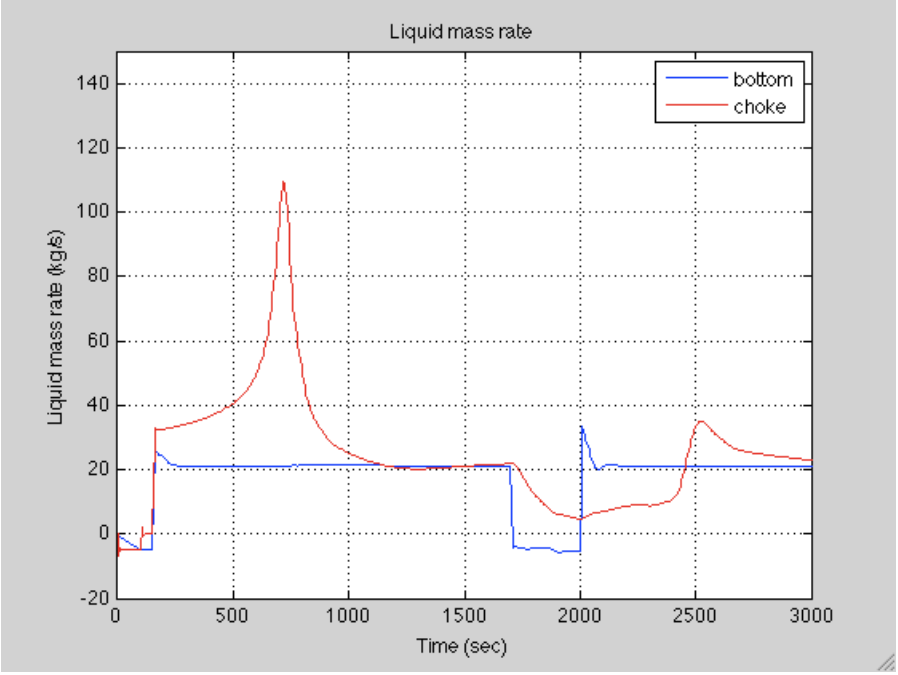

Figure (52) - Liquid Mass Rate as Function of Time

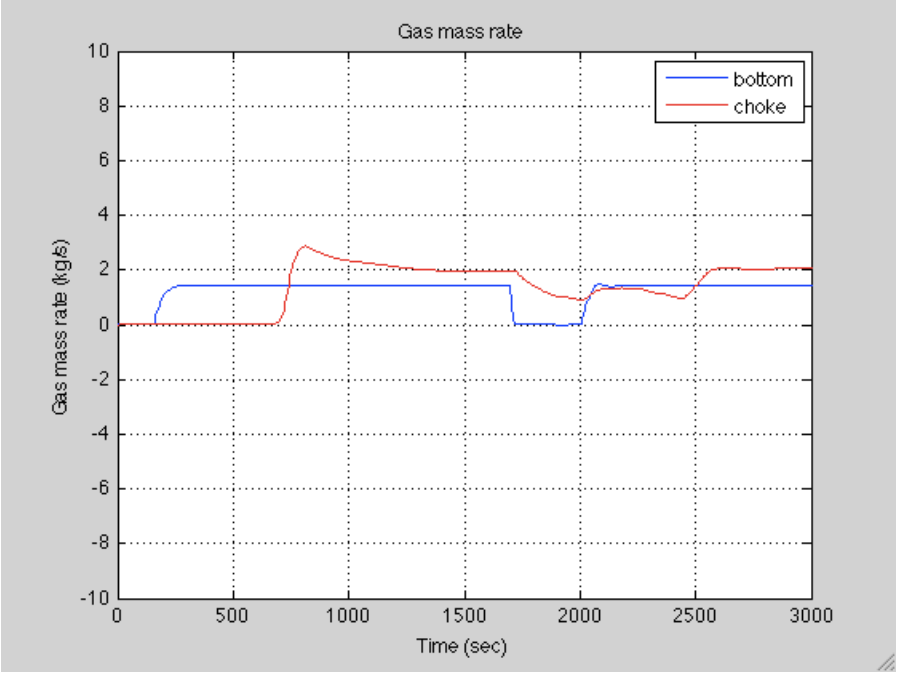

Figure (53) - Gas Mass Rate as Function of Time

However, due to the fact that all other simulations are performed using the boundary at 75 %, and that the BHP in figure (44) is smooth and are not experiencing any oscillations, this is the boundary that will be chosen for this model as well. Table (8), below, corresponds to table (5) and (7) for the original model and bubble flow model respectively. The "difference" values, in the parentheses in the "Pressure Peak" event, gives the pressure difference with respect to the BHP at time equals 1700 seconds. All

other differences are from the previous event. The values are gained from figure (49), (50) and (51).

Table (8) - Overview Flow Pattern Dependent Model

Event	Time [s]	BHP [bar]	Difference [bar]	Difference [%]
Start Unloading	150	194	-	-
Constant Circulation	160	203.5	+9.5	+4.9
Unloading Complete	1080	143.3	-60.2	-29.6
Start DP Connection	1700	145.5	+2.2	+1.5
Regain Circulation	2000	117.1	-28.4	-19.5
Pressure Peak	2475	154	+36.9 (+8.5)	+31.5 (+5.8)

12.3.1 Unloading Sequence

- Observation 1:

  The unloading sequence in this case lasts approximately in 930 seconds, see comment in figure (46). As seen in the same figure, the BHP is actually increasing with 2.2 bars after this time, however, this is considered to be the time that steady state occurs. In the original model the unloading sequence was done after 850 seconds of simulation, see values in table (5) for this model. This is a time difference of about 80 seconds. The bubble flow model, as presented in 12.2, did the unloading scenario in 1250 seconds.

- Observation 2:

  At time equals 1080 seconds; the pressure experienced in the bottom of the well will be 143.3 bar. This is 4.6 bar lower than for the original model, where the pressure was 147.9 bar. For the bubble flow model, the corresponding BHP was found to be 120.7 bar.

- Observation 3:

  Gas break through for the flow pattern dependent model is found at 715 seconds, see figure (50). For the original model, this was found at 640 seconds, and the bubble flow model experienced gas break through at time equals 740 seconds.

Comments to the unloading sequence:

Based on observation 1 and 2, it is expected that the slug flow model has played the biggest role during the unloading scenario. However, observation 3 suggests that the bubble flow model also has been used during the sequence. Figure (54) below shows the gas volume fraction as function of depth at the time for break through of gas for the original model, 640 seconds. The boundaries for the different flow patterns are drawn into figure (54). It is seen that, from 2000 meters and up to about 1100 meters, the transition flow parameters are used. From 800 and up to the surface, the bubble model will be used. This is why the profile looks more like the profile gained by the bubble flow model in figure (44) than the profile gained by the slug flow model in figure (21).

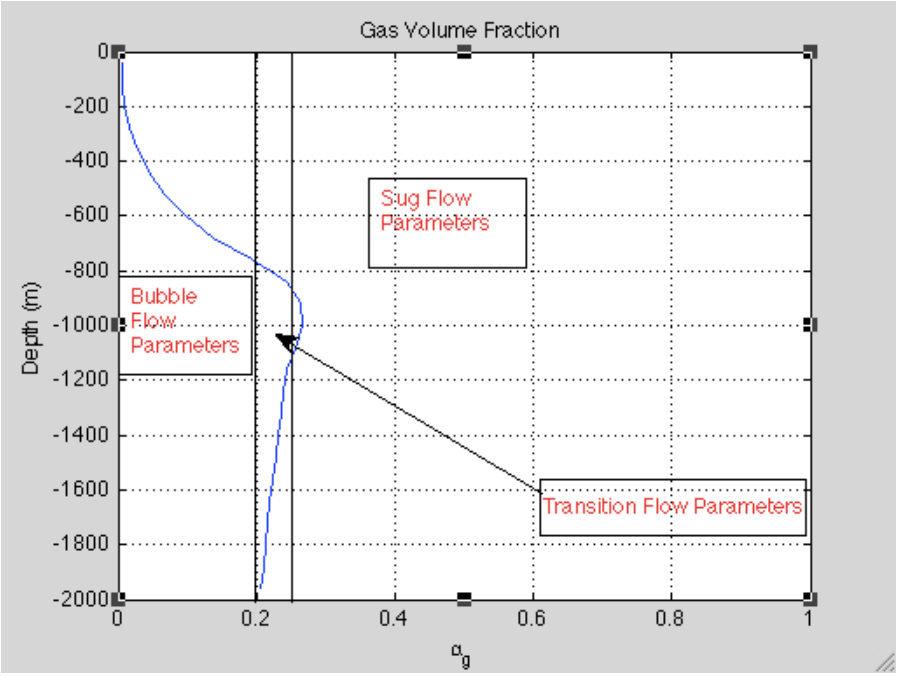

Figure (54) - Gas Volume Fraction as Function of Depth at Time Equals 640 s

As gas break through occurs at 715 seconds, the gas volume fraction profile is shifting to the right, more and more over towards the slug flow area. This is probably the explanation to observation 1 and 2, more and more parts of the wellbore is experiencing slug flow.

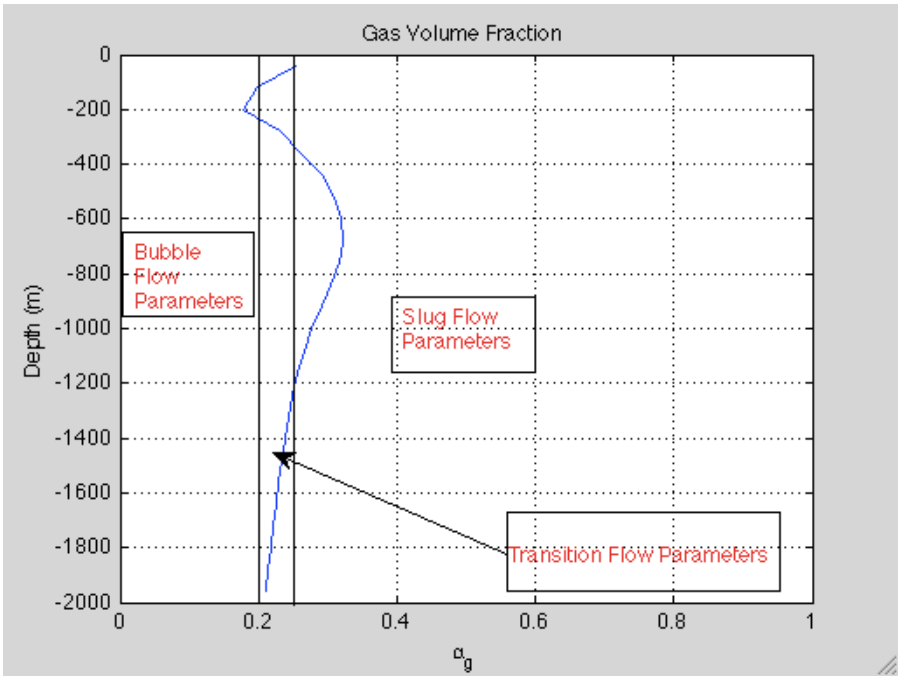

Figure (55) - Gas Volume Fraction as Function of Depth at Time Equals 715 s

Figure (56) below shows the gas volume fraction profile at steady state conditions, here it is seen that no parts of the wellbore is experiencing bubble flow. The bottom 500 meters are experiencing transition flow, but the interval between about 100 meters to 1500 meters are in the slug flow area. The very top of the well has gas fractions above 75 %, and is therefore dominated by the slip parameters for the approaching one-phase flow model.

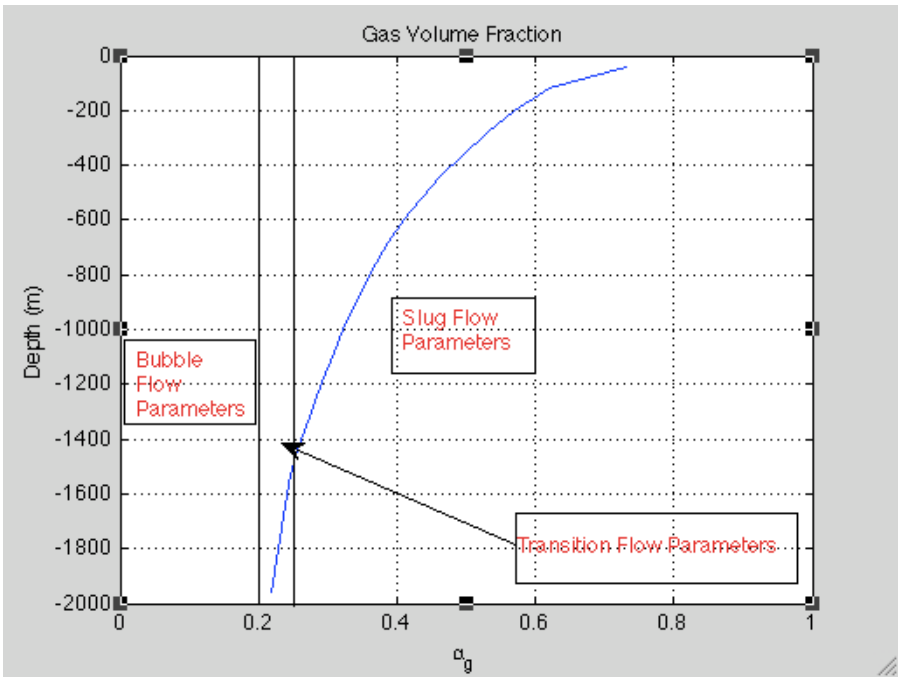

Figure (56) - Gas Volume Fraction as Function of Depth at Time Equals 850 s

12.3.2 Regaining Circulation After Drill Pipe Connection

- Observation 4:

  As the circulation starts again, the pressure build up modeled by the flow pattern dependent model gives a pressure peak of 154 bars at time equals 2475 seconds, before the pressure decrease down towards steady state again. This is a pressure increase of 8.5 bars, compared to the BHP at 1700 seconds. The original model will give a pressure peak of 161.8 bars at time equals 2480 seconds. This is a pressure increase of 13.8 bars from steady state conditions at 1700 seconds. For the bubble flow model the peak is found at 2650 seconds and a value of 129.4 bar, equaling an increase of 9 bars from steady-state conditions.

Comments to the pressure peak:

There are not big differences in the pressure differences between the steady-state conditions and the peak, but it is observed that the flow pattern depending model is closer to the value given by the bubble flow model. However, the time from starting circulation, until the liquid part at the bottom is circulated out is 175 seconds higher for the bubble model than for the flow pattern depending model. Time difference between slug flow model and flow pattern dependent is only 5 seconds. Figure (57), below, shows the gas volume fraction profile at time equals 2000 seconds. As seen in the figure, the bubble flow model will rule the bottom 400 meters. Then 100 meters with transition flow model and from here up to about 500 meters the slug flow model will be used. The final 500 meters are in the range where the transition to one-phase flow occurs, at 75 % gas.

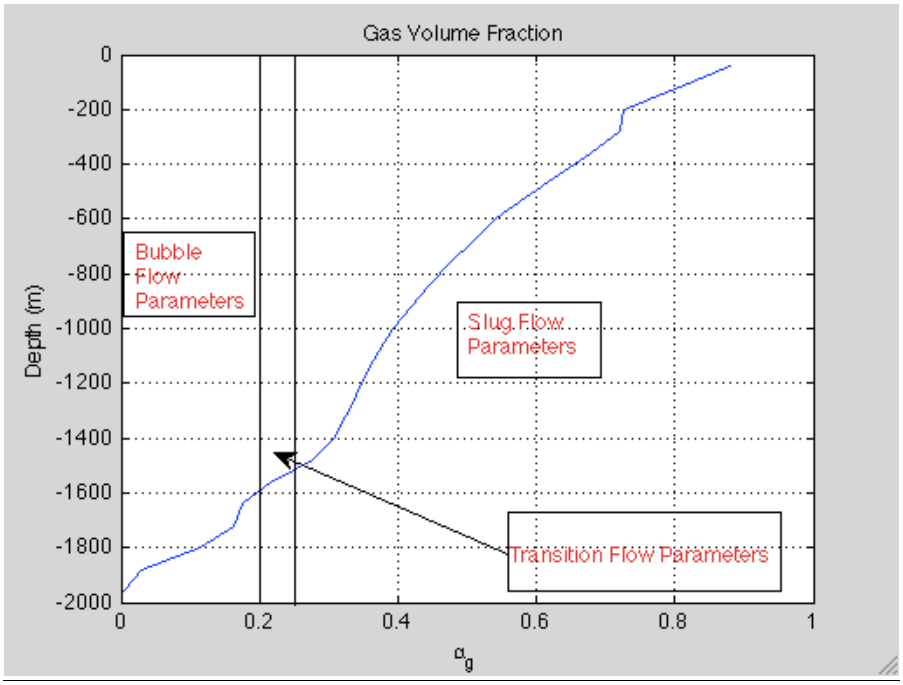

Figure (57) - Gas Volume Fraction as Function of Depth at Time Equals 2000 s

Now, as the circulation starts again, the pressure profile will shift to the left, due to the liquid is circulated out. This is shown in figure (58), below, and here it is seen that the slug flow model is only used between about 100 meters to 900 meters. Here the bubble flow model and the transition flow model will have more influence on the result.

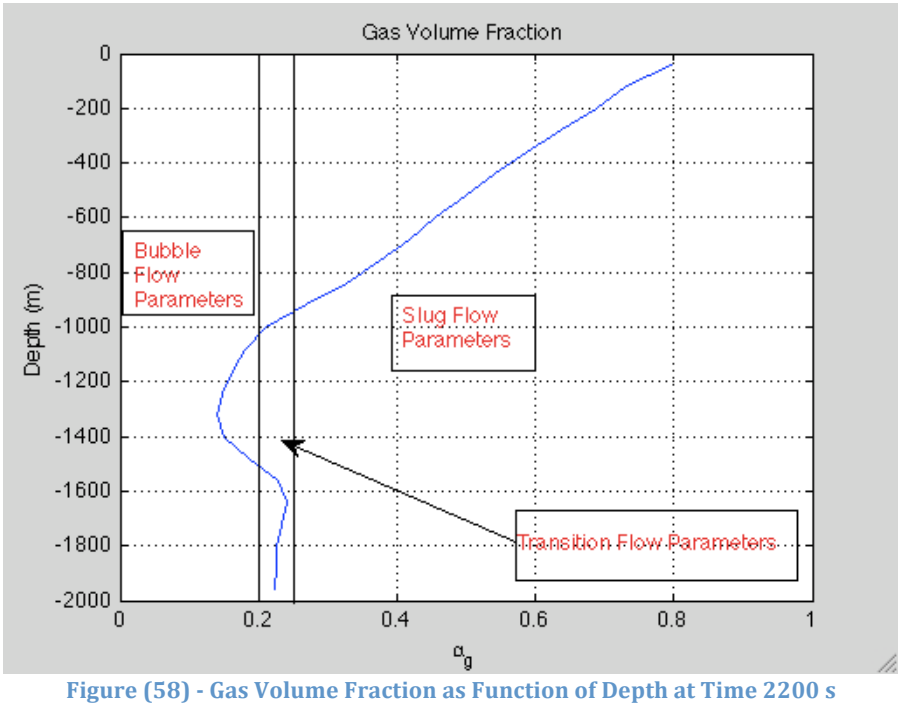

Figure (58) - Gas Volume Fraction as Function of Depth at Time 2200 s

Finally, at time equals 2475 seconds, the liquid slug is circulated out, the gas volume fraction profile here is given in figure (59) and now the slug flow model is the most dominant again, while the bubble flow model is not used.

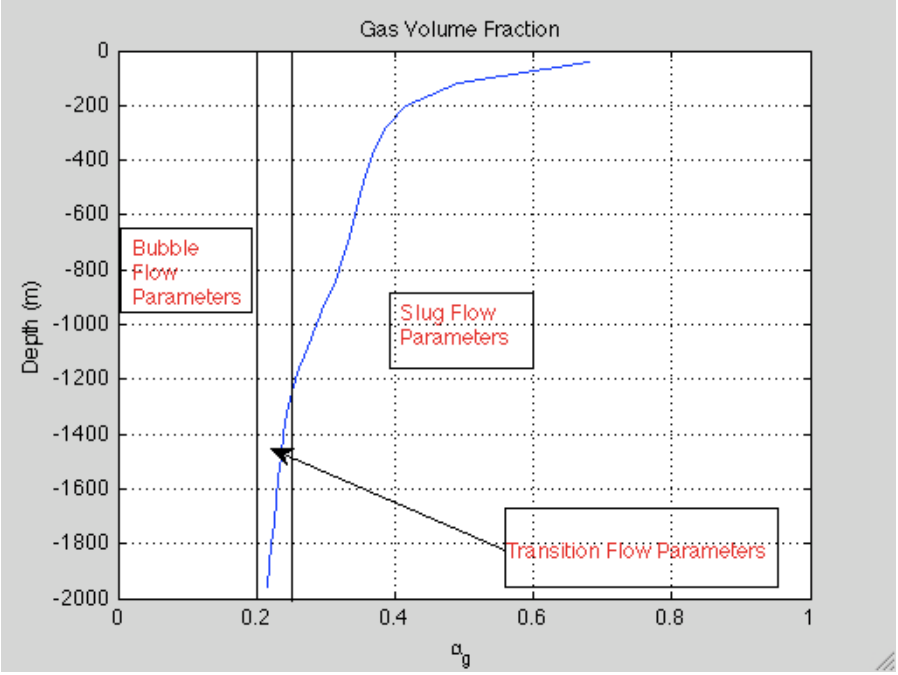

Figure (59) - Gas Fraction as Function of Depth at Time Equals 2475 s

From here the profile will shift more to the right as the system is regaining steady state conditions, resulting in a profile like in figure (60), which is found at time equals 3000 seconds.

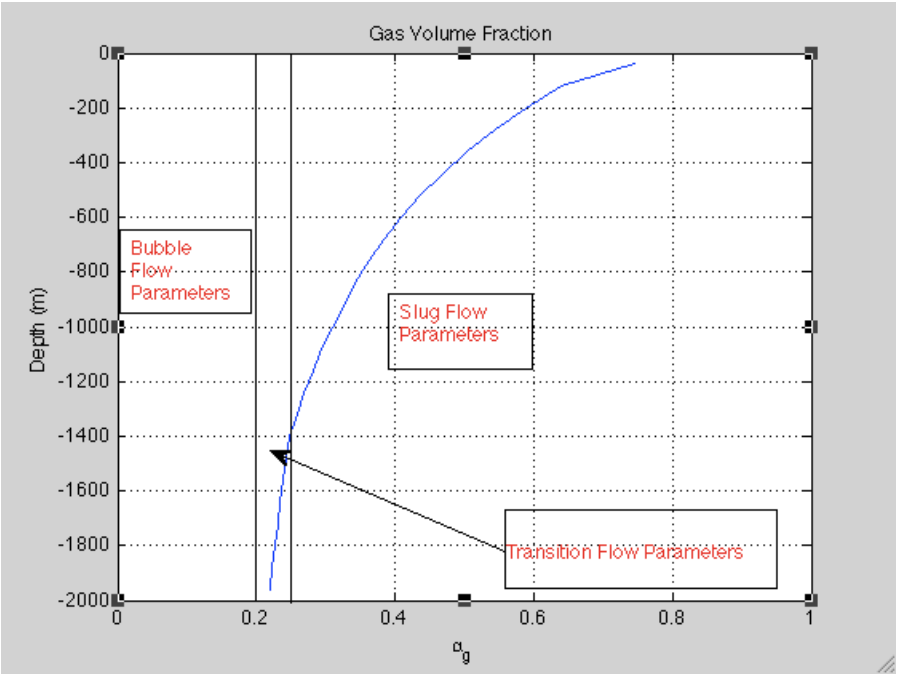

Figure (60) - Gas Volume Fraction as Function of Depth at Time Equals 3000 s

12.4 Overview of Observations

The main results from comparing the results gained from the bubble flow model to the results gained from the slug flow model are found in the unloading sequence. The sequence was found to last 400 seconds longer for the bubble flow model, as well as the steady-state pressure was 27.2 bars lower. In general, the pressure profile gained from simulating bubble flow is lower than the pressure profile for the slug flow simulations. This indicates higher gas fractions in the well when using the bubble flow model. Table (9) presents a comparison between the two models, during the different events. The pressure difference is the same from regaining circulation until the pressure peak, however, compared to the steady-state conditions, the pressure peak for the slug model represents a pressure increase of 9.3 % while the value for the bubble flow model is 7.5 %. See table (5) and (7).

Table (9) – Overview of Comparisons Between Slug- and Bubble Flow Model

Event	Slug Flow Model [bar]	Bubble Flow Model [bar]	Difference [bar]	Difference [%]
Start Unloading	194	194	-	-
Constant Circulation	203.5	203.5	-	-
Unloading Complete	147.8	120.7	27.1	18.3
Start DP Connection	148	120.4	27.6	18.7
Regain Circulation	121	88.6	32.4	26.8
Pressure Peak	161.8	129.4	32.4	20
Relative Pressure Peak	13.8	9	4.8	35

For the flow pattern depending model it is found that its nature is most like the slug flow model, as the gas volume fractions are over 0.20 most of the time. The events that were investigated were the unloading sequence and the circulation of the liquid at the bottom after drill pipe connection. The reason for choosing these events was due to the gas volume fractions was expected to have most variations here. Table (10) and (11) gives the differences in pressure between the flow pattern dependent model and the slug flow model, and between the flow pattern dependent model and the bubble flow model respectively.

Table (10) – Overview of Comparisons Between Slug- and Flow Pattern Dependent Model

Event	Flow Pattern Dependent Model [bar]	Slug Flow Model [bar]	Difference [bar]	Difference [%]
Start Unloading	194	194	-	-
Constant Circulation	203.5	203.5	-	-
Unloading Complete	143.3	147.8	-4.5	-3.1
Start DP Connection	145.5	148	45.5	-1.7
Regain Circulation	117.1	121	-3.9	-3.3
Pressure Peak	154	161.8	-7.8	-5.1

As seen in table (10) the values gained from the flow pattern dependent model does not vary much from the values gained from the original model.

Table (11) – Overview of Comparisons Between Bubble- and Flow Pattern Dependent Model

Event	Flow Pattern Dependent Model [bar]	Bubble Flow Model [bar]	Difference [bar]	Difference [%]
Start Unloading	194	194	-	-
Constant Circulation	203.5	203.5	-	-
Unloading Complete	143.3	120.7	22.6	15.8
Start DP Connection	145.5	120.4	25.1	17.3
Regain Circulation	117.1	88.6	28.5	24.3
Pressure Peak	154	129.4	24.6	16

As seen from table (11), the differences is larger when comparing the flow pattern dependent model to the bubble flow model. This is also quite logic, as gas fractions in the wellbore are higher than 0.25 for most of the simulation.

14 Conclusion and Further Work

Being able to maintain underbalanced conditions during an underbalanced drilling operation is of major importance. Modeling of the multiphase flow during drilling is considered to be critical for securing a successful job. The BHP reacts to changes in the circulation system, and this makes the transient simulations of a UBO hard when using jointed pipe drilling combined with gas injection through the drill string. A two-phase drift-flux model has been developed in Matlab to simulate the dynamic bottomhole pressure during transient conditions, such as the unloading sequence and drill pipe connections. The model is based on the AUSMV scheme and a description of the model has been made. The original drift-flux model only recognizes the slug flow region, giving slip parameters according to this. Extensions to the model were made, first defining slip parameters for the bubbly region. The velocity profile coefficient, $C_{0,B}$, was found in literature to have a value of 1.0 or 1.1, the value of 1.1 was selected after simulation test runs. Another extension made was to implement a simple procedure for flow pattern prediction, choosing between bubble flow, transition flow and slug flow. Slip values were found depending on what flow pattern that was recognized.

Simulations of a defined base case have been performed, including a unloading sequence and a drill pipe connection. The simulation runs was made using:

- Original slug flow parameters for slip
- Bubble flow parameters for slip
- Flow pattern dependent parameters for slip

The results showed that the bubble flow parameters for slip, in general gave a lower BHP and a more time consuming unloading sequence than for the original model. Time of the unloading sequence was found to be 47 % higher for the bubble flow model. Some of the comparisons are shown in table (12) below.

Table (12) - Some Comparison Results Between Slug- and Bubble Flow Model

Event	Slug Flow Model [bar]	Bubble Flow Model [bar]	Difference [bar]	Difference [%]
Start Unloading	194	194	-	-
Unloading Complete	147.8	120.7	27.1	18.3
Start DP Connection	148	120.4	27.6	18.7
Pressure Peak	161.8	129.4	32.4	20

From the simulations using the flow pattern depending slip parameters it was found some differences compared to the original model, however, it was shown that the slug flow region was the primary flow pattern throughout the simulation. During the unloading sequence, until gas break through, was found to be the sequence where the bubble- and transition flow model had most influence.

Future recommendations for the drift-flux model presented in this thesis include:

- Better description of the interfacial tension, as function of pressure.
  In this model a constant value of 0.0722 N/m is used, which is valid for standard conditions.
- Implement the geometrical limitation presented in 11.1
- Better description of what happens when approaching one-phase flow, some oscillations were found at mass rates during simulations using the flow pattern dependent model
- Implement friction model depending on the flow pattern found
- Implementation of flow model for churn-, annular- and dispersed bubble flow
- Include modeling of the two-phase downward flow in the drill string
- Model with influx from formation
- Validation from experimental data

References:

1. Bill Rehm, "Practical Underbalanced Drilling and Workover", PETROLEUM EXTENSION SERVICE, The university of Texas at Austin, Continuing & Extended Education, Austin, Texas-2002
2. Bernt S. Aadnøy – "An introduction to Petroleum Rock Mechanics" – Compendium Given in Course MPE680 – Brønnteknologi H-10 - UiS
3. Boyun Guo and Ali Ghalambor, "Gas Volume Requirements for Underbalanced Drilling Deviated Holes" University of Louisiana at Lafayette, PennWell Corporation, Tulsa, Oklahoma - 2002
4. Kjell K. Fjelde, Rolv Rommetveit, Antonio Merlo, Antonio C.V.M Lage "Improvements in Dynamic Modeling of Underbalanced Drilling"- IADC/SPE 81636, IADC/SPE Underbalanced Technology Conference and Exhibition, Houston, Texas, 25-26 March – 2003
5. Hani Qutob, "Underbalanced Drilling; Remedy for Formation Damage, Lost Circulation, & Other Related Conventional Drilling Problems" – 88698-MS, Abu Dhabi International Conference and Exhibition, Abu Dhabi, United Arab Emirates, 10-13 October - 2004
6. Thomas J. Danielson, Lloyd D. Brown and Kris M. Bansal, "Flow Management: Steady-State and Transient Multiphase Pipeline Simulation" - OTC 11965, Offshore Technology Conference, Houston, Texas, 1-4 May - 2000
7. Saponja, J., "Challenges with Jointed Pipe Underbalanced Operations" – 37066-PA, SPE Drilling & Completion, Volume 13, Number 2, June-1998
8. C. Mykytiw, P.V. Suryanarayana, P.R Brand, Blade Energy Partners, "Practical Use of a Multiphase Flow Simulator for Underbalanced Drilling Applications Design – The Tricks of the Trade" - SPE/IADC 91598, SPE/IADC Underbalanced Technology Conference and Exhibition, Houston, Texas, 11-12 October - 2004,
9. R. Rommetveit, O. Sævareid, A.C.V.M Lage, A. Guarneri, C. Georges, E. Nakagawa, A. Bijleveld – "Dynamic Underbalanced Drilling Effects are Predicted by Design Model" – 56920-MS, Conference Paper, Offshore Europe Oil and Gas Exhibition and Conference, Aberdeen United Kingdom, 7 – 10 September - 1999

10. Bernt S. Aadnoy, Iain Cooper, Stefan Z. Miska, Robert F. Mitchell and Michal L. Payne – "Advanced Drilling and Well Technology"- Copyright 2009 Society of Petroleum Engineers
11. Rune W. Time – Compendium Given in Part 2 of the Course MPE700 Petroleumsproduksjon V-11 – Multiphase Flow V-11, UiS
12. Faisal Abdullah ALAdwani – "Application of Mechanistic Models in Predicting Flow Behaviour in Deviated Wells Under UBD Conditions" – Masters Thesis Submitted to the Graduate Faculty of the Louisiana State Univeristy and Agricultural and Mechanical College – May – 2003
13. Boyun Guo and Gefei Liu – "Applied Drilling Circulation Systems Hydraulics, Calculations, and Models" Copyright 2011 Elsevier Inc.
14. M.M. Awad, Y.S. Muzychka "Effective Property Models for Homogeneous Two-Phase Flows" – Experimental Thermal and Fluid Science, Vol. 33, Issue 1, P. 106-113, October - 2008
15. James P. Brill - "Modeling Multiphase Flow in Pipes" – The Way Ahead - The Magazine by and for Young Professionals in Oil and Gas, SPE, Vol. 6, No. 2, P. 16-17, 2010
16. Beggs D.H and Brill J.P. – "A Study of Two-Phase Flow in Inclined Pipes" – 4007-PA, Journal of Petroleum Technology, Vol. 25, Number 5, P. 607-617, May - 1973
17. C. Perez – Tellez, J.R. Smith, J.K Edwards – "A New Comprehensive, Mechanistic Model for Underbalanced Drilling Improves Wellbore Pressure Predictions" – 74426-MS, SPE International Petroleum Conference and Exhibition in Mexico, Villahermosa, Mexico, 10-12 February - 2002
18. Carloz Perez-Tellez – "Improved Bottomhole Pressure Control for Underbalanced Drilling Operations" – Ph. D Dissertation, The Louisiana State University and Agricultural and Mechanical College, May - 2003
19. Bijleveld A.F, Koper M, Saponja – "Development and Application of an Underbalanced Drilling Simulator" – 39303-MS- IADC/SPE Drilling Conference, Dallas, Texas, 3-6 March – 1998

20. Hasan, A.R. and Kabir, C.S. - "Two-Phase Flow in Vertical and Inclined Annuli", International Journal of Multiphase Flow, Vol. 18, Issue 2, P. 279-293, March - 1992
21. Hasan, A.R. - "Void Fraction in Bubbly and Slug Flow in Downward Two-Phase Flow in Vertical and Inclined Wellbores" – 26522-PA, SPE Production and Facilities, Vol. 10, Number 3, P. 172-176, August - 1995
22. Caetano, E.F. - "Upward Two-Phase Flow Through an Annulus", Ph.D. Dissertation, The University of Tulsa - 1985.
23. Information Taken From the SPT Groups Website, http://www.sptgroup.com
For Chapter 7.4.1:
http://www.sptgroup.com/en/Products/Drillbench/UBD/
The different Modules are Selected in the "Module Solutions" in the Right Column
24. Baker Hughes Inteq – "Underbalanced Drilling Manual", Version 1.0, November - 1999
25. Definitions Taken From the IADC UBO & MPD Glosary of Terms dec. 2011, Website; http://www.iadc.org/wp-content/uploads/2011/12/UBO-MPD-Glossary-Dec11.pdf
26. Kenneth P. Malloy, C. Rick Stone, George H. Medley, Don Hannegan, Oliver Coker, Don Reitsma, Heilo Santos, Joseph Kinder, Johan Eck-Olsen, John McCaskill, James May, Kenneth Smith and Paul Sonneman – "Managed-Pressure Drilling: What It Is and What It Is Not" – 122281-MS, IADC/SPE Managed Pressure Drilling and Underbalanced Operations Conference & Exhibition, San Antonio, Texas, 12-13 February - 2009
27. Kenneth P. Malloy "Managed Pressure Drilling – What is it Anyway" World Oil, Issue: March 2007, P. 27-34
28. Øyvind Breyholtz, Gehard Nygaard and Hardy Siahaan – "Managed Pressure Drilling: A Multi-Level Control Approach" – 128151-MS, SPE Intelligent Energy Conference and Exhibition, Utrecht, The Netherlands, 23-25 March -2010

29. N. Zuber, J.A Findland – "Average Volumetric Concentration in Two-Phase Flow Systems" - Journal of Heat Transfer, Vol. 87, Issue 4, P. 453-468, ASME - 1965
30. H. Shi, J.A. Holmes, L.J. Durlofsky, K. Aziz, L.R. Diaz, B. Alkaya, G. Oddie – "Drift-Flux Modeling of Two-Phase Flow in Wellbores" – 84228-PA, SPE Journal, Volume 10, Number 1, March - 2005
31. Norsok Standard D-010, Rev. 3, August 2004 – Well integrity in drilling and well operations
32. Compendium Given in Course BIP200 Bore og Brønnvæsker V-10 by Helge Hodne, UiS-2010
33. Antonio C.V.M. Lage, Rune W. Time – "Mechanistic Model for Upward Two-Phase Flow in Annuli" – 63127-MS, SPE Annual Technical Conference and Exhibition, Dallas, Texas, 1-4 October - 2000
34. Antonio C.V.M. Lage, Rune W. Time – "An Experimental and Theoretical Investigation of Upward Two-Phase Flow in Annuli" – 64525-MS, SPE Asia Pacific Oil and Gas Conference and Exhibition, Brisbane, Australia, 16-18 October – 2000
35. Yehuda Taitel, Dvora Bornea and A. E. Dukler – "Modelling flow pattern transitions for steady upward gas-liquid flow in vertical tubes" – AIChe Journal, Volume 26, Issue 3, P. 345-354, May – 1980
36. Finn Paulsen: "Underbalanced drilling in hard formations in Algeria", Mag S6179 - Stavanger Universitets Bibliotek, Masteroppgave Petroleumsteknologi, UiS – 2005
37. Christian Callin, Øystein Falch, Karl Torstein Hetland, Jan Pålsgård, Jostein Walle: "Ergo Fysikk 2FY Grunnbok", P. 168, H. Aschehoug & Co – 1997
38. Figure Taken From Dr. Ove Bratlands – "The Flow Assurance Site" See: http://drbratland.com/PipeFlow2/chapter1.html
39. Stian Molvik "A Study of Two-Phase Drift-Flux Modeling in Wells and Corresponding Slip Relations" - Masters´s Thesis, UiS – 2011
40. Steinar Evje and Kjell Kåre Fjelde - "Hybrid Flux-Splitting Schemes for a Two-Phase Flow Model", Journal of Computational Physics, Volume 175, Issue 2, P. 674-701, 20. January - 2002